A Multimodal Sleep Foundation Model for Disease Prediction

Rahul Thapa[1,2,*], Magnus Ruud Kjaer[3,4,5,*], Bryan He[2], Ian Covert[2], Hyatt Moore IV[3,6], Umaer Hanif[5,7], Gauri Ganjoo[3], M. Brandon Westover[8], Poul Jennum[5,9], Andreas Brink-Kjaer[4], Emmanuel Mignot[3,+], and James Zou[1,2,+]

[1]Department of Biomedical Data Science, Stanford University, Stanford, CA, USA
[2]Department of Computer Science, Stanford University, Stanford, CA, USA
[3]Department of Psychiatry and Behavioral Sciences, Stanford University, Stanford, CA, USA
[4]Department of Health Technology, Technical University of Denmark, Kongens Lyngby, Denmark
[5]Department of Clinical Neurophysiology, Danish Center for Sleep Medicine, Rigshospitalet, Glostrup, Denmark
[6]Department of Systems Engineering, Naval Postgraduate School, Monterey, CA, USA
[7]Data Science, BioSerenity, Paris, France
[8]Department of Neurology, Beth Israel Deaconess Medical Center, Harvard Medical School, Boston, MA, USA
[9]Department of Clinical Medicine, University of Copenhagen, Copenhagen, Denmark
[*]These authors contributed equally.
[+]These authors jointly supervised this work.
Correspondence: mignot@stanford.edu, jamesz@stanford.edu

Abstract

Sleep is a fundamental biological process with broad implications for physical and mental health, yet its complex relationship with disease remains poorly understood. Polysomnography (PSG), the gold standard for sleep analysis, captures rich physiological signals but remains underutilized due to challenges in standardization, generalizability, and multimodal integration. To address these limitations, we developed SleepFM, a multimodal sleep foundation model trained with a novel contrastive learning approach that accommodates multiple PSG montages—the specific arrangements of electrodes and sensors used to record physiological signals during sleep. Trained on a curated dataset of over 585,000 hours of PSG recordings from approximately 65,000 participants across multiple cohorts, SleepFM produces latent sleep representations that capture the physiological and temporal structure of sleep and enable accurate prediction of future disease risk. SleepFM achieved a C-Index of at least 0.75 (Bonferroni-corrected $p < 0.01$) for 130 conditions, including all-cause mortality (C-Index: 0.84), dementia (0.85), myocardial infarction (0.81), heart failure (0.80), chronic kidney disease (0.79), stroke (0.78), and atrial fibrillation (0.78). Moreover, the model demonstrates strong transfer learning performance on a dataset from the Sleep Heart Health Study (SHHS), a dataset that was excluded from pretraining, and performs competitively with specialized sleep-staging models such as U-Sleep and YASA on common sleep analysis tasks, achieving mean F1 scores of 0.70–0.78 for sleep staging and accuracies of 0.69 and 0.87 for classifying sleep apnea severity and presence. This work shows that foundation models can extract clinically meaningful features from multi-modal sleep recordings, enabling scalable, label-efficient analysis and disease prediction.

Introduction

Sleep is a complex process characterized by intricate interactions across physiological systems, including brain, heart, respiratory, and muscle activity [1]. Polysomnography (PSG), the gold standard for sleep evaluation, captures these interactions through recordings of multiple modalities including brain activity signals (BAS, including EEG and EOG), electrocardiography (ECG), electromyography (EMG), and respiratory signals [2].

Sleep disorders affect millions of people and are increasingly recognized as indicators of and contributors to various health conditions [3]. Sleep disturbances often precede the clinical onset of numerous conditions, such as psychiatric disorders [4], neurodegenerative diseases [5] and cardiovascular disorders [6]. These associations highlight an important role sleep plays in maintaining overall health and underscores its predictive potential across a wide spectrum of diseases. However, most existing studies have focused on identifying links between sleep and specific diseases using isolated metrics or manual annotations, leaving much of the complexity of sleep physiology, as captured in PSG, underutilized.

Recent advances in deep learning have enabled the use of PSG's multimodal data for tasks ranging from sleep staging and apnea detection to predicting conditions like atrial fibrillation, biological aging, and narcolepsy [3, 7, 8, 9, 10]. Despite this progress, current approaches face key limitations: they focus on individual outcomes, depend on supervised learning with expert-labeled data, and are trained on relatively small datasets (2,500–15,913 recordings) [3, 7, 9, 10, 11]. Manual annotations are time-consuming and prone to inter-rater variability, making scaling difficult. Moreover, existing models lack flexibility across recording environments, generalize poorly across cohorts, and often fail to exploit the richness of multimodal sleep signals. There remains a need for robust, generalizable architectures and systematic evaluation of sleep's predictive value across a broad range of health conditions.

Foundation models have emerged as a transformative approach in machine learning, enabling robust representation learning from large-scale, unlabeled data [12]. By leveraging self-supervised learning, these models can be fine-tuned efficiently for diverse applications. In biomedicine, foundation models have demonstrated remarkable capabilities in analyzing complex, heterogeneous datasets, driving advances in disease prediction, patient stratification, and therapeutic discovery [13, 14]. Their ability to extract meaningful patterns from large-scale data has addressed many challenges associated with the diverse and high-dimensional nature of clinical datasets.

Despite these successes, their application to sleep remains limited. Sleep data, particularly from PSG, presents unique challenges due to its complexity and variability, including differences in the number and types of recording channels across clinical cohorts. Most sleep studies have narrowly focused on sleep-specific outcomes, constraining the broader potential of foundation models for disease prediction. In preliminary work, we explored self-supervised learning on PSG data in a smaller cohort of participants [11]. While this effort highlighted the potential of foundation models for analyzing sleep data, it primarily targeted sleep-specific outcomes and lacked the flexibility to accommodate the diverse configurations of PSG recordings. These limitations emphasize the need for models that can generalize across heterogeneous datasets and systematically uncover sleep's role in predicting a wider range of diseases.

In this paper, we present SleepFM, a foundation model trained on over 585,000 hours of PSG data from 65,000+ participants. SleepFM captures the diverse information present in multimodal sleep recordings—integrating EEG, ECG, EMG, and respiratory signals. Its channel-agnostic architecture enables joint learning across multiple modalities, producing representations that generalize across environments. We also introduce a new leave-one-out contrastive learning algorithm that aligns information across modalities during pretraining while remaining resilient to missing or heterogeneous channels during inference. Our model uses 5–25 times more data than previously trained supervised sleep [3, 7, 9, 10] or biosignal models [15, 16].

Inspired by phenome-wide association studies (PheWAS) [17], we examined whether sleep characteristics, as captured by SleepFM, can predict the onset of a wide range of diseases. Leveraging EHR disease codes, we develop a framework to systematically explore predictive associations between multimodal sleep and diverse health conditions.

Dataset and SleepFM architecture

We describe our dataset and training procedures in detail in Methods section. Briefly, we used PSG data from four primary cohorts: Stanford Sleep Clinic (SSC) [11], BioSerenity [18, 19], the Multi-Ethnic Study of Atherosclerosis (MESA) [20, 21], and the Outcomes of Sleep Disorders in Older Men (MrOS) [20, 22]. SSC

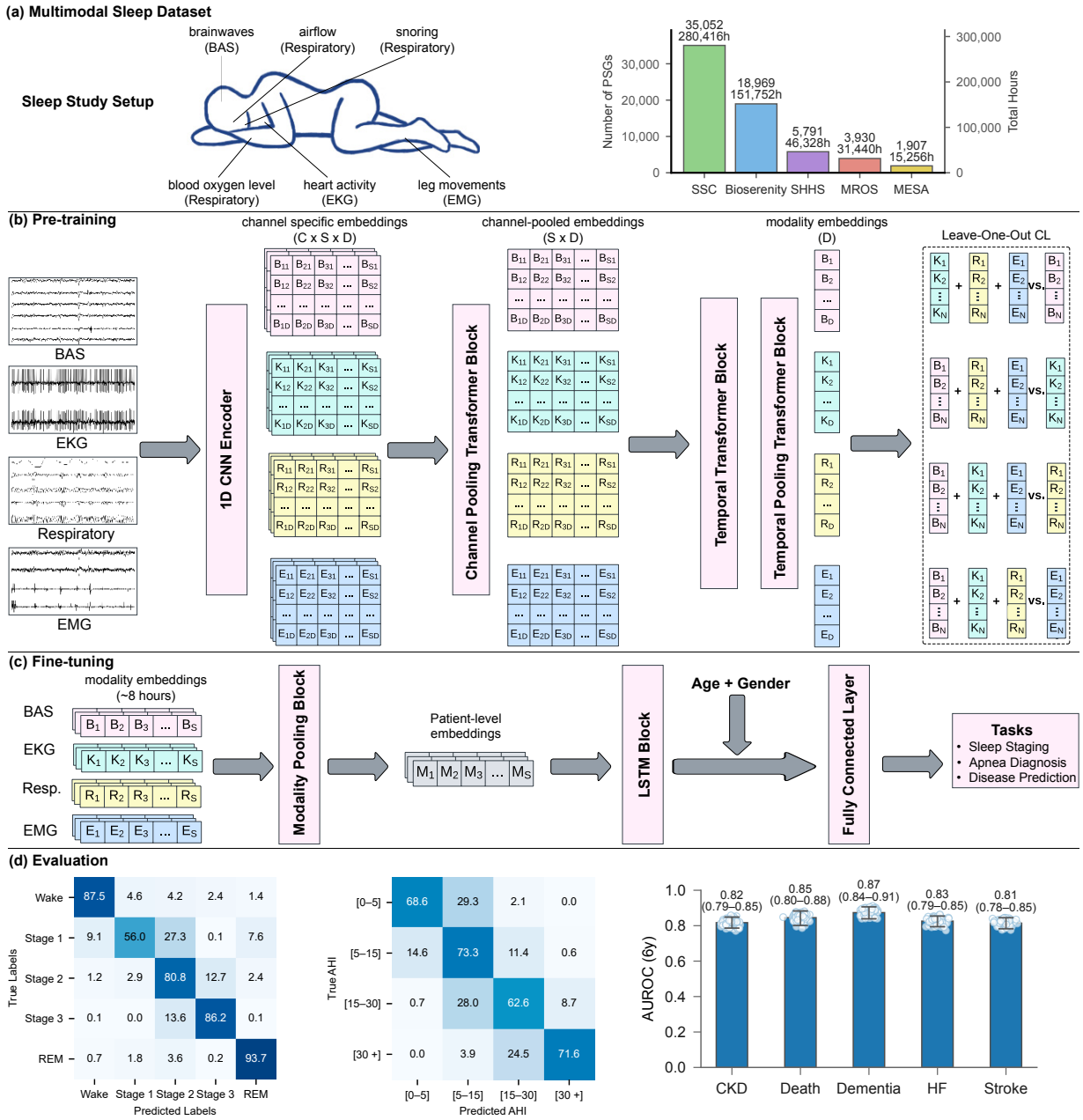

Figure 1: Overview of the SleepFM framework. (a) Polysomnography (PSG) setup and dataset statistics across multiple sleep centers. Bars show the number of independent PSG recordings (participants) per cohort and the corresponding total recording hours. (b) Multimodal contrastive pre-training: raw signals from each modality are encoded by a CNN, channel embeddings are pooled within modality, and a temporal transformer with temporal pooling yields sequence-level representations for leave-one-out contrastive learning (CL). C: channels, S: sequence length, D: embedding dimension. (c) Fine-tuning using frozen embeddings for downstream tasks (sleep staging, apnea detection, disease prediction). Eight hours of multimodal embeddings are aggregated to patient-level representations, concatenated with age and gender, and passed to an LSTM followed by a fully connected layer. (d) Evaluation across representative tasks and clinical applications. Left and middle, confusion matrices for sleep staging (SHHS) and AHI categories (SSC) shown as row-normalized percentages. Right, disease-prediction performance on the Stanford cohort (n=5,019 participants). Box plots summarize 1,000 patient-level bootstrap resamples: faint dots (individual bootstrap draws), and vertical line with end caps (95% bootstrap percentile CI). Numeric labels are means. The number of positive samples for each disease is as follows: CKD (354), Death (224), Dementia (221), HF (283), and Stroke (297). **Abbreviations:** BAS, brain activity signal; EKG, electrocardiogram; EMG, electromyogram; SSC, Stanford Sleep Cohort; SHHS, Sleep Heart Health Study; MROS, Outcomes of Sleep Disorders in Older Men; MESA, Multi-Ethnic Study of Atherosclerosis; CKD, chronic kidney disease; HF, heart failure.

includes 35,052 studies from participants aged 1–100 years; BioSerenity adds 18,900 studies from individuals aged 7–90; MESA and MrOS contribute 2,237 and 3,930 PSGs, respectively, from older adults. Together, these cohorts span 65,000 participants and over 585,000 hours of sleep recordings. We further evaluated generalization using the Sleep Heart Health Study (SHHS) [20, 23], a multi-center dataset of 6,441 adults aged 40+, held out from pretraining and used solely for transfer learning. Dataset distributions post-filtering are shown in Table 1. Demographics for SSC and BioSerenity appear in Extended Table 1 and Extended Table 2, while details for SHHS, MrOS, and MESA are available in their respective publications.

Our pre-processing pipeline begins by resampling all signals to 128 Hz for consistency across cohorts. Signals are then segmented into 5-second windows, which serve as the model's fundamental input tokens. The architecture includes 1D convolutional layers for feature extraction, followed by channel-agnostic attention pooling to address variability in channel number and order across cohorts. A transformer block captures temporal dependencies over a 5-minute context window. During pre-training, we use a multimodal contrastive learning objective to align representations across all modalities. The model's robustness stems from its channel-agnostic design, enabling it to accommodate missing channels, varying channel counts, and heterogeneous signal types.

For downstream tasks, we leverage the pre-trained model's embeddings through lightweight fine-tuning. The token embeddings from different modalities are pooled again and processed by a 2-layer Long Short-Term Memory (LSTM) network before passing through task-specific output heads. For patient-level prediction tasks (e.g., disease prediction), an additional temporal pooling layer before the output layer compresses all token embeddings into a single 128-dimensional embedding.

To evaluate model performance across tasks, we use appropriate task-specific metrics. For classification tasks such as gender classification, we report AUROC and AUPRC; for sleep apnea classification we show confusion matrices and report accuracy; for age estimation, we use mean absolute error (MAE) and Pearson correlation. Sleep staging is evaluated using the F1 score, which is well-suited for class-imbalanced settings. For disease prediction, we report AUROC and Harrell's concordance index (C-Index), a standard survival analysis metric that measures the proportion of correctly ranked risk pairs. All metrics range from 0 to 1, with higher values indicating better performance. Confidence intervals (95%) are computed using bootstrapping.

SleepFM Supports Standard Sleep Analysis Tasks

After pre-training SleepFM, we assessed the general utility of its learned representations by fine-tuning on four common benchmark tasks: age estimation, gender classification, sleep stage classification, and sleep apnea classification. While these tasks are not the main focus of our work, they are useful validations showing that the model captures fundamental sleep patterns. For all tasks, we trained lightweight LSTM-based heads on top of the frozen multimodal embeddings derived from entire nights of PSG data.

For age estimation, we assessed the model's ability to predict chronological age. Overall performance is shown in Extended Figure 1, with the model achieving a MAE of 7.33 years and a correlation coefficient of 0.88. Performance varied across age groups, with higher accuracy in pediatric and middle-aged participants and greater error in elderly adults, suggesting that age prediction is more challenging at the extremes of the age spectrum. Gender classification yielded an AUROC of 0.86 [0.85–0.87] and AUPRC of 0.90 [0.89–0.91]. For sleep stage classification, we fine-tuned a LSTM-based classifier to distinguish Wake, Stage 1, Stage 2, Stage 3, and REM using 5-second windows—a more granular resolution than the standard 30-second epochs, which has been shown to improve precision in certain conditions (e.g., narcolepsy [10]). As shown in Supplementary Figure 1, SleepFM performs well on Wake, Stage 2, and REM, with expected confusion in transitional stages like Stage 1—consistent with known human scoring variability. We report results across SSC, MESA, MrOS, and SHHS, where SleepFM achieves competitive performance compared to U-Sleep [7], YASA [24], GSSC [25], and STAGES [10], state-of-the-art sleep staging models, as shown in Extended Table 3 and Extended Table 4. Additionally, we compare SleepFM to three PhysioEx [26] models on the public datasets DCSM [27] and HMC [28] in a fully external validation setting, achieving an F1-score of 0.68 on DCSM—outperforming all models—and 0.55 on HMC (see Supplementary Table 1). While the source alone has little impact, using multiple datasets for pretraining and fine-tuning improves generalization, boosting macro F1 by around 0.1 (see Supplementary Tables 2, 3, and 4), consistent with prior work [26].

For sleep apnea classification, we performed patient-level severity classification to distinguish between four commonly used severity groups based on the apnea-hypopnea index (AHI): none (AHI < 5), mild ($5 \leq$ AHI < 15), moderate ($15 \leq$ AHI < 30), and severe (AHI ≥ 30). Across MESA, MrOs, and SHHS, we observe competitive performance, with a severity classification accuracy of 0.69 and a presence classification accuracy (none/mild vs. moderate/severe) of 0.87. The confusion matrix for apnea classification is shown in Figure 1.

SleepFM Enables Comprehensive Disease Prediction from Sleep Data

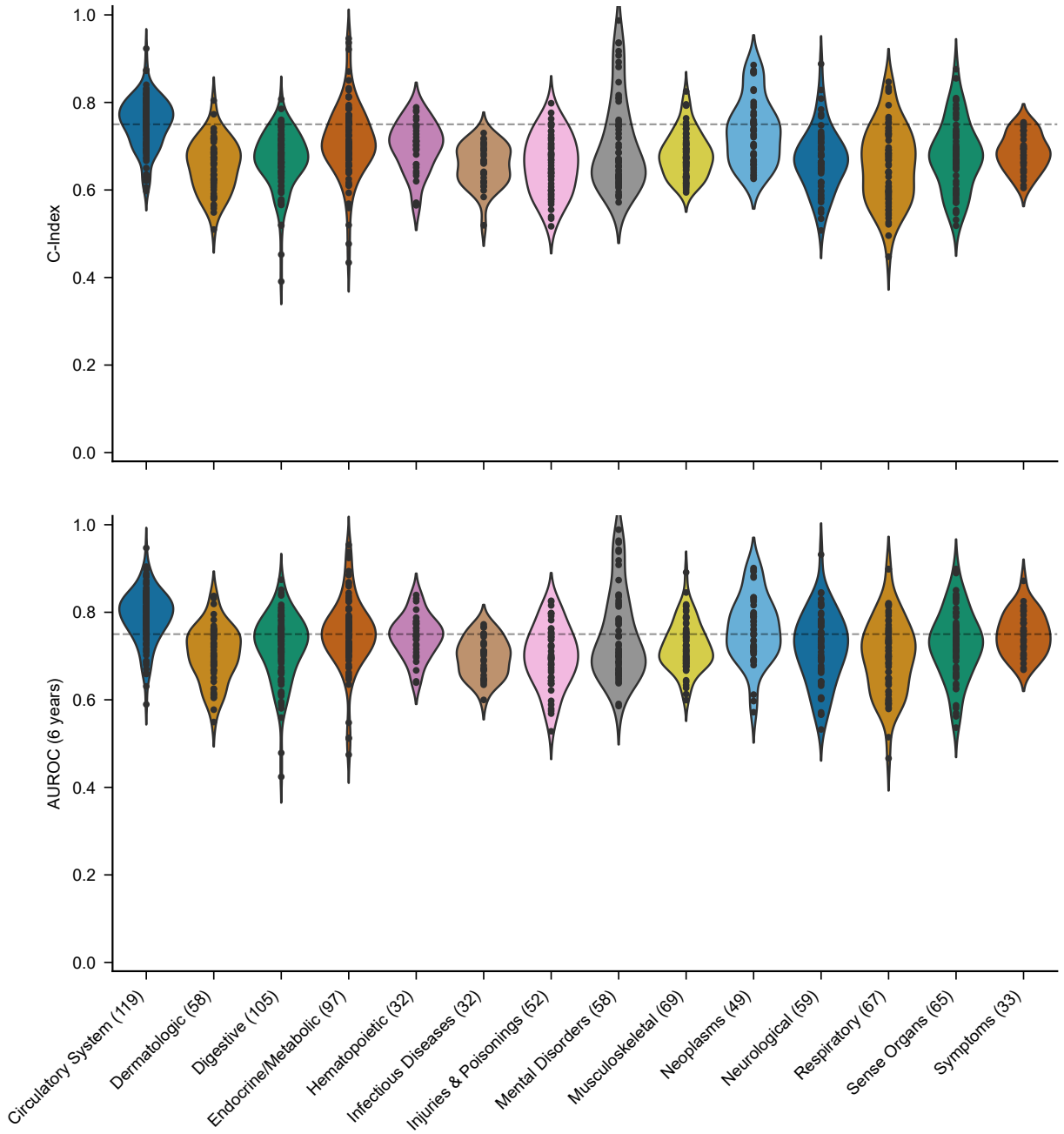

Figure 2: Performance of SleepFM on the held-out test set (n=5,019) as stratified by disease categories. Individual dots represents a disease within a category. The results are evaluated using two metrics: the C-Index, which measures the model's ability to rank patient risk accurately, and the 6-year AUROC, which assesses the model's discrimination performance by evaluating its ability to distinguish between patients who experience the event of interest and those who do not within a 6-year prediction window. For reference, the horizontal dashed line indicates a threshold of 0.75.

To enable disease prediction, we paired SSC data with EHRs, extracting all diagnostic codes (ICD-9 and ICD-10) and their timestamps. These codes were mapped to phecodes—a hierarchical system of 1,868 disease categories designed for PheWAS [29]. Each phecode's timestamp was defined as the earliest among its

corresponding ICD codes. Positive cases were defined as patients whose first phecode instance occurred more than 7 days after the sleep study, avoiding trivial associations. We excluded phecodes with prevalence below 1.5% to ensure statistical power, resulting in 1,041 phecodes for evaluation. For model fine-tuning, we used a multi-label extension of the Cox proportional hazards (CoxPH) loss, averaging independent losses computed for each label.

Figure 2 illustrates SleepFM's performance across disease categories on the test set. While performance varies across categories, SleepFM demonstrates strong results in several areas, including neoplasms, pregnancy complications, circulatory conditions, and mental disorders. Overall, 130 future diseases achieved a C-Index and AUROC of at least 0.75 on held-out participants (and Bonferroni-corrected $p < 0.01$), as summarized in Supplementary Table 5. AUROC was calculated using a six-year horizon, meaning a condition is considered positive if the patient develops the disease within six years of their PSG study. The six-year horizon for AUROC calculation was chosen to balance performance and account for both long-term and short-term conditions. Supplementary Figure 2 shows AUROC values across 1–6 year horizons for multiple conditions.

The model showed high accuracy for mild cognitive impairment (AUROC: 0.84 [0.80–0.88]), aligning with studies showing sleep disturbances as early markers of cognitive decline [30]. Strong performance was observed for Parkinson's disease (0.93 [0.89–0.96]), where sleep disorders are increasingly recognized as potential early indicators [31], and developmental delays and disorders (0.84 [0.79–0.87]). Among circulatory conditions, the model effectively predicted hypertensive heart disease (0.88 [0.85–0.91]) and intracranial hemorrhage (0.82 [0.73–0.90]), consistent with established links between sleep disorders and cardiovascular risk [32]. In the Neoplasm category, the model showed strong predictive performance for several cancers: prostate cancer (0.90 [0.87–0.93]), breast cancer (0.90 [0.86–0.93]), and melanomas of skin (0.83 [0.76–0.90]). These findings align with existing literature linking sleep patterns to cancer risk [33, 34].

Drawing on sleep expertise and prior literature, we identified 14 conditions with strong potential links to sleep patterns. Prior studies associate sleep regularity with mortality [35], prolonged sleep with early neurodegeneration [36], and sleep disturbances with dementia [37], stroke [38], and cardiovascular outcomes [9]. Related phecodes were grouped into unified disease categories in consultation with a medical doctor (see Supplementary Table 6). Results for selected conditions—including death, stroke, heart failure, and dementia—are shown in Extended Figure 2. SleepFM demonstrates strong predictive performance, with particularly high accuracy for death (AUROC: 0.84 [0.80–0.88]), heart failure (0.83 [0.79–0.86]), chronic kidney disease (0.82 [0.79–0.85]), dementia (0.87 [0.84–0.91]), and stroke (0.81 [0.78–0.85]). All reported associations are statistically significant ($p < 0.01$, Bonferroni-corrected).

To better understand the physiological basis of disease prediction, we analyzed model performance stratified by both sleep stages and signal modalities. We found that while most sleep stages contribute similarly to disease prediction, certain stages such as Stage 1/2 and REM can offer slightly better predictive power for specific conditions, including cardiovascular and neurodegenerative diseases. Likewise, different signal modalities showed nuanced differences, with BAS signals better capturing mental and neurological conditions, RESP signals more predictive of respiratory and metabolic disorders, and EKG signals more informative for circulatory diseases. While these differences align with known physiology, the overall predictive performance was highest when combining all modalities. Full results and condition-specific breakdowns are provided in Supplementary Figures 3 and 4, and Supplementary Tables 7 and 8. Additionally, we trained separate SleepFM models on each modality to directly assess modality-level importance. Performance comparisons stratified by disease category, presented in Supplementary Tables 9 and 10, further confirm that combining all modalities yields the optimal performance.

SleepFM Demonstrates Robust Generalization Across Time and cohorts

We evaluate SleepFM's generalization capabilities across temporal distribution shifts and external site validation. For temporal generalization, we test the model on a separate cohort comprising Stanford patients from 2020 onwards. All model pre-training and training was done on data prior to 2020. Despite the limited follow-up period, SleepFM maintains strong predictive performance. Extended Figure 3 shows results for our 14 selected conditions, with particularly robust and statistically significant performance (Bonferroni-corrected $p < 0.01$) for death (0.83 [0.73–0.91]), heart failure (0.80 [0.75–0.85]), and dementia (0.83 [0.76–0.89]). Comprehensive temporal-split performance across all disease phenotypes and categories is provided in Supplementary Figures 5 and 6. Supplementary Figure 7 further reports temporal-split performance comparisons with baseline models, stratified by disease category.

To assess cross-site generalization, we evaluate SleepFM's transfer learning capabilities on SHHS, a dataset entirely excluded from the pre-training phase. We use the pretrained model to extract embeddings and then

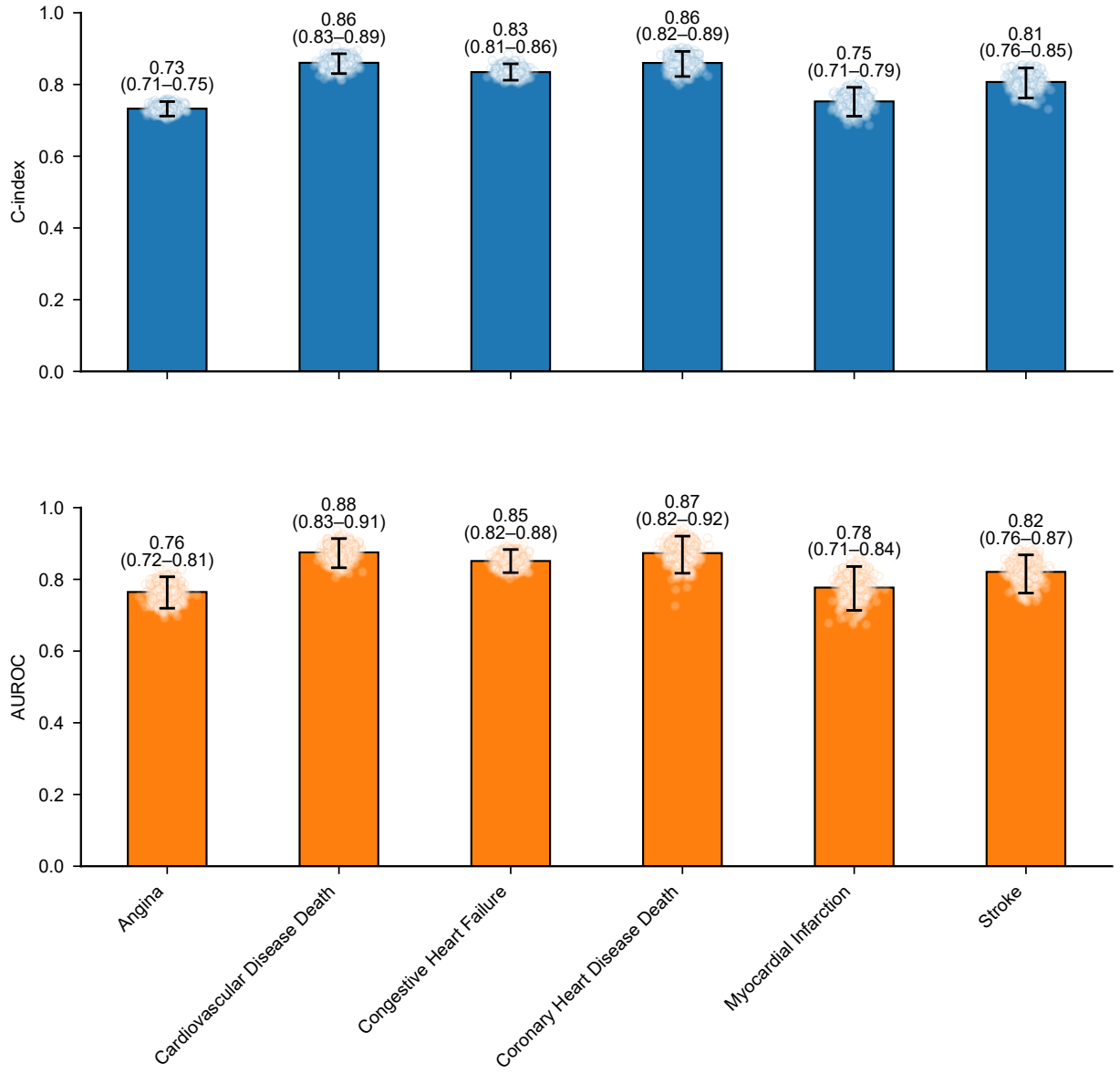

Figure 3: SleepFM prediction performance on the Sleep Heart Health Study (SHHS) test set (n=2,000 participants). Due to differences in available outcome data between SHHS and Stanford datasets, evaluation was limited to a subset of conditions. Results demonstrate transfer learning capabilities across these key clinical outcomes, including stroke, congestive heart failure, and cardiovascular disease-related mortality. Each panel uses bar plots derived from 1000 patient-level bootstrapping: faint points are individual bootstrap draws, and the vertical line with end caps marks the 95% bootstrap percentile CI. Numbers above bars report the mean. Metrics are C-index (top) and AUROC at 6 years (bottom). The number of positive samples for each outcome is as follows: Angina (704), Cardiovascular disease death (128), Congestive heart failure (190), Coronary heart disease death (80), Myocardial infarction (103), and Stroke (95). All conditions are statistically significant with a p-value < 0.01 after Bonferroni correction.

fine-tune it on a subset of SHHS. Specifically, the SHHS fine-tuning set includes 3,291 participants, and the test set includes 2,000 participants. Due to differences in task availability between SSC and SHHS, our evaluation focuses on six overlapping cardiovascular conditions. This setup mimics real-world deployment scenarios where foundation models must be adapted to new clinical sites with minimal supervision.

As shown in Figure 3, SleepFM demonstrates strong transfer learning performance across key outcomes. For example, the model achieves statistically significant predictive accuracy (Bonferroni-corrected $p < 0.01$) for stroke (0.82 [0.76–0.87]), congestive heart failure (0.85 [0.82–0.88]), and cardiovascular disease-related mortality (0.88 [0.83–0.91]).

SleepFM Surpasses Supervised Baselines in Disease Prediction

We compare SleepFM against two supervised baselines: Demographics and End-to-End PSG. The demographics baseline is a multi-layer perceptron (MLP) trained on structured clinical features (age, gender, race/ethnicity, and BMI). This baseline includes more demographic variables than the SleepFM-based models, which only use age and gender. The End-to-End PSG model is trained directly on raw PSG data using the same architecture and parameter count as SleepFM, and it includes age and gender but does not use any pretraining. From Figure 4, we observe that the percentage difference in AUROC between SleepFM and both baseline models ranges from 5% to 17%. The magnitude of improvement varies across disease categories; for example, gains are more pronounced in neurological and hematopoietic conditions, whereas in neoplasm-related conditions, the improvements are comparatively modest. Supplementary Figure 8 reports the overall test-set performance comparison between SleepFM and the baseline models across all disease phenotypes.

Next, we evaluate three different variants of SleepFM using identical training configurations, as shown in Table 2 and Extended Table 5. SleepFM-LSTM (w/o Demo) uses SleepFM embeddings with a 2-layer LSTM fine-tuning head but no demographic features. SleepFM-Linear uses SleepFM embeddings with a simple linear prediction head and includes age and gender. Finally, SleepFM-LSTM, combines the pretrained SleepFM embeddings with a 2-layer LSTM head and includes age and gender.

As seen in Table 2, the demographics-only baseline performs well, reflecting the fact that many diseases are strongly associated with age, gender, BMI, and race/ethnicity. For example, in the Neoplasm category, older age is a strong predictor of cancer risk. Nevertheless, all SleepFM-based models, including the SleepFM-LSTM (w/o Demo) variant, consistently outperform the demographics and End-to-End PSG baselines across most disease categories. This demonstrates the benefit of using pretrained SleepFM embeddings for disease prediction. Additionally, SleepFM-LSTM (w/o Demo) achieves over +5 AUROC points in 9 out of 14 conditions, while SleepFM-Linear and SleepFM-LSTM achieve over +5 AUROC points in 12 out of 14 conditions, compared to supervised demographics baseline. Importantly, as seen from the 95% CI bars, these improvements are robust, with most differences being larger than the uncertainty intervals. Finally, SleepFM-Linear performs comparably to SleepFM-LSTM, suggesting that the strength of the model lies in the pretrained embeddings rather than the complexity of the downstream head. Percentage improvement comparisons across models are provided in Supplementary Figure 9, and a scatter-plot comparison of all disease phenotypes across different fine-tuning architectures on top of SleepFM is shown in Supplementary Figure 10.

To further examine disease-specific performance, full results are provided in Supplementary Tables 11, 12, and 13, and clinician-selected conditions are presented in Supplementary Figure 11. These comparisons show that SleepFM achieves substantial gains across multiple neurological, mental, circulatory, endocrine/metabolic, and respiratory conditions. For neurological and mental disorders, SleepFM attains higher C-Index scores for senile dementia (0.99 [0.98–1.00] vs. 0.87 [0.75–0.96]), myoneural disorders (0.81 [0.73–0.88] vs. 0.42 [0.28–0.55]), and developmental delays (0.80 [0.77–0.84] vs. 0.58 [0.51–0.64]). For circulatory diseases, SleepFM outperforms in atherosclerosis (0.92 [0.88–0.95] vs. 0.74 [0.64–0.89]) and acute pulmonary heart disease (0.80 [0.75–0.85] vs. 0.74 [0.68–0.80]). Improvements in endocrine/metabolic conditions include diabetes type 2 with circulatory complications (0.87 [0.83–0.91] vs. 0.79 [0.74–0.85]) and diabetic retinopathy (0.81 [0.77–0.85] vs. 0.75 [0.69–0.80]). For respiratory conditions, SleepFM achieves higher C-Index in respiratory insufficiency (0.79 [0.72–0.85] vs. 0.59 [0.51–0.67]) and failure (0.77 [0.73–0.80] vs. 0.70 [0.65–0.74]). These findings highlight the versatility of SleepFM in predicting a broad range of diseases beyond what is captured by demographics alone.

Similarly, full comparisons with the End-to-End PSG model are provided in Supplementary Table 14. This comparison highlights the value of foundation model pre-training: although both models share similar architecture and input signals, SleepFM benefits from self-supervised pre-training, enabling more robust and

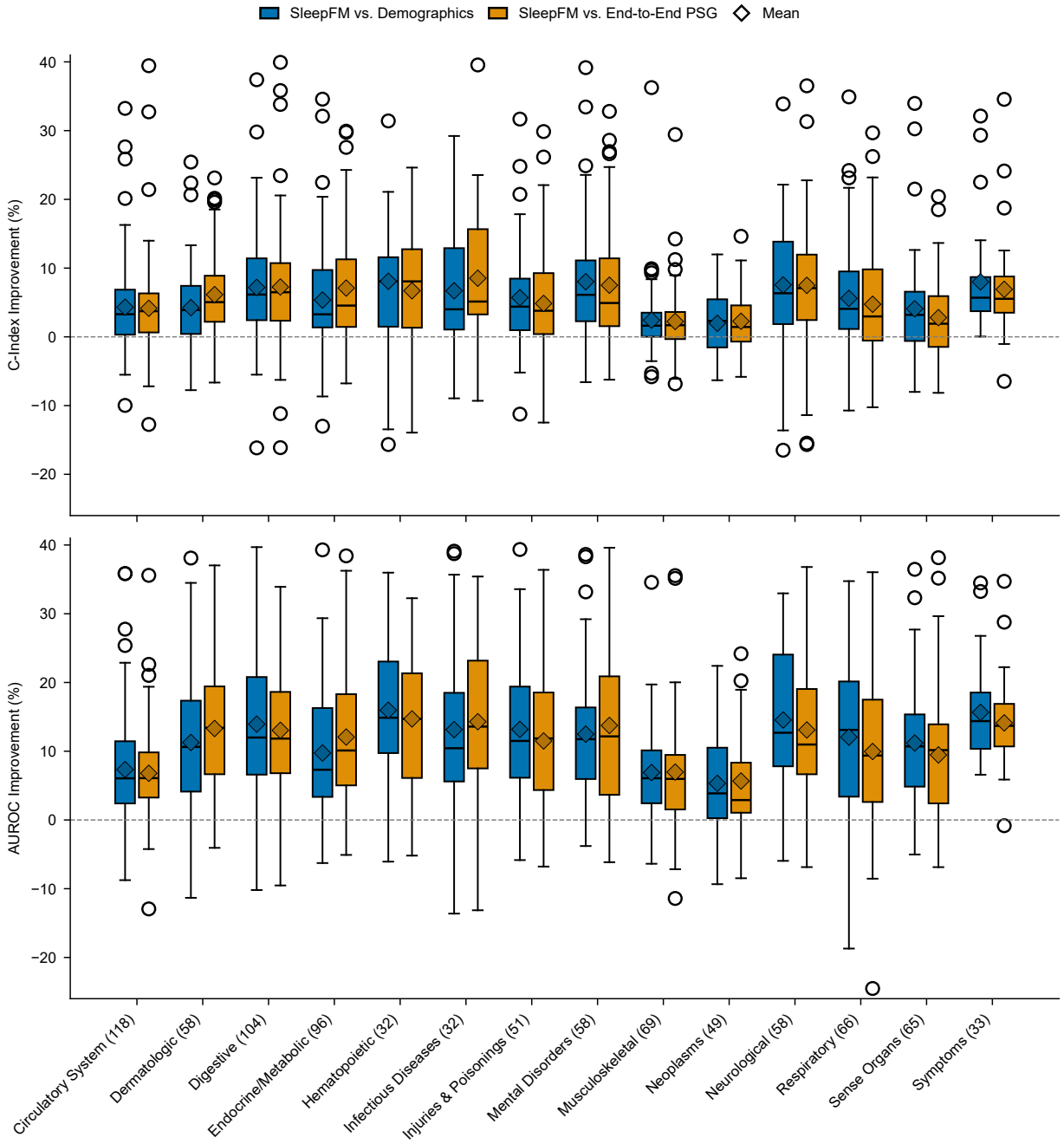

Figure 4: Performance improvements of SleepFM over baseline models across disease categories on Stanford test set (n=5,019 participants). SleepFM and the End-to-End PSG model include age and gender demographic features, whereas the demographics-only model includes age, gender, body mass index (BMI), and race/ethnicity. Each box shows the distribution of disease-level percentage improvements of SleepFM relative to each baseline within the indicated disease category. Improvements are shown for both C-index (top) and 6-year AUROC (bottom) metrics. Boxes represent the interquartile range (IQR), with whiskers extending to 1.5 × IQR and outliers shown as points. Diamonds denote the mean improvement within each category. The horizontal dashed line at zero indicates no improvement.

informative representations. This advantage is reflected in consistent performance gains across neurological, circulatory, endocrine/metabolic, and respiratory conditions. For neurological and mental disorders, SleepFM outperforms the end-to-end model in myoneural disorders (0.84 [0.75–0.91] vs. 0.54 [0.40–0.69]), developmental delays (0.84 [0.79, 0.87] vs. 0.61 [0.52, 0.69]), and speech/language disorders (0.83 [0.74, 0.90] vs. 0.71 [0.60, 0.83]). For circulatory conditions, improvements are observed in atherosclerosis of native arteries of the extremities (0.95 [0.92, 0.98] vs. 0.65 [0.61, 0.69]), atherosclerosis of the extremities (0.84 [0.75, 0.90] vs. 0.78 [0.71, 0.85]), and acute pulmonary heart disease (0.84 [0.77, 0.90] vs. 0.76 [0.69, 0.83]). In endocrine/metabolic disorders, SleepFM demonstrates stronger performance for predicting diabetes with circulatory complications (0.89 [0.85, 0.93] vs. 0.79 [0.70, 0.87]), neurological manifestations (0.86 [0.81, 0.90] vs. 0.73 [0.67, 0.78]), and diabetic retinopathy (0.84 [0.79, 0.89] vs. 0.76 [0.69, 0.82]). Respiratory conditions also benefit, with better performance in predicting respiratory insufficiency (0.82 [0.72, 0.91] vs. 0.64 [0.54, 0.73]) and respiratory failure (0.76 [0.71, 0.82] vs. 0.68 [0.62, 0.74]). In predicting all-cause mortality, SleepFM achieves a AUROC of 0.85 [0.80–0.89], outperforming both the demographic baseline and end-to-end PSG model, which achieve AUROC of 0.78 [0.72–0.82].

Finally, we compare fine-tuning scalability by evaluating SleepFM alongside two baseline models as we increase the amount of fine-tuning data and measure performance on the same test set. These results are shown in Extended Figure 4 for SHHS and Extended Figure 5 and Supplementary Figure 12 for SSC. In both plots, the key observation is that SleepFM consistently outperforms the supervised baselines, with its performance steadily improving as more data is used, remaining above the baseline curves for nearly all conditions. For SHHS, SleepFM surpasses the Demographics baseline in 5 out of 6 conditions across all data percentages, with particularly large improvements in smaller dataset splits. For example, SleepFM trained on just 10% of the data outperforms the Demographics baseline trained on five times more data across all conditions in SSC and 4 out of 6 conditions in SHHS (e.g., cardiovascular disease death, congestive heart failure, myocardial infarction, and stroke). SleepFM also outperforms the End-to-End PSG baseline in 5 out of 6 conditions, although the gap is slightly smaller than with the Demographics baseline. Importantly, SleepFM exhibits stable scaling behavior across data percentages, with smoother performance improvements, while the baseline models show greater variability.

Table 1: **Distribution of polysomnography recordings across cohorts and data splits**. The model was first pre-trained on SSC, BioSerenity, MESA, and MROS data, following which these same recordings were used for task-specific fine-tuning. The SHHS dataset is reserved exclusively for evaluating transfer learning capabilities and was used only during fine-tuning not during pre-training. The temporal test set consists of SSC recordings from 2020 onwards, used to evaluate model robustness to temporal distribution shifts. Dashes (-) indicate that no data is available for that split.

Split	**SSC**	**BioSerenity**	**MESA**	**MROS**	**SHHS**	**Total**
Train	24,137	18,869	1,747	3,340	3,291	51,384
Validation	764	100	10	18	500	1,392
Test	5,019	—	150	286	2,000	7,455
Temporal Test	5,132	—	—	—	—	5,132
Total	35,052	18,969	1,907	3,644	5,791	65,363

Discussion

This study presents a large-scale foundation model for sleep analysis, developed on over 585,000 hours of PSG data from 65,000 subjects. Our work makes several contributions. First, we address challenges in sleep analysis by leveraging self-supervised learning to train a foundation model that learns from unlabeled data and is agnostic to channel type and number, enabling broad exploration of sleep data across diverse clinical settings. Second, through extensive evaluation across 1,041 disease phenotypes, we demonstrate sleep's broad predictive power for diverse health outcomes. The model shows strong performance in predicting death (C-Index: 0.84), dementia (0.85), heart failure (0.80), and chronic kidney disease (0.79). Third, we demonstrated transfer learning capabilities through strong performance on the SHHS dataset. Despite SHHS being entirely excluded from pre-training, our model maintains robust predictive power for key outcomes such as stroke (C-Index: 0.81), congestive heart failure (0.83), and death related to cardiovascular disease (0.86). Finally, SleepFM achieves competitive performance on standard sleep analysis tasks, including sleep staging and apnea detection, with mean F1 scores ranging from 0.70 to 0.78 across cohorts—comparable to

Table 2: **Comparison of category-averaged AUROC across SleepFM variants and baselines.** Category-averaged 6-year AUROC (mean with 95% CI) comparing SleepFM variants with two baselines across disease categories on Stanford cohort (n=5,019). The Demographics baseline ("Demo") uses only structured clinical features (age, gender, BMI, and race/ethnicity). The End-to-End PSG baseline ("E2E-PSG") is trained directly on raw PSG signals with age and gender, without any pretraining. SleepFM-1 denotes SleepFM-LSTM (w/o Demo), using two LSTM layers in the fine-tuning prediction module and no demographic features. SleepFM-2 denotes SleepFM-Linear, a linear prediction module on SleepFM embeddings with age and gender. SleepFM-3 denotes SleepFM-LSTM, which uses two LSTM layers in the fine-tuning prediction module with age and gender. Values are averaged within each category across conditions. Uncertainty is estimated via nonparametric bootstrapping (n=1000 resamples): for each resample, conditions within a category are sampled with replacement and the category mean is computed; 95% CIs are the 2.5th–97.5th percentiles across resamples.

Category	Demo	E2E-PSG	SleepFM-1	SleepFM-2	SleepFM-3
Circulatory System	0.74 (0.73, 0.74)	0.74 (0.73, 0.75)	0.78 (0.77, 0.78)	0.79 (0.78, 0.80)	0.79 (0.78, 0.80)
Dermatologic	0.64 (0.63, 0.65)	0.63 (0.62, 0.64)	0.68 (0.67, 0.69)	0.71 (0.70, 0.72)	0.70 (0.70, 0.71)
Digestive	0.63 (0.62, 0.64)	0.64 (0.63, 0.65)	0.69 (0.69, 0.70)	0.72 (0.71, 0.73)	0.72 (0.71, 0.73)
Endocrine/Metabolic	0.68 (0.68, 0.69)	0.67 (0.66, 0.68)	0.74 (0.73, 0.75)	0.75 (0.74, 0.76)	0.75 (0.74, 0.76)
Hematopoietic	0.64 (0.63, 0.66)	0.66 (0.64, 0.67)	0.73 (0.72, 0.75)	0.75 (0.73, 0.76)	0.74 (0.73, 0.76)
Infectious Diseases	0.62 (0.61, 0.64)	0.62 (0.60, 0.63)	0.67 (0.65, 0.69)	0.70 (0.68, 0.71)	0.70 (0.68, 0.71)
Injuries & Poisonings	0.62 (0.61, 0.63)	0.63 (0.61, 0.64)	0.68 (0.67, 0.69)	0.70 (0.69, 0.71)	0.70 (0.69, 0.71)
Mental Disorders	0.66 (0.65, 0.67)	0.66 (0.66, 0.67)	0.72 (0.71, 0.73)	0.74 (0.73, 0.75)	0.74 (0.74, 0.75)
Musculoskeletal	0.68 (0.67, 0.68)	0.68 (0.67, 0.69)	0.70 (0.69, 0.71)	0.72 (0.72, 0.73)	0.72 (0.71, 0.73)
Neoplasms	0.73 (0.71, 0.74)	0.73 (0.71, 0.74)	0.73 (0.72, 0.74)	0.76 (0.75, 0.77)	0.76 (0.75, 0.77)
Neurological	0.62 (0.61, 0.63)	0.63 (0.62, 0.64)	0.70 (0.69, 0.71)	0.72 (0.71, 0.73)	0.72 (0.71, 0.73)
Respiratory	0.63 (0.62, 0.64)	0.64 (0.63, 0.65)	0.69 (0.68, 0.70)	0.69 (0.69, 0.70)	0.70 (0.69, 0.71)
Sense Organs	0.66 (0.65, 0.67)	0.67 (0.66, 0.68)	0.71 (0.70, 0.72)	0.73 (0.72, 0.74)	0.73 (0.72, 0.74)
Symptoms	0.65 (0.64, 0.66)	0.66 (0.64, 0.67)	0.72 (0.71, 0.73)	0.75 (0.74, 0.76)	0.75 (0.74, 0.76)

state-of-the-art models such as U-Sleep [7], GSSC [25], STAGES [10], and YASA [24]. Additionally, in a fully external validation setting, SleepFM outperforms all models on DCSM (F1 = 0.68) and is competitive with the PhysioEx [26] models. For apnea classification, SleepFM achieves 87% accuracy in MESA, MrOS, and SHHS, comparable to state-of-the-art [8].

SleepFM predicts all-cause mortality more accurately than both the demographics-based model and the end-to-end PSG model, achieving a higher C-Index of 0.84 [0.81–0.87], compared to 0.79 [0.75–0.82]. This indicates that pre-training efficiently captures subtle mortality-related signals in the PSG data. Research shows strong association between all-cause mortality and sleep-related factors, including high arousal burden [39], low REM sleep [40], sleep-disordered breathing [41], hypoxemia, and low sleep efficiency [42]. Increased "brain age" derived from EEG has also been identified as a significant predictor of mortality [3]. SleepFM likely integrates these multifactorial contributors, capturing respiratory events, sleep fragmentation, arousal burden, and sleep efficiency, along with markers of cardiovascular, metabolic, and other diseases.

Predictive and prognostic models for neurological and mental disorders are rapidly advancing, offering the potential for earlier and more individualized treatment. Among the top conditions predicted by SleepFM were Alzheimer's disease and Parkinson's disease, with C-indices of 0.91 [0.87–0.98] and 0.89 [0.85–0.92], respectively. Sleep disorders are strongly associated with preclinical Alzheimer's disease [43], including abnormalities in Non-REM sleep, such as reduced slow-wave activity [44], REM sleep disturbances [45], and decreased spindle activity [46]. In early Alzheimer's disease, REM sleep abnormalities have been linked to basal forebrain cholinergic lesions, which likely contribute to cognitive decline [47]. Similarly, Parkinson's disease is frequently preceded by REM sleep behavior disorder (RBD), characterized by REM sleep without atonia and abnormalities in BAS and ECG patterns [48]. Recent studies have also shown that respiratory signals can capture phenotypes specific to Parkinson's disease [49].

Consistent with these findings, SleepFM identified BAS as the strongest predictor of neurological and mental disorders, while respiratory signals were particularly effective in predicting senile dementia. Most studies in this domain rely on imaging modalities such as MRI and fMRI to predict dementia. For example, one study

using hippocampal MRI achieved a C-index of 0.86 [50], while another using fMRI reported an AUROC of 0.82 for predicting dementia up to nine years in advance [51]. Although direct performance comparisons are challenging due to differences in sample distributions, the ability of SleepFM to leverage PSG data to predict neurological and mental disorders underscores its potential as an alternative to imaging-based approaches.

Other established biomarkers for Alzheimer's disease—such as amyloid PET, decreased CSF β-amyloid$_{42}$, and increased CSF phosphorylated tau (e.g., p-tau$_{129}$) [52, 53]—have been widely used for diagnosis and prognosis. More recently, plasma p-tau$_{217}$ has emerged as a promising less invasive marker [54]. Sleep biomarkers from PSG data offer a complementary, non-invasive tool for the prognosis of dementia and mild cognitive impairment.

SleepFM accurately modeled cardiovascular disease in both the SSC and SHHS datasets, leveraging data-driven methods commonly used in prognostic modeling of cardiovascular disease, particularly with ECG data [55] and lead II ECG from PSG studies [9]. Foundation models have demonstrated state-of-the-art performance with ECG data in various cross-sectional tasks [15]. For predicting cardiovascular mortality over 10 years, a previous study reported an AUROC of 0.84 [0.78–0.89] in a subset of SHHS participants with sleep apnea, whereas SleepFM achieved a slightly higher AUROC of 0.88 [0.83–0.91]. Similarly, for atrial fibrillation, earlier work reported an AUROC of 0.82 [9], which aligns with SleepFM's performance of 0.81 [0.78–0.84]. Our ablation study further demonstrated that both ECG and respiratory signals contribute to the prediction of circulatory system phenotypes, suggesting that SleepFM integrates information on sleep apnea and heart activity in ways that are consistent with known disease mechanisms [56].

Most disease categories, including neurological, circulatory, hematopoietic, mental disorders, and endocrine/metabolic, were predicted with significantly improved performance by SleepFM compared to the demographics-based and end-to-end PSG baseline models. Many of these diseases are either associated with sleep (e.g., type 2 diabetes [57]) or directly influenced by the signal modalities (e.g., heart arrhythmia). Disrupted and unhealthy sleep contributes to dysfunction across multiple physiological systems, increasing the risk of diseases such as obesity, type 2 diabetes, hypertension, stroke, and cardiovascular disease [58]. Sleep-specific conditions, including sleep apnea [56] and less conclusively periodic leg movements [59], are also linked to cardiovascular outcomes. Additionally, specific EEG waveforms, such as coupled slow-wave and spindle activity, have been identified as markers of next-day blood glucose regulation [60].

Despite these promising results, several limitations should be acknowledged. While our dataset is large, it primarily consists of patients referred for sleep studies due to suspected sleep disorders or other medical conditions requiring overnight monitoring. This selection bias means our cohort is not representative of the general population, as individuals without sleep complaints or those with limited access to specialized sleep clinics are underrepresented. The model's performance shows some degradation in temporal test sets, highlighting the challenge of maintaining predictive accuracy over time as clinical practices and patient populations evolve. Additionally, interpreting the predictions made by SleepFM is inherently challenging due to the complexity of the learned features during training by a deep model. To mitigate this, we stratified the model's performance across sleep stages and data modalities, and conducted evaluations on temporal test sets and unseen datasets to gain insights into its behavior. However, further work is needed to enhance case-level interpretability and understand the specific sleep patterns and features driving these predictions.

In building our model, we selected hyperparameters for SleepFM based on prior work and ensured all training converged in loss; more extensive hyperparameter searches may further boost performance. Furthermore, while we evaluated SleepFM's transfer learning performance on an independent dataset, SHHS, only a subset of the full 1,041 conditions could be assessed in this sample due to limited diagnostic overlap with SSC; this prevented a comprehensive evaluation of generalization across the full spectrum of diseases. Our sleep apnea analysis was limited to binary and four-class classification based on AHI thresholds; we did not explore more granular formulations such as AHI regression or event detection, we leave this for future research. Similarly, while SleepFM achieves competitive results on sleep staging tasks across most datasets, it lags behind specialized sleep staging models on certain external validation datasets (e.g., HMC). Further specialized modeling may be necessary to optimize SleepFM for sleep staging.

This study underscores the potential of sleep-based foundation models for risk stratification and longitudinal health monitoring. By integrating multiple physiological signals and leveraging large-scale pretraining, SleepFM performs consistently well across diverse disease categories and outperforms supervised baselines. Its stable performance across fine-tuning splits suggests that pretraining may improve model generalizability, particularly in clinical contexts with limited labeled data. These results suggest that SleepFM can complement existing risk assessment tools and help identify early signs of diseases. As wearable sleep technologies continue to advance, models like SleepFM may offer opportunities for non-invasive, real-time health monitoring. Future

efforts should explore how combining sleep-based models with data from electronic health records, omics, and imaging can further enhance their utility.

Acknowledgements

The Multi-Ethnic Study of Atherosclerosis (MESA) Sleep Ancillary study was funded by NIH-NHLBI Association of Sleep Disorders with Cardiovascular Health Across Ethnic Groups (RO1 HL098433). MESA is supported by NHLBI funded contracts HHSN268201500003I, N01-HC-95159, N01-HC-95160, N01-HC-95161, N01-HC-95162, N01-HC-95163, N01-HC-95164, N01-HC-95165, N01-HC-95166, N01-HC-95167, N01-HC-95168 and N01-HC-95169 from the National Heart, Lung, and Blood Institute, and by cooperative agreements UL1-TR-000040, UL1-TR-001079, and UL1-TR-001420 funded by NCATS. The National Sleep Research Resource was supported by the National Heart, Lung, and Blood Institute (R24 HL114473, 75N92019R002).

The National Heart, Lung, and Blood Institute provided funding for the ancillary MrOS Sleep Study, "Outcomes of Sleep Disorders in Older Men," under the following grant numbers: R01 HL071194, R01 HL070848, R01 HL070847, R01 HL070842, R01 HL070841, R01 HL070837, R01 HL070838, and R01 HL070839. The National Sleep Research Resource was supported by the National Heart, Lung, and Blood Institute (R24 HL114473, 75N92019R002).

The Sleep Heart Health Study (SHHS) was supported by National Heart, Lung, and Blood Institute cooperative agreements U01HL53916 (University of California, Davis), U01HL53931 (New York University), U01HL53934 (University of Minnesota), U01HL53937 and U01HL64360 (Johns Hopkins University), U01HL53938 (University of Arizona), U01HL53940 (University of Washington), U01HL53941 (Boston University), and U01HL63463 (Case Western Reserve University). The National Sleep Research Resource was supported by the National Heart, Lung, and Blood Institute (R24 HL114473, 75N92019R002).

R.T. is supported by the Knight-Hennessy Scholars funding. E.M. and B.W. are supported by a grant from the National Heart, Lung, and Blood Institute of the NIH (R01HL161253). J.Z. is supported by funding from the Chan-Zuckerberg Biohub.

We would also like to acknowledge Ethan Steinberg for his valuable insights into survival analysis.

Author Contributions Statement

R.T. and M.R.K. contributed equally to brainstorming the project, running experiments, and writing the manuscript. B.H., I.C., P.J., A.B.K., and B.W. provided high-level brainstorming and contributed to writing and editing the paper. U.H., G.G. and H.M. assisted with data access. E.M. and J.Z., as senior co-authors, conceived the project and provided overall guidance. All authors reviewed and approved the final manuscript.

Competing Interests Statement

B.W. is a co-founder, scientific advisor, consultant to, and has personal equity interest in Beacon Biosignals. The remaining authors declare no competing interests.

References

[1] Richard B Berry, Rita Brooks, Charlene E Gamaldo, Susan M Harding, C Marcus, Bradley V Vaughn, et al. The AASM manual for the scoring of sleep and associated events. *Rules, Terminology and Technical Specifications, Darien, Illinois, American Academy of Sleep Medicine*, 176:2012, 2012.

[2] Meir H Kryger, Thomas Roth, and William C Dement. Principles and practice of sleep medicine fifth edition, 2010.

[3] Andreas Brink-Kjaer, Eileen B Leary, Haoqi Sun, M Brandon Westover, Katie L Stone, Paul E Peppard, Nancy E Lane, Peggy M Cawthon, Susan Redline, Poul Jennum, et al. Age estimation from sleep studies using deep learning predicts life expectancy. *NPJ Digital Medicine*, 5(1):103, 2022.

[4] Dieter Riemann. Insomnia and comorbid psychiatric disorders. *Sleep medicine*, 8:S15–S20, 2007.

[5] Claire André, Stéphane Rehel, Elizabeth Kuhn, Brigitte Landeau, Inès Moulinet, Edelweiss Touron, Valentin Ourry, Gwendoline Le Du, Florence Mézenge, Clémence Tomadesso, et al. Association of sleep-disordered breathing with alzheimer disease biomarkers in community-dwelling older adults: a secondary analysis of a randomized clinical trial. *JAMA Neurology*, 77(6):716–724, 2020.

[6] Prince Nii Ossah Addo, Paddington T Mundagowa, Longgang Zhao, Mufaro Kanyangarara, Monique J Brown, and Jihong Liu. Associations between sleep duration, sleep disturbance and cardiovascular disease biomarkers among adults in the united states. *BMC Public Health*, 24(1):947, 2024.

[7] Mathias Perslev, Sune Darkner, Lykke Kempfner, Miki Nikolic, Poul Jørgen Jennum, and Christian Igel. U-sleep: resilient high-frequency sleep staging. *NPJ Digital Medicine*, 4(1):72, 2021.

[8] Thijs E Nassi, Wolfgang Ganglberger, Haoqi Sun, Abigail A Bucklin, Siddharth Biswal, Michel JAM van Putten, Robert J Thomas, and M Brandon Westover. Automated scoring of respiratory events in sleep with a single effort belt and deep neural networks. *IEEE transactions on biomedical engineering*, 69(6):2094–2104, 2021.

[9] Zuzana Koscova, Ali Bahrami Rad, Samaneh Nasiri, Matthew A. Reyna, Reza Sameni, Lynn M. Trotti, Haoqi Sun, Niels Turley, Katie L. Stone, Robert J. Thomas, Emmanuel Mignot, Brandon Westover, and Gari D. Clifford. From sleep patterns to heart rhythm: Predicting atrial fibrillation from overnight polysomnograms. *Journal of Electrocardiology*, 86:153759, 2024.

[10] Jens B Stephansen, Alexander N Olesen, Mads Olsen, Aditya Ambati, Eileen B Leary, Hyatt E Moore, Oscar Carrillo, Ling Lin, Fang Han, Han Yan, et al. Neural network analysis of sleep stages enables efficient diagnosis of narcolepsy. *Nature Communications*, 9(1):5229, 2018.

[11] Rahul Thapa, Bryan He, Magnus Ruud Kjær, Hyatt Moore, Gauri Ganjoo, Emmanuel Mignot, and James Zou. Sleepfm: multi-modal representation learning for sleep across brain activity, ecg and respiratory signals. In *Proceedings of the 41st International Conference on Machine Learning*, ICML'24. JMLR.org, 2024.

[12] Rishi Bommasani, Drew A. Hudson, Ehsan Adeli, Russ Altman, Simran Arora, Sydney von Arx, Michael S. Bernstein, Jeannette Bohg, Antoine Bosselut, Emma Brunskill, Erik Brynjolfsson, S. Buch, Dallas Card, Rodrigo Castellon, Niladri S. Chatterji, Annie S. Chen, Kathleen A. Creel, Jared Davis, Dora Demszky, Chris Donahue, Moussa Doumbouya, Esin Durmus, Stefano Ermon, John Etchemendy, Kawin Ethayarajh, Li Fei-Fei, Chelsea Finn, Trevor Gale, Lauren E. Gillespie, Karan Goel, Noah D. Goodman, Shelby Grossman, Neel Guha, Tatsunori Hashimoto, Peter Henderson, John Hewitt, Daniel E. Ho, Jenny Hong, Kyle Hsu, Jing Huang, Thomas F. Icard, Saahil Jain, Dan Jurafsky, Pratyusha Kalluri, Siddharth Karamcheti, Geoff Keeling, Fereshte Khani, O. Khattab, Pang Wei Koh, Mark S. Krass, Ranjay Krishna, Rohith Kuditipudi, Ananya Kumar, Faisal Ladhak, Mina Lee, Tony Lee, Jure Leskovec, Isabelle Levent, Xiang Lisa Li, Xuechen Li, Tengyu Ma, Ali Malik, Christopher D. Manning, Suvir P. Mirchandani, Eric Mitchell, Zanele Munyikwa, Suraj Nair, Avanika Narayan, Deepak Narayanan, Benjamin Newman, Allen Nie, Juan Carlos Niebles, Hamed Nilforoshan, J. F. Nyarko, Giray Ogut, Laurel Orr, Isabel Papadimitriou, Joon Sung Park, Chris Piech, Eva Portelance, Christopher Potts, Aditi Raghunathan, Robert Reich, Hongyu Ren, Frieda Rong, Yusuf H. Roohani, Camilo Ruiz, Jack Ryan, Christopher R'e, Dorsa Sadigh, Shiori Sagawa, Keshav Santhanam, Andy Shih, Krishna Parasuram Srinivasan, Alex Tamkin, Rohan Taori, Armin W. Thomas, Florian Tramèr, Rose E. Wang, William Wang, Bohan Wu, Jiajun Wu, Yuhuai Wu, Sang Michael Xie, Michihiro Yasunaga, Jiaxuan You, Matei A. Zaharia, Michael Zhang, Tianyi Zhang, Xikun Zhang, Yuhui Zhang, Lucia Zheng, Kaitlyn Zhou, and Percy Liang. On the opportunities and risks of foundation models. *ArXiv*, 2021.

[13] Khaled Saab, Tao Tu, Wei-Hung Weng, Ryutaro Tanno, David Stutz, Ellery Wulczyn, Fan Zhang, Tim Strother, Chunjong Park, Elahe Vedadi, et al. Capabilities of Gemini models in medicine. *arXiv preprint arXiv:2404.18416*, 2024.

[14] Theodore Zhao, Yu Gu, Jianwei Yang, Naoto Usuyama, Ho Hin Lee, Sid Kiblawi, Tristan Naumann, Jianfeng Gao, Angela Crabtree, Jacob Abel, et al. A foundation model for joint segmentation, detection and recognition of biomedical objects across nine modalities. *Nature methods*, 22(1):166–176, 2025.

[15] Shaoting Zhang, Yishan Du, Wenji Wang, Xianying He, Fangfang Cui, Liang Zhao, Bei Wang, Zhiqiang Hu, Ziqiang Wang, Qing Xia, Tian Shen, and Jie Zhao. Ecgfm: A foundation model for ecg analysis trained on a multi-center million-ecg dataset. *Information Fusion*, 124:103363, 2025.

[16] Wenhui Cui, Woojae Jeong, Philipp Thölke, Takfarinas Medani, Karim Jerbi, Anand A Joshi, and Richard M Leahy. Neuro-gpt: Towards a foundation model for eeg. In *2024 IEEE International Symposium on Biomedical Imaging (ISBI)*, pages 1–5. IEEE, 2024.

[17] SA Pendergrass, K Brown-Gentry, SM Dudek, ES Torstenson, JL Ambite, CL Avery, S Buyske, C Cai, MD Fesinmeyer, C Haiman, et al. The use of phenome-wide association studies (PheWAS) for exploration of novel genotype-phenotype relationships and pleiotropy discovery. *Genetic epidemiology*, 35(5):410–422, 2011.

[18] Umaer Hanif, Ulysse Gimenez, Alyssa Cairns, Daniel Lewin, Nisar Ashraf, and Emmanuel Mignot. Automatic detection of chronic insomnia from polysomnographic and clinical variables using machine learning. In *2023 45th Annual International Conference of the IEEE Engineering in Medicine & Biology Society (EMBC)*, pages 1–5. IEEE, 2023.

[19] Umaer Hanif, Alyssa Cairns, Vincent Mysliwiec, Ruggero G Bettinardi, Maxime Elbaz, Ulysse Gimenez, and Emmanuel JM Mignot. Associations between self-reported parasomnias and psychiatric illness in 370,000 patients with sleep disorders. *Psychiatry and Clinical Neurosciences*, 78(11):667–677, 2024.

[20] Guo-Qiang Zhang, Licong Cui, Remo Mueller, Shiqiang Tao, Matthew Kim, Michael Rueschman, Sara Mariani, Daniel Mobley, and Susan Redline. The national sleep research resource: towards a sleep data commons. *Journal of the American Medical Informatics Association*, 25(10):1351–1358, 2018.

[21] Xiaoli Chen, Rui Wang, Phyllis Zee, Pamela L Lutsey, Sogol Javaheri, Carmela Alcántara, Chandra L Jackson, Michelle A Williams, and Susan Redline. Racial/ethnic differences in sleep disturbances: the multi-ethnic study of atherosclerosis (MESA). *Sleep*, 38(6):877–888, 2015.

[22] Terri Blackwell, Kristine Yaffe, Sonia Ancoli-Israel, Susan Redline, Kristine E Ensrud, Marcia L Stefanick, Alison Laffan, Katie L Stone, and Osteoporotic Fractures in Men Study Group. Associations between sleep architecture and sleep-disordered breathing and cognition in older community-dwelling men: the osteoporotic fractures in men sleep study. *Journal of the American Geriatrics Society*, 59(12):2217–2225, 2011.

[23] Stuart F Quan, Barbara V Howard, Conrad Iber, James P Kiley, F Javier Nieto, George T O'Connor, David M Rapoport, Susan Redline, John Robbins, Jonathan M Samet, et al. The sleep heart health study: design, rationale, and methods. *Sleep*, 20(12):1077–1085, 1997.

[24] Raphael Vallat and Matthew P Walker. An open-source, high-performance tool for automated sleep staging. *Elife*, 10:e70092, 2021.

[25] Jevri Hanna and Agnes Flöel. An accessible and versatile deep learning-based sleep stage classifier. *Frontiers in Neuroinformatics*, 17:1086634, 2023.

[26] Guido Gagliardi, Luca Alfeo, Mario GCA Cimino, Gaetano Valenza, and Maarten De Vos. Physioex, a new python library for explainable sleep staging through deep learning. *Physiological Measurement*, 2025.

[27] Mathias Perslev, Sune Darkner, Jacob Kempfner, Mladen Nikolic, Poul J. Jennum, and Christian Igel. DCSM Sleep Staging Dataset. `https://erda.ku.dk/public/archives/db553715ecbe1f3ac66c1dc569826eef/published-archive.html`, 2021. Data set, University of Copenhagen.

[28] Diego Alvarez-Estevez and Roselyne Rijsman. Haaglanden Medisch Centrum Sleep Staging Database (version 1.1). `https://doi.org/10.13026/t79q-fr32`, 2022. PhysioNet, Data set.

[29] Patrick Wu, Aliya Gifford, Xiangrui Meng, Xue Li, Harry Campbell, Tim Varley, Juan Zhao, Robert Carroll, Lisa Bastarache, Joshua C Denny, et al. Mapping ICD-10 and ICD-10-CM codes to phecodes: workflow development and initial evaluation. *JMIR medical informatics*, 7(4):e14325, 2019.

[30] Alexandra MV Wennberg, Mark N Wu, Paul B Rosenberg, and Adam P Spira. Sleep disturbance, cognitive decline, and dementia: a review. In *Seminars in neurology*, volume 37, pages 395–406. Thieme Medical Publishers, 2017.

[31] Ambra Stefani and Birgit Högl. Sleep in parkinson's disease. *Neuropsychopharmacology*, 45(1):121–128, 2020.

[32] Rakshana Ravichandran, Lovish Gupta, Mansi Singh, Aiswarya Nag, Jingle Thomas, and Binay K Panjiyar. The interplay between sleep disorders and cardiovascular diseases: A systematic review. *Cureus*, 15(9), 2023.

[33] Maryssa Shigesato, Yosuke Kawai, Cherie Guillermo, Fadi Youkhana, Yurii B Shvetsov, Veronica W Setiawan, Christopher A Haiman, Loïc Le Marchand, and Gertraud Maskarinec. Association between sleep duration and breast cancer incidence: the multiethnic cohort. *International journal of cancer*, 146(3):664–670, 2020.

[34] Joshua R Freeman, Pedro F Saint-Maurice, Eleanor L Watts, Steven C Moore, Marissa M Shams-White, Dana L Wolff-Hughes, Daniel E Russ, Jonas S Almeida, Neil E Caporaso, Hyokyoung G Hong, et al. Actigraphy-derived measures of sleep and risk of prostate cancer in the uk biobank. *JNCI: Journal of the National Cancer Institute*, 116(3):434–444, 2024.

[35] Daniel P Windred, Angus C Burns, Jacqueline M Lane, Richa Saxena, Martin K Rutter, Sean W Cain, and Andrew JK Phillips. Sleep regularity is a stronger predictor of mortality risk than sleep duration: A prospective cohort study. *Sleep*, 47(1):zsad253, 2024.

[36] Andrew J Westwood, Alexa Beiser, Nikita Jain, Jayandra J Himali, Charles DeCarli, Sanford H Auerbach, Matthew P Pase, and Sudha Seshadri. Prolonged sleep duration as a marker of early neurodegeneration predicting incident dementia. *Neurology*, 88(12):1172–1179, 2017.

[37] Le Shi, Si-Jing Chen, Meng-Ying Ma, Yan-Ping Bao, Ying Han, Yu-Mei Wang, Jie Shi, Michael V Vitiello, and Lin Lu. Sleep disturbances increase the risk of dementia: a systematic review and meta-analysis. *Sleep medicine reviews*, 40:4–16, 2018.

[38] Christine Eileen Mc Carthy, Salim Yusuf, Conor Judge, Alberto Alvarez-Iglesias, Graeme J Hankey, Shahram Oveisgharan, Albertino Damasceno, Helle Klingenberg Iversen, Annika Rosengren, Alvaro Avezum, et al. Sleep patterns and the risk of acute stroke: results from the interstroke international case-control study. *Neurology*, 100(21):e2191–e2203, 2023.

[39] Sobhan Salari Shahrbabaki, Dominik Linz, Simon Hartmann, Susan Redline, and Mathias Baumert. Sleep arousal burden is associated with long-term all-cause and cardiovascular mortality in 8001 community-dwelling older men and women. *European heart journal*, 42(21):2088–2099, 2021.

[40] Eileen B Leary, Kathleen T Watson, Sonia Ancoli-Israel, Susan Redline, Kristine Yaffe, Laurel A Ravelo, Paul E Peppard, James Zou, Steven N Goodman, Emmanuel Mignot, et al. Association of rapid eye movement sleep with mortality in middle-aged and older adults. *JAMA neurology*, 77(10):1241–1251, 2020.

[41] Terry Young, Laurel Finn, Paul E Peppard, Mariana Szklo-Coxe, Diane Austin, F Javier Nieto, Robin Stubbs, and K Mae Hla. Sleep disordered breathing and mortality: eighteen-year follow-up of the wisconsin sleep cohort. *Sleep*, 31(8):1071–1078, 2008.

[42] Meredith L Wallace, Timothy S Coleman, Lucas K Mentch, Daniel J Buysse, Jessica L Graves, Erika W Hagen, Martica H Hall, Katie L Stone, Susan Redline, and Paul E Peppard. Physiological sleep measures predict time to 15-year mortality in community adults: application of a novel machine learning framework. *Journal of sleep research*, 30(6):e13386, 2021.

[43] Omonigho M Bubu, Michael Brannick, James Mortimer, Ogie Umasabor-Bubu, Yuri V Sebastião, Yi Wen, Skai Schwartz, Amy R Borenstein, Yougui Wu, David Morgan, et al. Sleep, cognitive impairment, and alzheimer's disease: a systematic review and meta-analysis. *Sleep*, 40(1):zsw032, 2017.

[44] Yo-El S Ju, Sharon J Ooms, Courtney Sutphen, Shannon L Macauley, Margaret A Zangrilli, Gina Jerome, Anne M Fagan, Emmanuel Mignot, John M Zempel, Jurgen AHR Claassen, et al. Slow wave sleep disruption increases cerebrospinal fluid amyloid-β levels. *Brain*, 140(8):2104–2111, 2017.

[45] Neus Falgàs and Christine M Walsh. The importance of rem sleep and its implications for alzheimer's disease, 2024.

[46] Yuan-Yuan Weng, Xu Lei, and Jing Yu. Sleep spindle abnormalities related to alzheimer's disease: a systematic mini-review. *Sleep medicine*, 75:37–44, 2020.

[47] Claire André, Marie-Ève Martineau-Dussault, Véronique Daneault, Hélène Blais, Sonia Frenette, Dominique Lorrain, Carol Hudon, Célyne Bastien, Dominique Petit, Alexandre Lafrenière, et al. Rem sleep is associated with the volume of the cholinergic basal forebrain in amci individuals. *Alzheimer's Research & Therapy*, 15(1):151, 2023.

[48] Andreas Brink-Kjaer, Katarina Mary Gunter, Emmanuel Mignot, Emmanuel During, Poul Jennum, and Helge BD Sorensen. End-to-end deep learning of polysomnograms for classification of rem sleep behavior disorder. In *2022 44th Annual International Conference of the IEEE Engineering in Medicine & Biology Society (EMBC)*, pages 2941–2944. IEEE, 2022.

[49] Yuzhe Yang, Yuan Yuan, Guo Zhang, Hao Wang, Ying-Cong Chen, Yingcheng Liu, Christopher G Tarolli, Daniel Crepeau, Jan Bukartyk, Mithri R Junna, et al. Artificial intelligence-enabled detection and assessment of parkinson's disease using nocturnal breathing signals. *Nature medicine*, 28(10):2207–2215, 2022.

[50] Hongming Li, Mohamad Habes, David A Wolk, Yong Fan, Alzheimer's Disease Neuroimaging Initiative, et al. A deep learning model for early prediction of alzheimer's disease dementia based on hippocampal magnetic resonance imaging data. *Alzheimer's & Dementia*, 15(8):1059–1070, 2019.

[51] Sam Ereira, Sheena Waters, Adeel Razi, and Charles R Marshall. Early detection of dementia with default-mode network effective connectivity. *Nature Mental Health*, pages 1–14, 2024.

[52] Oskar Hansson, Henrik Zetterberg, Peder Buchhave, Elisabet Londos, Kaj Blennow, and Lennart Minthon. Association between csf biomarkers and incipient alzheimer's disease in patients with mild cognitive impairment: a follow-up study. *The Lancet Neurology*, 5(3):228–234, 2006.

[53] William E Klunk, Henry Engler, Agneta Nordberg, Yanming Wang, Gunnar Blomqvist, Daniel P Holt, Mats Bergström, Irina Savitcheva, Guo-Feng Huang, Sergio Estrada, et al. Imaging brain amyloid in alzheimer's disease with pittsburgh compound-b. *Annals of Neurology: Official Journal of the American Neurological Association and the Child Neurology Society*, 55(3):306–319, 2004.

[54] Shorena Janelidze, Niklas Mattsson, Sebastian Palmqvist, Ruben Smith, Thomas G Beach, Geidy E Serrano, Xiyun Chai, Nicholas K Proctor, Udo Eichenlaub, Henrik Zetterberg, et al. Plasma p-tau181 in alzheimer's disease: relationship to other biomarkers, differential diagnosis, neuropathology and longitudinal progression to alzheimer's dementia. *Nature medicine*, 26(3):379–386, 2020.

[55] Pedro A Moreno-Sánchez, Guadalupe García-Isla, Valentina DA Corino, Antti Vehkaoja, Kirsten Brukamp, Mark van Gils, and Luca Mainardi. Ecg-based data-driven solutions for diagnosis and prognosis of cardiovascular diseases: A systematic review. *Computers in Biology and Medicine*, page 108235, 2024.

[56] Amal K Mitra, Azad R Bhuiyan, and Elizabeth A Jones. Association and risk factors for obstructive sleep apnea and cardiovascular diseases: a systematic review. *Diseases*, 9(4):88, 2021.

[57] Mark TU Barone and Luiz Menna-Barreto. Diabetes and sleep: a complex cause-and-effect relationship. *Diabetes research and clinical practice*, 91(2):129–137, 2011.

[58] Chao Yang, Peijing Yan, Xueyao Wu, Wenqiang Zhang, Huijie Cui, Li Zhang, Zhengxing Xu, Shanshan Peng, Mingshuang Tang, Yutong Wang, et al. Associations of sleep with cardiometabolic risk factors and cardiovascular diseases: an umbrella review of observational and mendelian randomization studies. *Sleep Medicine Reviews*, page 101965, 2024.

[59] Michela Figorilli, Monica Puligheddu, Patrizia Congiu, and Raffaele Ferri. The clinical importance of periodic leg movements in sleep. *Current treatment options in neurology*, 19:1–15, 2017.

[60] Raphael Vallat, Vyoma D Shah, and Matthew P Walker. Coordinated human sleeping brainwaves map peripheral body glucose homeostasis. *Cell Reports Medicine*, 4(7), 2023.

Methods

Dataset and Preprocessing

Our dataset includes PSG recordings from four different sites: SSC, BioSerenity, MESA [20, 21], and MROS [20, 22], with SHHS [20, 23] serving as an external validation dataset. Among these, MESA, MROS, and SHHS are publicly available datasets, while SSC is our proprietary dataset. The BioSerenity dataset, provided by the BioSerenity company, contains 18,869 overnight recordings lasting 7-11 hours each. This dataset is a subset of a larger collection from SleepMed and BioSerenity sleep laboratories, gathered between 2004

and 2019 across 240 US facilities [19]. At the time of this study, approximately 20K de-identified PSGs were available for analysis. The dataset distribution across different splits is shown in Figure 1, with SSC constituting the largest cohort. To prevent data leakage, participants with multiple PSG recordings were assigned to a single split. For MESA, MROS, and SHHS details, we refer readers to their original publications. Below, we describe our internal SSC dataset in more detail.

The SSC dataset comprises 35,052 recordings, each lasting approximately 8 hours overnight. It includes diverse waveforms such as BAS, ECG, EMG, and respiratory channels, making it a high-quality resource for sleep-related research. The dataset spans recordings from 1999 to 2024 and includes participants aged 2 to 96. The patient demographic statistics for SSC and BioSerenity are summarized in Extended Table 1 and Extended Table 2 respectively.

Our preprocessing strategy minimizes alterations to preserve raw signal characteristics crucial for identifying nuanced patterns. Each recording contains up to four modalities: BAS, ECG, EMG, and respiratory, with variable numbers of channels. For BAS, we allowed up to 10 channels, for ECG 2 channels, for EMG 4 channels, and for respiratory 7 channels. The number and type of channels vary across sites and even between patients within the same site, depending on the study type. The types of channels available across sites are described in Supplementary Tables 15, 16, 17, 18, and 19. BAS includes channels that measure brain activity from different regions (frontal, central, occipital) as well as EOG for eye movements. EMG records electrical activity in muscles, while ECG captures cardiac electrical function. Respiratory channels measure chest and abdominal movements, pulse readings, and nasal/oral airflow. These channels were selected based on their relevance to sleep studies, guided by sleep experts [1].

Each PSG recording is resampled to 128 Hz to standardize sampling rates across participants and sites. Before downsampling, we utilized a 4th-order low-pass Butterworth filter to prevent aliasing, applied in a zero-phase setting to avoid phase distortion. Finally, we standardized the signal to have zero mean and unit variance. For any signals that needed to be upsampled, this was done using linear interpolation. Due to the channel agnostic model design, we did not need any other data-harmonization. Signals are segmented into 5-second patches, with each segment embedded into a vector representation for transformer model processing. To prevent data leakage, PSGs were split into pre-train, train, validation, test, and temporal test sets early in the preprocessing pipeline. While there is overlap between the pre-training and training sets, no overlap exists with the validation, test, or temporal test sets. The SHHS serves as an independent dataset not used during pre-training, instead being used to evaluate the model's ability to adapt to a new site through lightweight fine-tuning.

During pre-training, the only required labels are the modality types of the signals. A self-supervised contrastive learning (CL) objective is employed for pre-training. For downstream evaluations, we consider canonical tasks such as age/gender prediction, sleep stage classification, sleep apnea classification, and various patient conditions extracted from EHR data. Sleep staging and apnea labels for SSC, MESA, MROS, and SHHS were annotated by sleep experts. To ensure consistency across and within datasets, R&K labels were converted to AASM by mapping R&K stages 3 and 4 to AASM N3. SHHS also includes diagnostic information for conditions such as myocardial infarction, stroke, angina, congestive heart failure, and death. For SSC, we paired PSG data with Stanford EHR data using de-identified patient IDs to extract demographic and diagnostic information. As BioSerenity lacks associated labels, it was used exclusively for pre-training.

SleepFM Model Architecture

Our model architecture is illustrated in Figure 1. The architecture includes several key components that differ slightly between the pre-training and fine-tuning stages. During pre-training, we employ contrastive learning (CL) as the objective function for representation learning. A single model processes all four modalities.

The first component of the architecture is the *Encoder*, a 1D convolutional neural network (CNN) that processes raw signal data for each modality separately. The encoder takes raw input vectors, where the length of each vector corresponds to a 5-second segment of the signal, referred to as a token. The input dimensions are (B, T, C), where B is the batch size, T is the raw temporal length of the input, and C is the number of channels for each modality. These inputs are reshaped into (B, C, S, L), where S is the sequence length representing the number of tokens ($S = T/L$), and L corresponds to the raw vector length for a single token (e.g., 640 samples). Each token is then processed individually through a stack of six convolutional layers, each followed by normalization and ELU activation layers. These layers progressively reduce the temporal resolution while increasing the number of feature channels, converting the input from one channel to 128 channels. After this, adaptive average pooling further reduces the temporal dimensions, and a fully connected

layer compresses the representation into a 128-dimensional embedding for each token. The final output of the encoder has dimensions (B, C, S, D), where $D = 128$.

Following the encoder, a sequence of transformer-based operations is applied to extract and aggregate modality-specific and temporal features. The first step is *channel pooling*, which aggregates token embeddings from all channels within a given modality. This operation uses an attention pooling mechanism based on a transformer layer to compute attention scores for each channel and produces a single aggregated embedding per time segment by averaging over the channel dimension. The resulting embeddings, with dimensions (B, S, D), are then passed through a *temporal transformer*, which operates along the temporal dimension to capture dependencies between tokens. The *temporal transformer* applies sinusoidal positional encoding to the token embeddings, followed by 2 transformer blocks consisting of self-attention and feedforward layers, enabling the model to learn contextual relationships across the sequence. After temporal modeling, the embeddings are processed through *temporal pooling*, which aggregates token embeddings over the sequence length (S) for each modality. Similar to *channel pooling*, *temporal pooling* uses an attention mechanism to compute weighted averages, generating a compact representation of size $(B, 128)$ per modality. These steps collectively ensure that the model captures both spatial and temporal dependencies while reducing dimensionality for computational efficiency.

The final output is a single 128-dimensional embedding for each modality, used for contrastive learning during pre-training. While the 5-minute recordings are used exclusively for pre-training, we retain the 5-second-level embeddings for each modality for downstream tasks such as sleep staging and disease classification.

Baseline Models

We evaluate SleepFM against two carefully chosen baseline approaches to demonstrate the value of our foundation model methodology.

The first baseline is a simple demographic model that processes only patient characteristics, including age, gender, body mass index (BMI), and race/ethnicity information. This demographic baseline is implemented as a one-layer multi-layer perceptron (MLP) to establish a minimum performance threshold using only basic patient data available in most clinical settings.

The second baseline is a more sophisticated end-to-end PSG model that directly processes raw sleep recordings. This model uses the same architecture as SleepFM, including the 1D CNN encoder, channel pooling transformer block, temporal transformer block, temporal pooling transformer block, and the LSTM layers, and is trained from scratch on the same dataset used for downstream evaluation. It also includes age and gender demographic features to ensure a fair comparison, but does not leverage any pretraining—serving to isolate the benefit of task-specific supervised learning on PSG signals without a foundation model.

All baseline models were trained using dataset splits shown in Table 1. The foundation model was first pretrained on the training dataset using a self-supervised objective, and subsequently fine-tuned on the same data. In contrast, the supervised baseline models were trained end-to-end without any pretraining. Although all models share identical architectures, training objectives, and data splits, SleepFM consistently outperforms both baselines across a range of clinical prediction tasks. While this may seem counterintuitive—given that the supervised PSG baseline is trained on the same data—these results align with well-established benefits of pretraining in representation learning. Self-supervised pretraining enables the model to learn more generalizable physiological representations, facilitates better convergence through improved initialization, and makes more efficient use of sparse or noisy supervision during fine-tuning, as demonstrated in prior work [11].

Model Training

Model training can be categorized into two segments: pre-training and fine-tuning. Pre-training stage involves self-supervised representation learning with a CL objective and fine-tuning involves training the model with supervised learning objective for specific tasks such as sleep stage classification, sleep apnea classification, and disease prediction. We describe these in more details below.

Pre-training

Model pre-training is performed using a self-supervised learning objective called CL. Specifically, we employ a CL objective for multiple modalities, referred to as leave-one-out contrastive learning (LOO-CL). The key idea behind CL is to bring positive pairs of embeddings from different modalities closer in the latent space while pushing apart negative pairs. Positive pairs are derived from temporally aligned 5-minute aggregated

embeddings, obtained after temporal pooling, across four different modalities. All other non-matching instances within a training batch are treated as negative pairs.

In LOO-CL, we define a predictive task where an embedding from one modality attempts to identify the corresponding embeddings from the remaining modalities. For each modality i, we construct an embedding $\bar{x}_k^{-i}$ by averaging over embeddings from all other modalities, excluding modality i. We then apply a contrastive loss between the embedding of modality i and this leave-one-out representation:

$$\mathcal{L}_{i,k} = -\log \frac{\exp\left(\text{sim}(x_k^i, \bar{x}_k^{-i})/\tau\right)}{\sum_{m=1}^{N} \exp\left(\text{sim}(x_k^i, \bar{x}_m^{-i})/\tau\right)},$$

where $\mathcal{L}_{i,k}$ is the loss for a sample k from modality i in a given batch, $\text{sim}(\cdot)$ represents a similarity function (e.g., cosine similarity), and τ is a temperature scaling parameter. The numerator computes the similarity between the embedding of modality i and the leave-one-out representation of the corresponding sample, while the denominator sums the similarities across all samples within the batch. The motivation behind the leave-one-out method is to encourage each embedding to align semantically with all other modalities.

Fine-tuning

After pre-training with the CL objective, we extract 5-second embeddings for all patient PSG data across modalities. We standardize the temporal context to 9 hours for all patients - longer recordings are cropped and shorter ones are zero-padded to ensure consistent input dimensions. For example, for a patient's standardized 9-hour sleep data, the resulting patient matrix has dimensions $(4 \times 6480 \times 128)$, where 4 represents the number of modalities, 6480 is the number of 5-second embeddings for 9 hours of sleep, and 128 is the embedding vector dimension.

During fine-tuning, we first apply a channel pooling operation across different modalities, reducing the dimensions to (6480×128) for our example patient matrix. The pooled embeddings are then processed through a 2-layer LSTM block, which is designed to handle temporal sequences. For sleep staging tasks, these 5-second embeddings are directly passed through a classification layer. For all other tasks, the embeddings are first pooled along the temporal dimension before being passed through an output layer.

For disease classification, we append age and gender features to the mean-pooled embedding vector after the LSTM block, before passing it to the final output layer. This addition empirically improves performance and surpasses the demographic baseline.

The fine-tuning objective for disease prediction uses the CoxPH loss function, a standard approach in survival analysis for modeling time-to-event data. The CoxPH loss maximizes the partial likelihood and is defined for a single label as:

$$\mathcal{L}_{\text{CoxPH}} = -\frac{1}{N_e} \sum_{i=1}^{n} \delta_i \left(h_i - \log \sum_{j \in R(t_i)} \exp(h_j) \right),$$

where h_i is the predicted hazard for the i-th patient, δ_i is the event indicator (1 for event occurrence, 0 otherwise), t_i is the event or censoring time, $R(t_i)$ represents the risk set of all patients with event times greater than or equal to t_i, n is the total number of patients, and $N_e = \sum_{i=1}^{n} \delta_i$ is the number of events.

For our multi-label setup with 1,041 labels, we extend the CoxPH loss by computing it independently for each label and summing the results:

$$\mathcal{L}_{\text{total}} = \sum_{k=1}^{L} \mathcal{L}_{\text{CoxPH}}^{(k)},$$

where L is the total number of labels.

Given the large dataset size, computing the loss for all patients in a single batch is computationally infeasible. Therefore, we calculate the loss in smaller batches of 32 samples, with patients sorted by event time in descending order to ensure correct computation of the partial likelihood. This batching strategy, combined with the summation of per-label losses, provides an efficient and scalable approach for multi-label time-to-event modeling.

Architectural Details

We provide additional implementation-level details to clarify how SleepFM is constructed and trained. The design of SleepFM was developed through an empirical and iterative process, informed by domain knowledge and guided by practical training considerations. While we did not perform an exhaustive hyperparameter search, we systematically evaluated architectural variants through trial-and-error by monitoring loss convergence, training stability, and downstream performance.

Each 5-second segment of raw PSG signals (640 timepoints at 128Hz) is passed through a tokenizer composed of six convolutional layers with increasing feature maps: $1 \rightarrow 4 \rightarrow 8 \rightarrow 16 \rightarrow 32 \rightarrow 64 \rightarrow 128$. Each convolutional block includes BatchNorm, ELU activation, and LayerNorm. After convolution, adaptive average pooling reduces the temporal axis to 1, and a linear layer projects the features to a fixed 128-dimensional token embedding. The resulting output shape is $(B, C, S, 128)$, where C is the number of channels and S is the number of 5-second tokens.

To accommodate variability in the number and ordering of channels across different PSG datasets, we introduced an attention-based spatial pooling layer that operates across channels using a transformer encoder. This design makes the model robust to inconsistencies in recording configurations across sites. Specifically, embeddings from multiple channels within a modality are pooled using multi-head self-attention, producing a modality-specific sequence of shape $(B, S, 128)$.

To capture long-range temporal dependencies in sleep signals, the pooled token sequence is passed through three transformer encoder layers (each with 8 heads, batch-first configuration, and a dropout rate of 0.3), along with sinusoidal positional encoding and LayerNorm. This component enables modeling of contextual relationships across the sleep sequence. The output shape remains $(B, S, 128)$.

An additional attention-based pooling layer aggregates the temporal sequence across time steps, resulting in a single 128-dimensional embedding for each modality (e.g., BAS, ECG, EMG, or respiratory). These fixed-size modality-specific embeddings are used for pretraining with a self-supervised contrastive learning objective.

For downstream disease prediction, 5-second token embeddings spanning a standardized 9-hour window are processed by a fine-tuning head. This head includes spatial pooling followed by a two-layer bidirectional LSTM (hidden size = 64). Temporal mean pooling is applied across valid time steps, and normalized age and sex features are concatenated with the pooled output. The combined vector is then passed through a final linear layer to generate hazard scores for each disease. The total number of learnable parameters in this setup is approximately 0.91 million.

The supervised baseline model uses the same architecture as SleepFM but is trained from scratch without pretraining. The demographics-only baseline passes four input features—age, sex, BMI, and race/ethnicity—through a shallow MLP with dimensions $4 \rightarrow 128 \rightarrow$ output.

Implementation Details

All implementations were carried out using PyTorch, a widely used library for deep learning. The PSG data was gathered and processed within a HIPAA-compliant and secure compute cluster on Google Cloud Platform. Patient electronic health record data was likewise stored and analyzed exclusively within this secure environment.

For pre-training, the model was trained with a batch size of 32, a learning rate of 0.001, 8 pooling heads, 3 transformer layers, and a dropout rate of 0.3. As previously described, each patch size corresponds to a 5-second segment, and the total sequence length is 5 minutes for the transformer model. The total parameter count for the model was approximately 4.44 million. Pre-training was performed on 432,000 hours of sleep data collected from 48,000 participants for one epoch, using an NVIDIA A100 GPU. The entire pre-training process took approximately 15 hours.

For fine-tuning, the batch size was also set to 32, with a learning rate of 0.001, 4 pooling heads, 2 LSTM layers, and a dropout rate of 0.3. The fine-tuned model had approximately 0.91 million learnable parameters. Training was conducted on patient data, with each token embedding represented as a 128-dimensional vector, over 10 epochs. The fine-tuning process was performed on an NVIDIA A100 GPU, with the total training time per epoch ranging from 2 to 5 minutes, depending on the task.

All data analysis and preprocessing were performed using Python (version 3.10.14) and its data analysis libraries, including Pandas (2.1.1), NumPy (1.25.2), SciPy (1.11.3), scikit-survival (0.23.0), scikit-learn (1.5.2), and PyTorch (2.0.1).

Data Availability

Of the five data sources used in this study, four datasets are publicly available and can be accessed at the following links: SHHS (`https://sleepdata.org/datasets/shhs`), MrOS (`https://sleepdata.org/datasets/mros`), MESA (`https://sleepdata.org/datasets/mesa`), and SSC (`https://sleepdata.org/datasets/ssc`). The BioSerenity dataset is proprietary and owned by BioSerenity, which has granted Stanford University access under a research and development agreement; please contact BioSerenity directly for data agreement. Stanford sleep data is available upon publication at this link: `https://bdsp.io/content/hsp/2.0/`. Access to these data is provided solely for research purposes and is subject to data use restrictions that prohibit redistribution or sharing with third parties.

Code Availability

All of the SleepFM code is open source and available at `https://github.com/zou-group/sleepfm-clinical`

Extended Tables and Figures

Extended Data Table 1. **Demographic characteristics of the Stanford Sleep Clinic (SSC) cohort.** Values are shown by dataset split and reported as mean ± 2 standard deviations for age, and as counts (percentages) for categorical variables.

Demographics	**Train**	**Validation**	**Test**	**Temporal Test**
Age (mean ± 2SD)	45.00 ± 40.59	44.65 ± 42.89	45.71 ± 40.21	49.25 ± 39.36
Male	13230 (58.95%)	418 (59.80%)	2819 (60.27%)	2693 (54.61%)
Female	9205 (41.02%)	281 (40.20%)	1856 (39.68%)	2237 (45.37%)
Unknown	8 (0.04%)	0 (0.00%)	2 (0.04%)	1 (0.02%)
White	12807 (57.06%)	381 (54.51%)	2748 (58.76%)	2476 (50.21%)
Asian	2864 (12.76%)	95 (13.59%)	571 (12.21%)	914 (18.54%)
Black	628 (2.80%)	23 (3.29%)	144 (3.08%)	205 (4.16%)
Pacific Islander	225 (1.00%)	9 (1.29%)	34 (0.73%)	52 (1.05%)
Native American	76 (0.34%)	1 (0.14%)	16 (0.34%)	31 (0.63%)
Other	2290 (10.20%)	65 (9.30%)	476 (10.18%)	896 (18.17%)
Unknown	3553 (15.83%)	125 (17.88%)	688 (14.71%)	357 (7.24%)
Non-Hispanic	16914 (75.36%)	513 (73.39%)	3600 (76.97%)	3828 (77.63%)
Hispanic/Latino	1978 (8.81%)	57 (8.15%)	392 (8.38%)	736 (14.93%)
Other	2290 (10.20%)	65 (9.30%)	476 (10.18%)	896 (18.17%)
Unknown	3551 (15.82%)	129 (18.45%)	685 (14.65%)	367 (7.44%)

Extended Data Table 2. **Demographic characteristics of the Bioserenity cohort**. Values are presented as mean ± 2 standard deviations for age, and as counts (percentages) for categorical variables.

Demographics	**Train**	**Validation**
Age (mean ± 2SD)	48.71 ± 38.59	49.11 ± 41.44
Female	9684 (52.06%)	47 (47.00%)
Male	8916 (47.94%)	53 (53.00%)
African American	4636 (24.92%)	29 (29.00%)
Alaska Native	0 (0.00%)	0 (0.00%)
American Indian	124 (0.67%)	1 (1.00%)
Asian	105 (0.56%)	0 (0.00%)
Hispanic	538 (2.89%)	4 (4.00%)
Native Hawaiian	3 (0.02%)	0 (0.00%)
Pacific Islander	22 (0.12%)	0 (0.00%)
White (Caucasian)	12755 (68.58%)	64 (64.00%)
Unknown	417 (2.24%)	2 (2.00%)

Extended Data Table 3. **Per–sleep-stage F1 performance of SleepFM across four cohorts.** Per–sleep-stage F1 scores for SleepFM across four cohorts (SSC, MESA, MrOS and SHHS), with comparison to U-Sleep. Values for SleepFM are mean F1 with 95% confidence intervals from 1,000 bootstrap resamples of test recordings (CIs shown in parentheses beneath each estimate). The bold "Mean" row reports the macro-average across stages. U-Sleep values are the corresponding F1 scores reported for the same cohorts; confidence intervals were not available.

	SleepFM				**U-Sleep**			
Stage	**SSC**	**MESA**	**MROS**	**SHHS**	**SSC**	**MESA**	**MROS**	**SHHS**
Wake	$0.92_{(0.92,\ 0.93)}$	$0.94_{(0.94,\ 0.94)}$	$0.94_{(0.94,\ 0.94)}$	$0.92_{(0.92,\ 0.92)}$	0.81	0.92	0.93	0.93
Stage 1	$0.48_{(0.48,\ 0.48)}$	$0.56_{(0.56,\ 0.56)}$	$0.41_{(0.40,\ 0.41)}$	$0.49_{(0.48,\ 0.49)}$	0.35	0.59	0.46	0.51
Stage 2	$0.87_{(0.87,\ 0.87)}$	$0.83_{(0.83,\ 0.83)}$	$0.86_{(0.86,\ 0.86)}$	$0.84_{(0.84,\ 0.84)}$	0.75	0.87	0.87	0.87
Stage 3	$0.39_{(0.38,\ 0.39)}$	$0.68_{(0.68,\ 0.69)}$	$0.65_{(0.64,\ 0.65)}$	$0.72_{(0.72,\ 0.72)}$	0.51	0.65	0.68	0.76
REM	$0.86_{(0.86,\ 0.86)}$	$0.88_{(0.88,\ 0.88)}$	$0.90_{(0.90,\ 0.90)}$	$0.91_{(0.91,\ 0.91)}$	0.84	0.90	0.88	0.92
Mean	**0.70**	**0.78**	**0.75**	**0.78**	**0.65**	**0.79**	**0.77**	**0.80**

Extended Data Table 4. **Sleep staging performance on the SSC cohort.** Sleep staging results (F1) for SleepFM, U-Sleep, YASA, GSSC, and STAGES on the SSC cohort. The **bold** bottom row reports the macro-average (mean) across stages.

Stage	**SleepFM**	**U-Sleep**	**YASA**	**GSSC**	**STAGES**
Wake	0.92	0.81	0.61	0.84	0.73
Stage 1	0.48	0.35	0.05	0.39	0.33
Stage 2	0.87	0.75	0.69	0.79	0.82
Stage 3	0.39	0.51	0.56	0.56	0.63
REM	0.86	0.84	0.71	0.85	0.79
Mean	**0.70**	**0.65**	**0.52**	**0.68**	**0.66**

Extended Data Table 5. **Comparison of category-averaged C-Index across SleepFM variants and baselines.** Category-averaged C-Index (mean with 95% CI) comparing SleepFM variants with two baselines across disease categories on Stanford cohort (n=5,019). The Demographics baseline ("Demo") uses only structured clinical features (age, gender, BMI, and race/ethnicity). The End-to-End PSG baseline ("E2E-PSG") is trained directly on raw PSG signals with age and gender, without any pretraining. SleepFM-1 denotes SleepFM-LSTM (w/o Demo), using two LSTM layers in the fine-tuning prediction module and no demographic features. SleepFM-2 denotes SleepFM-Linear, a linear prediction module on SleepFM embeddings with age and gender. SleepFM-3 denotes SleepFM-LSTM, which uses two LSTM layers in the fine-tuning prediction module with age and gender. Values are averaged within each category across conditions. Uncertainty is estimated via nonparametric bootstrapping (n=1000 resamples): for each resample, conditions within a category are sampled with replacement and the category mean is computed; 95% CIs are the 2.5th–97.5th percentiles across resamples.

Category	Demo	E2E PSG	SleepFM-1	SleepFM-2	SleepFM-3
Circulatory System	$0.72_{(0.72,\ 0.73)}$	$0.72_{(0.72,\ 0.73)}$	$0.75_{(0.75,\ 0.75)}$	$0.76_{(0.75,\ 0.76)}$	$0.75_{(0.75,\ 0.76)}$
Dermatologic	$0.63_{(0.62,\ 0.64)}$	$0.62_{(0.61,\ 0.63)}$	$0.65_{(0.64,\ 0.65)}$	$0.66_{(0.65,\ 0.66)}$	$0.66_{(0.65,\ 0.66)}$
Digestive	$0.62_{(0.62,\ 0.63)}$	$0.63_{(0.62,\ 0.63)}$	$0.66_{(0.65,\ 0.67)}$	$0.67_{(0.66,\ 0.68)}$	$0.67_{(0.66,\ 0.67)}$
Endocrine/Metabolic	$0.68_{(0.67,\ 0.68)}$	$0.66_{(0.66,\ 0.67)}$	$0.70_{(0.70,\ 0.71)}$	$0.71_{(0.71,\ 0.72)}$	$0.71_{(0.71,\ 0.72)}$
Hematopoietic	$0.65_{(0.64,\ 0.66)}$	$0.66_{(0.65,\ 0.67)}$	$0.70_{(0.69,\ 0.71)}$	$0.70_{(0.69,\ 0.72)}$	$0.70_{(0.69,\ 0.71)}$
Infectious Diseases	$0.62_{(0.61,\ 0.63)}$	$0.61_{(0.60,\ 0.62)}$	$0.65_{(0.64,\ 0.66)}$	$0.66_{(0.64,\ 0.67)}$	$0.66_{(0.64,\ 0.67)}$
Injuries & Poisonings	$0.62_{(0.61,\ 0.63)}$	$0.63_{(0.62,\ 0.64)}$	$0.65_{(0.64,\ 0.66)}$	$0.66_{(0.65,\ 0.67)}$	$0.66_{(0.65,\ 0.67)}$
Mental Disorders	$0.66_{(0.65,\ 0.66)}$	$0.66_{(0.65,\ 0.67)}$	$0.69_{(0.68,\ 0.70)}$	$0.69_{(0.69,\ 0.70)}$	$0.70_{(0.70,\ 0.71)}$
Musculoskeletal	$0.67_{(0.66,\ 0.67)}$	$0.67_{(0.66,\ 0.68)}$	$0.67_{(0.67,\ 0.68)}$	$0.68_{(0.67,\ 0.69)}$	$0.68_{(0.67,\ 0.69)}$
Neoplasms	$0.72_{(0.71,\ 0.73)}$	$0.72_{(0.71,\ 0.73)}$	$0.71_{(0.70,\ 0.72)}$	$0.73_{(0.72,\ 0.74)}$	$0.73_{(0.72,\ 0.74)}$
Neurological	$0.62_{(0.61,\ 0.63)}$	$0.63_{(0.62,\ 0.63)}$	$0.66_{(0.66,\ 0.67)}$	$0.67_{(0.66,\ 0.67)}$	$0.67_{(0.66,\ 0.68)}$
Respiratory	$0.63_{(0.62,\ 0.64)}$	$0.63_{(0.63,\ 0.64)}$	$0.66_{(0.65,\ 0.66)}$	$0.66_{(0.65,\ 0.66)}$	$0.66_{(0.65,\ 0.67)}$
Sense Organs	$0.65_{(0.65,\ 0.66)}$	$0.66_{(0.66,\ 0.67)}$	$0.68_{(0.67,\ 0.68)}$	$0.68_{(0.67,\ 0.68)}$	$0.68_{(0.67,\ 0.68)}$
Symptoms	$0.64_{(0.63,\ 0.64)}$	$0.64_{(0.64,\ 0.65)}$	$0.68_{(0.67,\ 0.69)}$	$0.69_{(0.68,\ 0.69)}$	$0.68_{(0.68,\ 0.69)}$

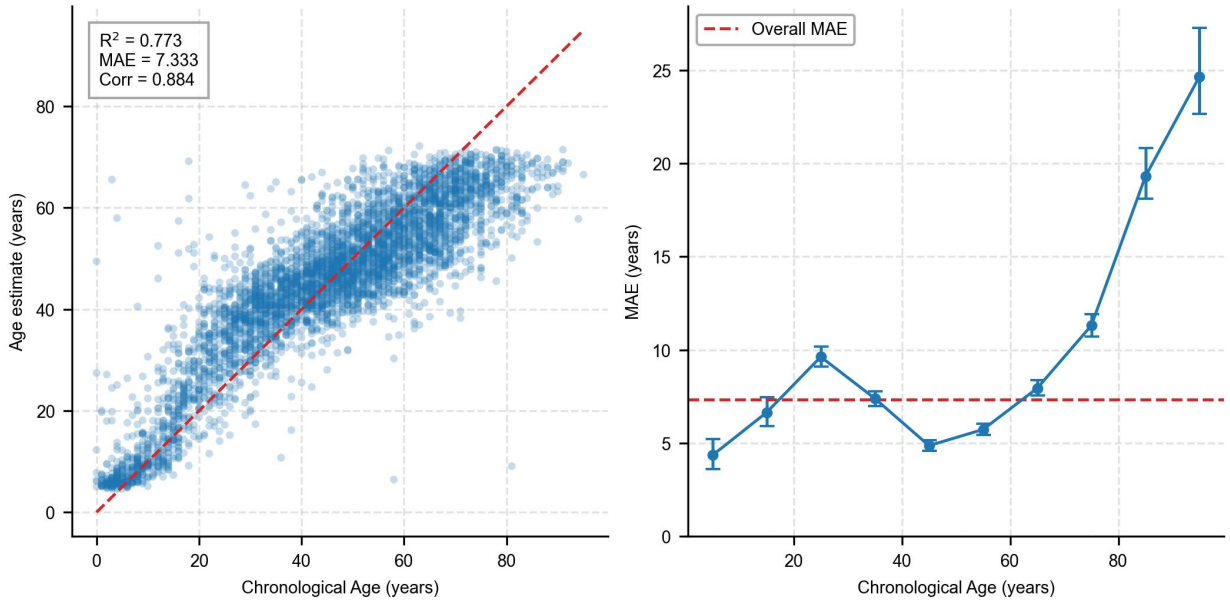

Extended Data Figure 1. Age estimation performance on the Stanford cohort. Left: Scatter plot showing predicted versus chronological age across all patients ($n = 5{,}019$), with the diagonal line representing perfect prediction. The coefficient of determination (R^2), mean absolute error (MAE), and Pearson correlation coefficient (Corr) are shown in the top left corner. Right: Mean Absolute Error (MAE) across chronological age groups, with vertical error bars indicating the standard error of the mean (SEM) within each age bin. The horizontal dashed line represents the overall MAE. Our model achieves an MAE comparable to state-of-the-art models and demonstrates improved age estimation performance for younger age groups compared to older ones.

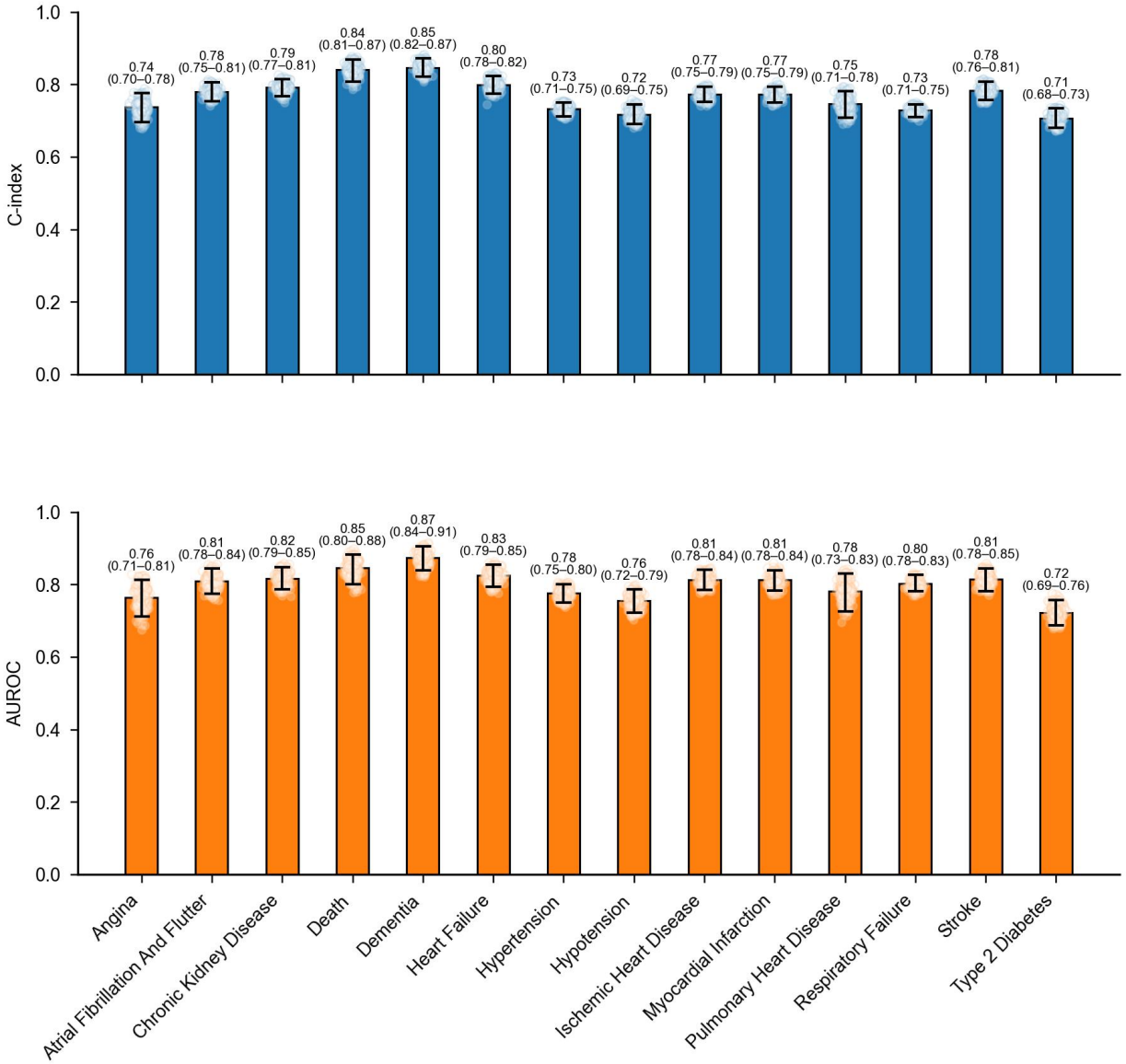

Extended Data Figure 2. Performance across clinically relevant diseases evaluated on the Stanford test set (n=5019). Performance is evaluated using multiple metrics: C-Index and AUROC. The selected conditions include critical health outcomes such as death, heart failure, stroke, and dementia. Each panel uses violin/point plots derived from 1000 patient-level bootstrapping: the violin encodes the distribution of bootstrap estimates, faint points are individual bootstrap draws, the filled dot is the mean, and the vertical line with end caps marks the 95% bootstrap percentile CI. Numbers above violins report the mean. Metrics are C-index (top) and AUROC at 6 years (bottom).

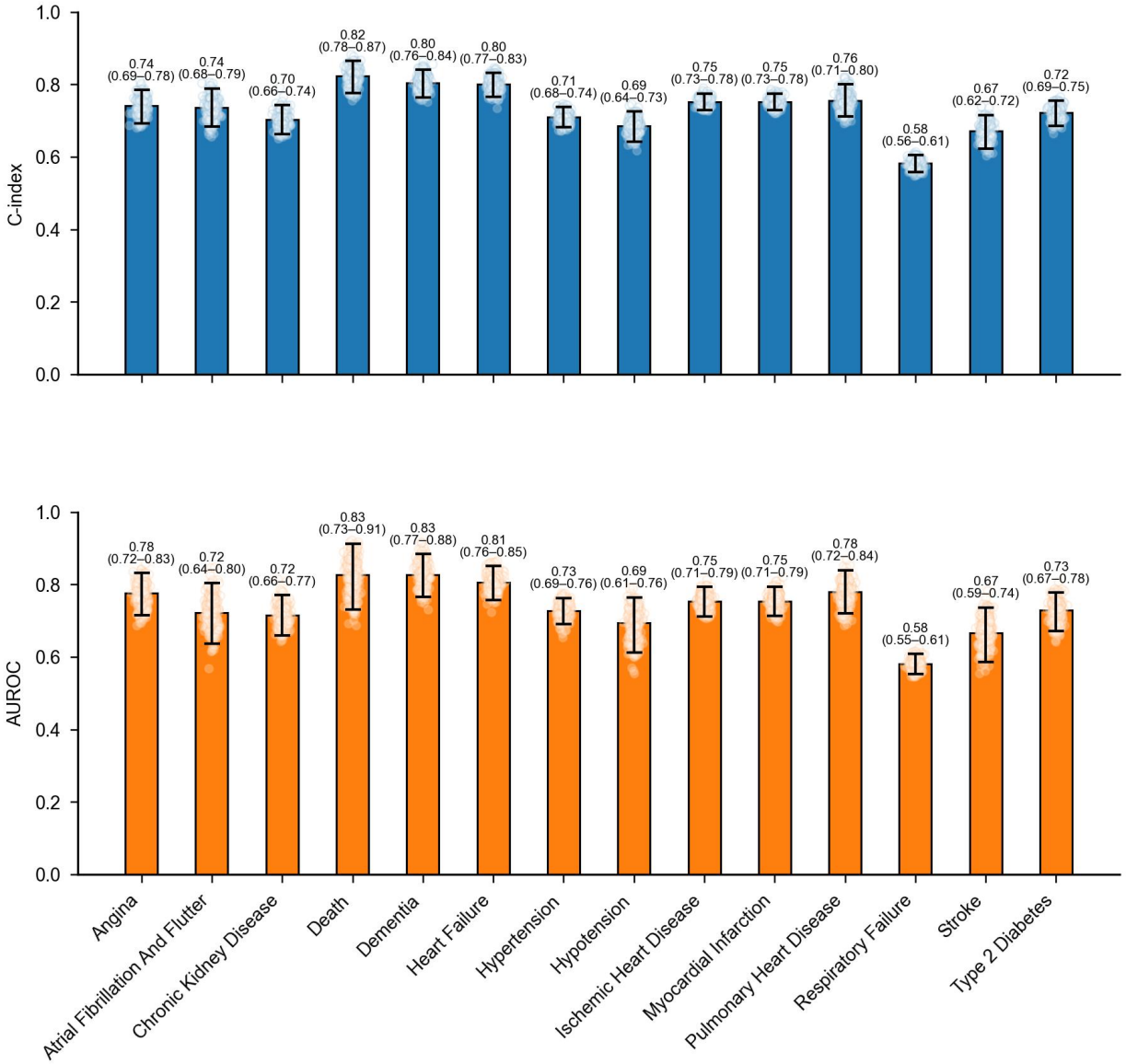

Extended Data Figure 3. Prediction performance of SleepFM for key clinical outcomes on the temporal test set, including C-Index and AUROC metrics for critical conditions such as death, heart failure, chronic kidney disease, dementia, and stroke. Each panel uses violin/point plots derived from 1000 patient-level bootstrapping: the violin encodes the distribution of bootstrap estimates, faint points are individual bootstrap draws, the filled dot is the mean, and the vertical line with end caps marks the 95% bootstrap percentile CI. Numbers above violins report the mean. Metrics are C-index (top) and AUROC (bottom). All conditions are statistically significant with a p-value < 0.01 after Bonferroni correction.

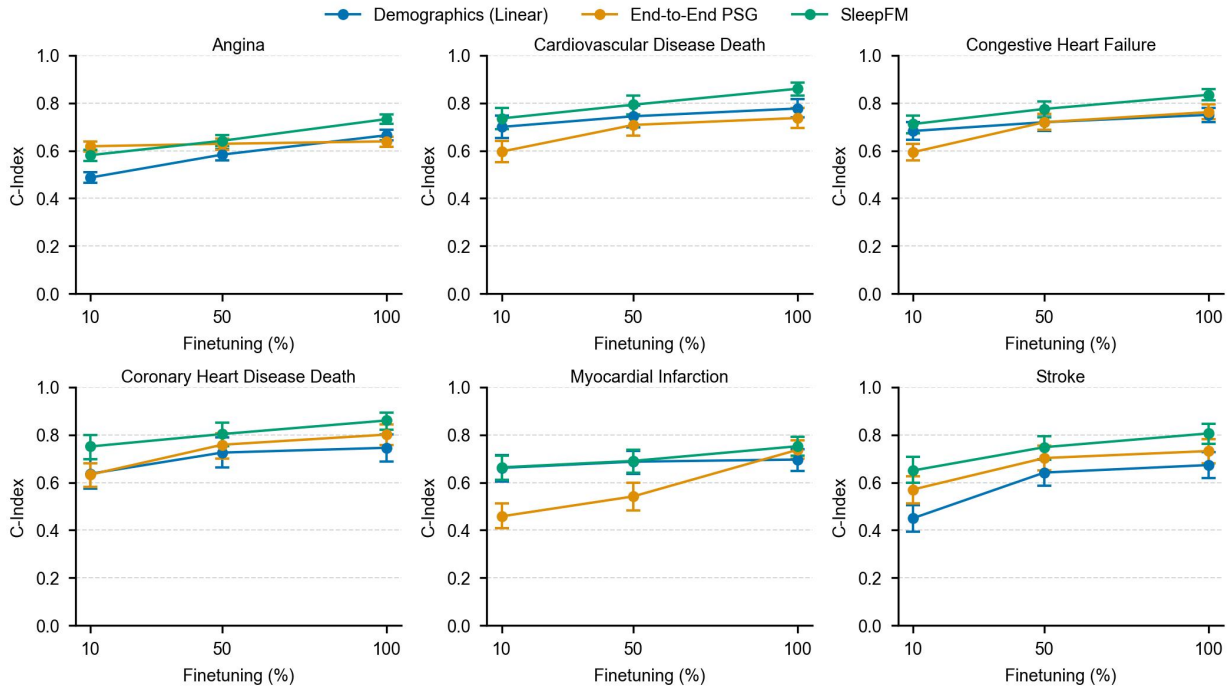

Extended Data Figure 4. Scaling behavior of fine-tuning SleepFM on the SHHS dataset. Scaling behavior of fine-tuning SleepFM on the SHHS dataset (test size = 2,000 participants). We progressively increased the percentage of labeled SHHS data used during fine-tuning from 10% to 100%. The plots show C-Index performance across six cardiovascular outcomes, comparing SleepFM with Demographics and End-to-End PSG baselines. Error bars indicate 95% confidence intervals derived from 1,000 participant-level bootstrap resamples with replacement. Even with as little as 10% of training data (~330 samples), SleepFM demonstrates strong predictive accuracy and consistent performance improvements as more labeled data becomes available. SleepFM outperforms both baseline models in most conditions, particularly when the dataset size is smaller, and its performance scaling is more stable across all outcomes.

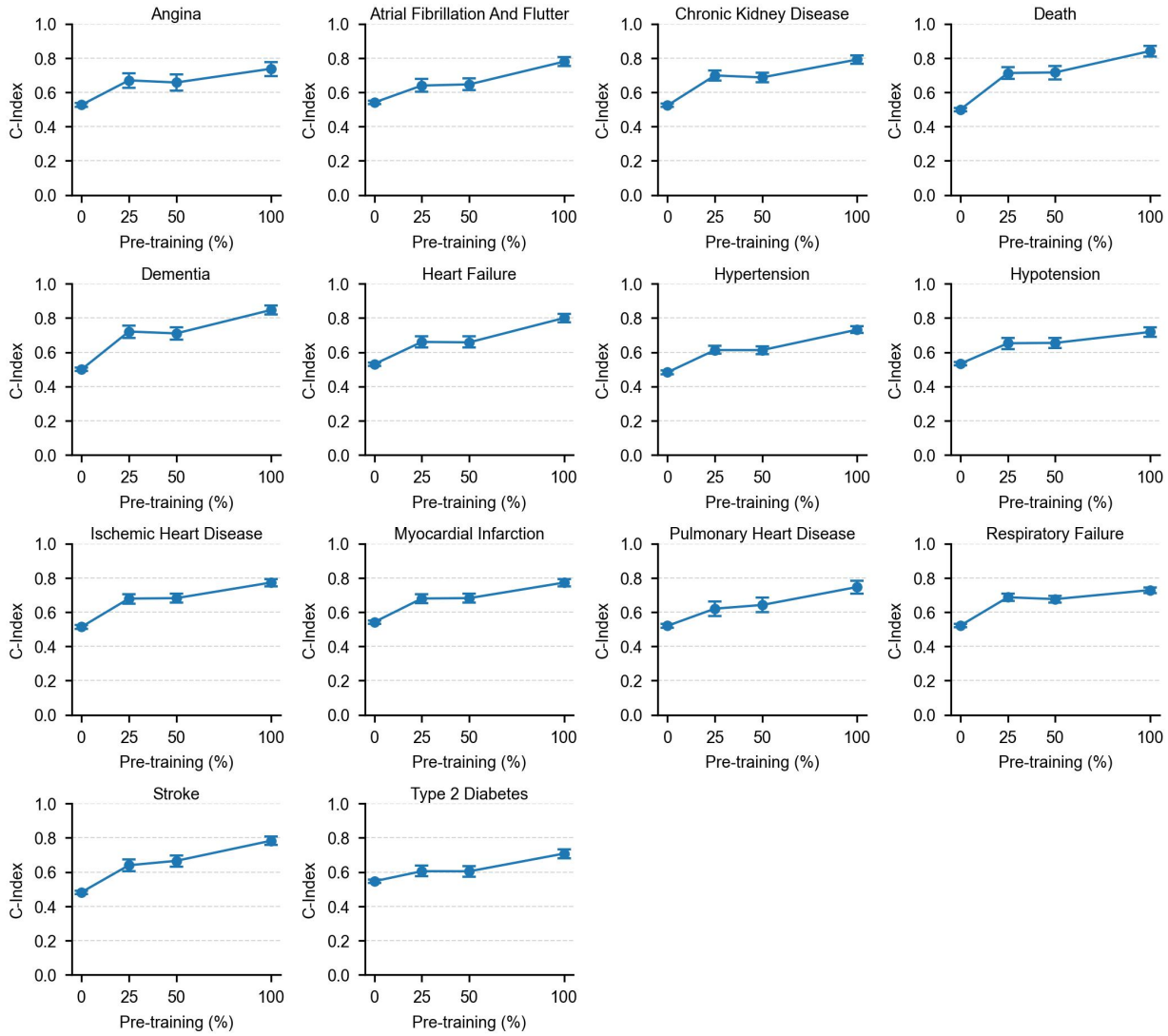

Extended Data Figure 5. Impact of pretraining dataset size on downstream performance on the Stanford cohort. Each subplot shows C-Index performance for a specific disease as a function of the percentage of pretraining data used (0%, 25%, 50%, 100%). The downstream fine-tuning and test datasets are held constant. Error bars represent 95% confidence intervals estimated via 1,000 participant-level bootstrap resamples with replacement. The 100% mark corresponds to a full epoch of pretraining on the entire dataset ($n = 24,137$). Intermediate checkpoints at 25% and 50% represent models saved partway through that epoch, while the 0% point denotes a model with no pretraining, resulting in near-random performance. Performance improves consistently with more pretraining data, highlighting the value of large-scale self-supervised pretraining across diverse phenotypes, including cardiovascular, metabolic, neurological, and respiratory conditions.

Supplementary Section

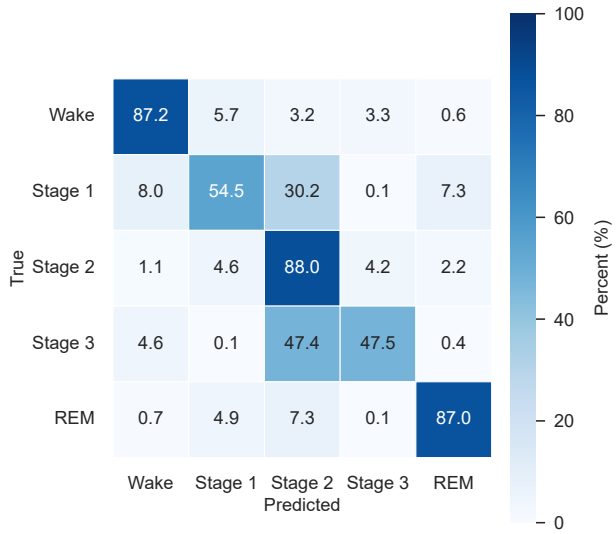

(a) SSC

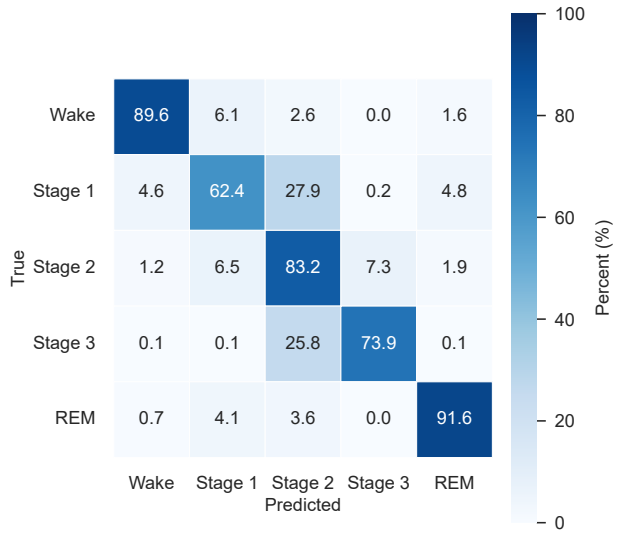

(b) MESA

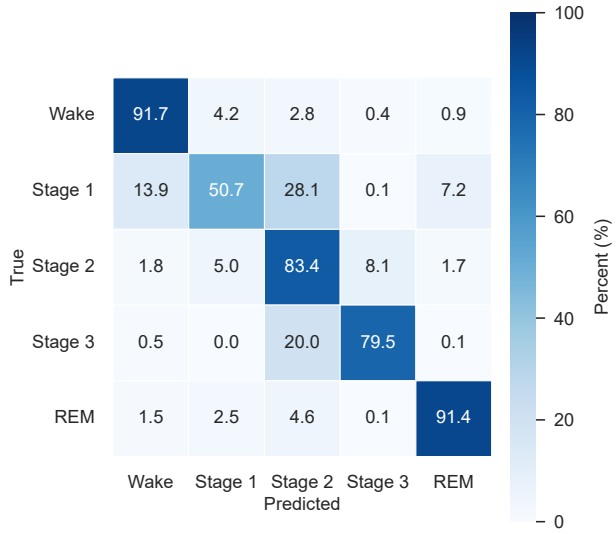

(c) MROS

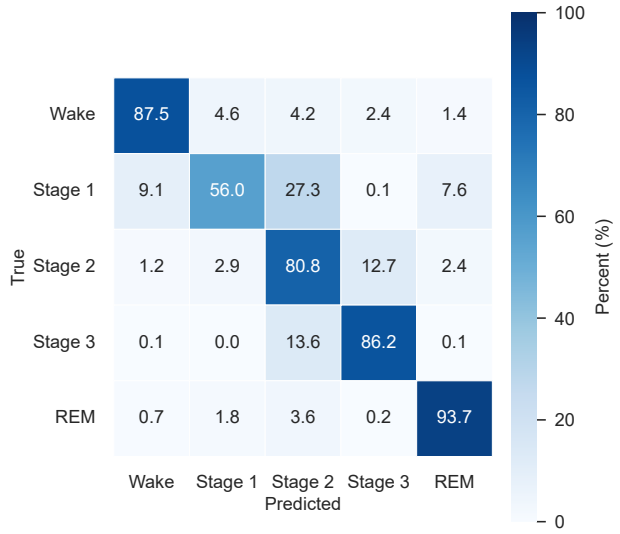

(d) SHHS

Supplementary Figure 1. SleepFM sleep staging confusion matrices for the Stanford, MESA, MROS, and SHHS cohorts. SleepFM generally performs well in differentiating between sleep stages, with mild confusion observed between Stage 1 and Stage 2, as well as between Stage 2 and Stage 3.

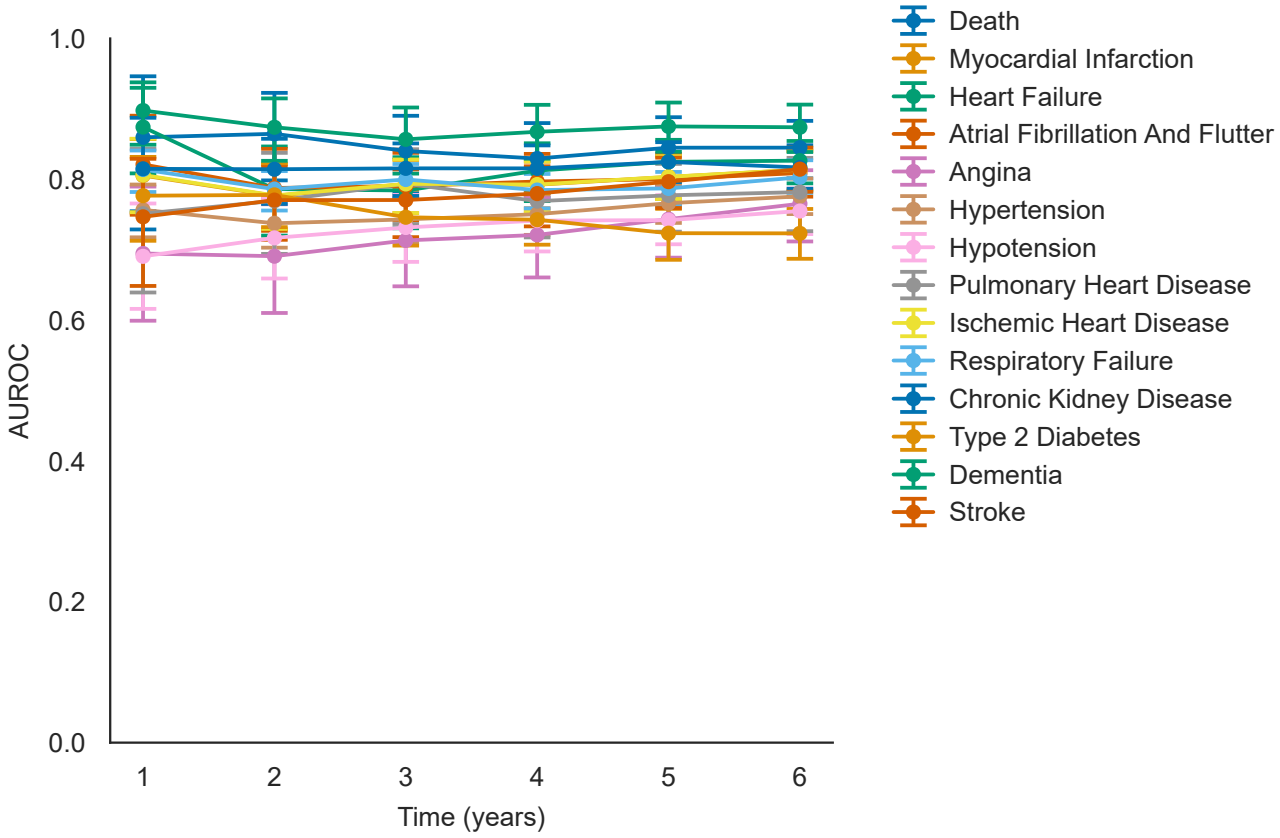

Supplementary Figure 2. AUROC trends across prediction windows from 1 to 6 years. While we report 6-year AUROC as our primary metric to accommodate the range of conditions—both acute and chronic—we acknowledge that different time horizons may be more appropriate for specific conditions. The plot above demonstrates that AUROC remains robust across multiple conditions over the 1–6 year range.

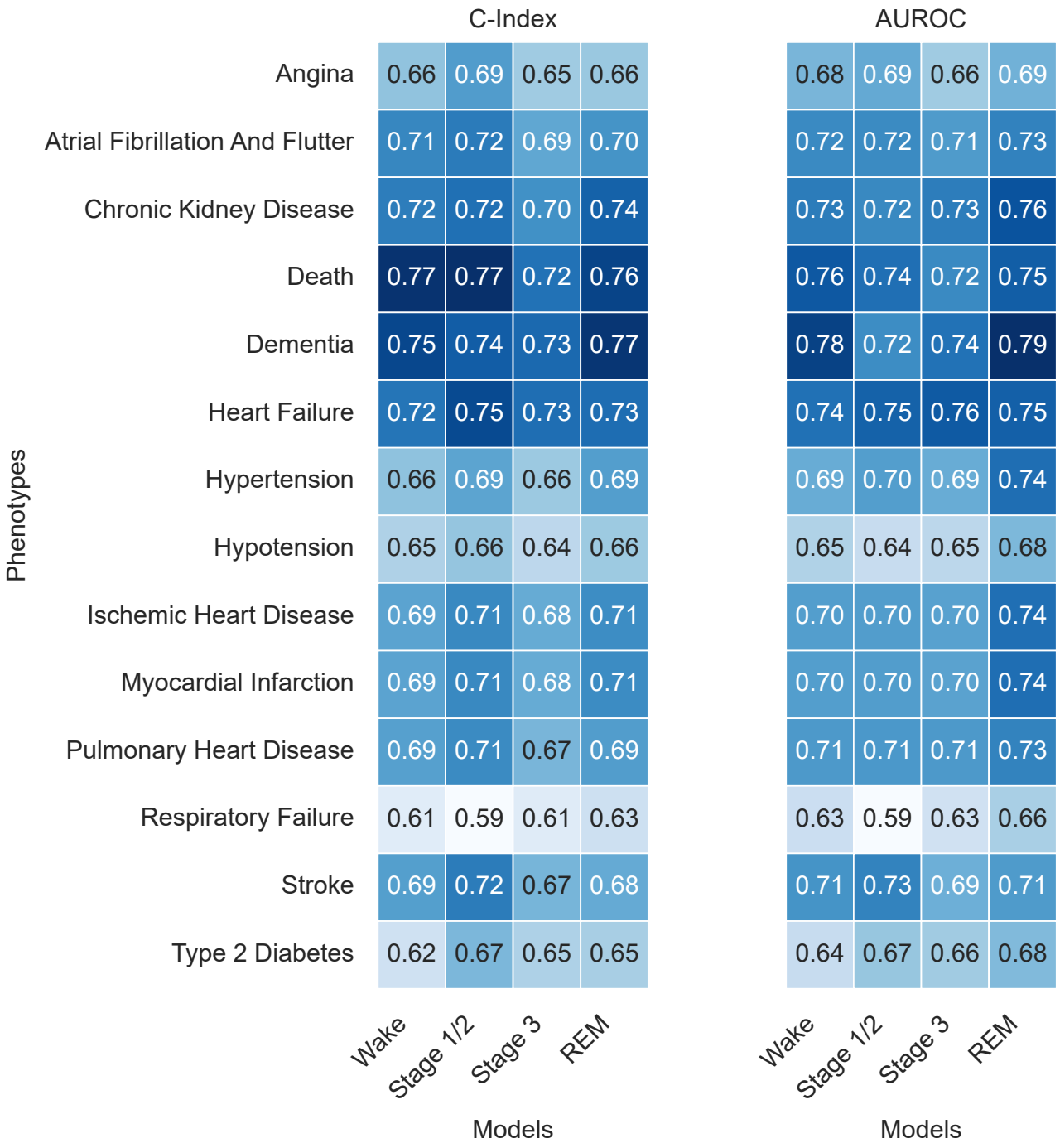

Supplementary Figure 3. Performance comparison of models trained on different sleep stages across selected conditions. Metrics presented are C-Index and AUROC.

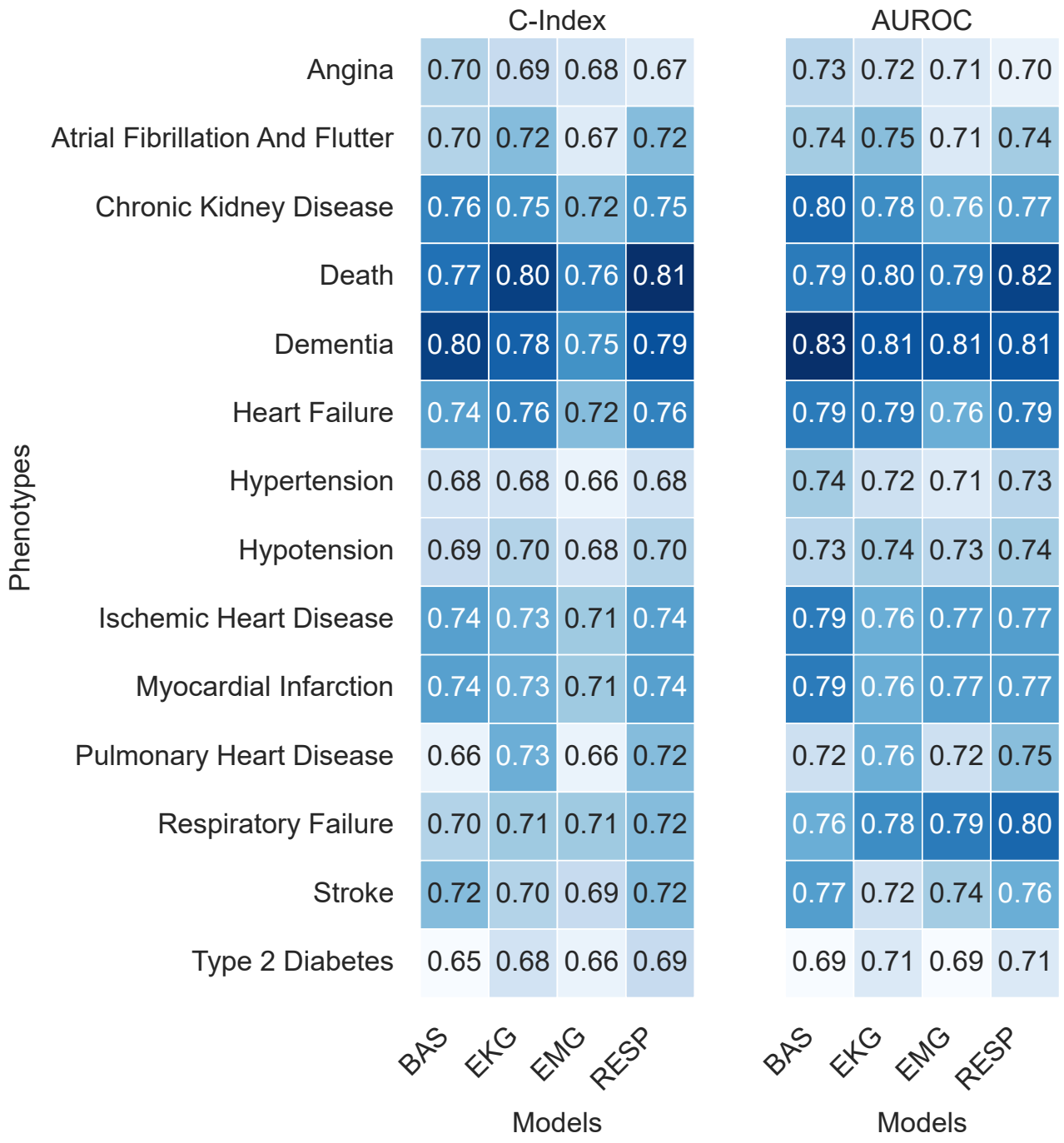

Supplementary Figure 4. Performance comparison of models trained on different sleep modalities across selected conditions. BAS, EKG, and RESP exhibit similar predictive performance across various conditions, while EMG is the least predictive.

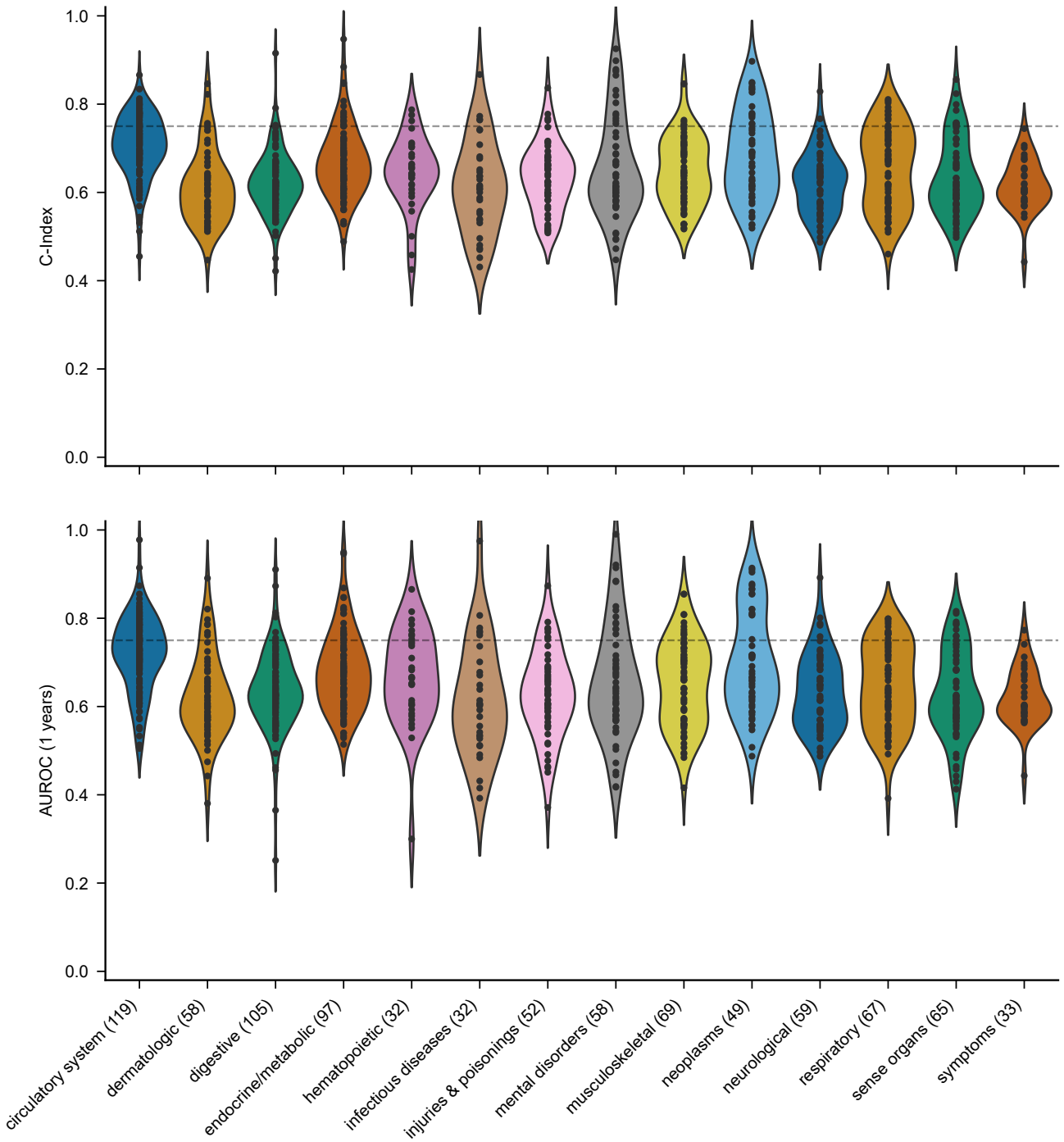

Supplementary Figure 5. SleepFM performance across disease categories on the temporal test set (Stanford data from 2020 onwards). Performance is measured using C-Index and 6-year AUROC metrics to assess the model's robustness to temporal distribution shifts. Despite these shifts, SleepFM maintains strong performance across a broad spectrum of diseases.

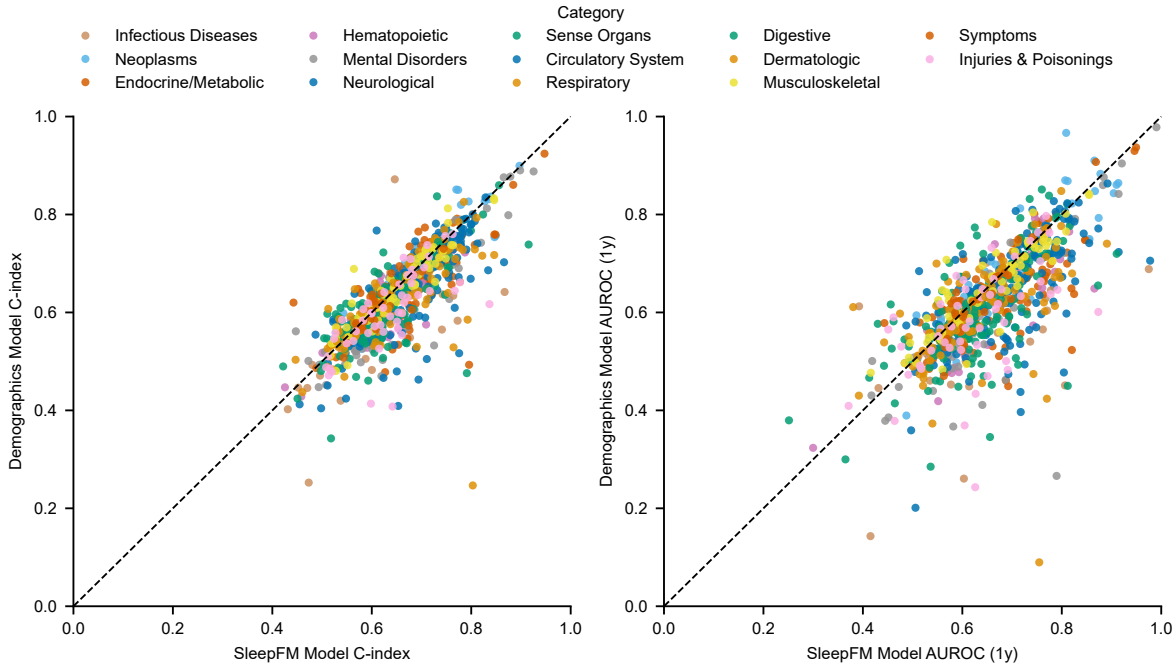

(a) Comparison with demographics-only baseline

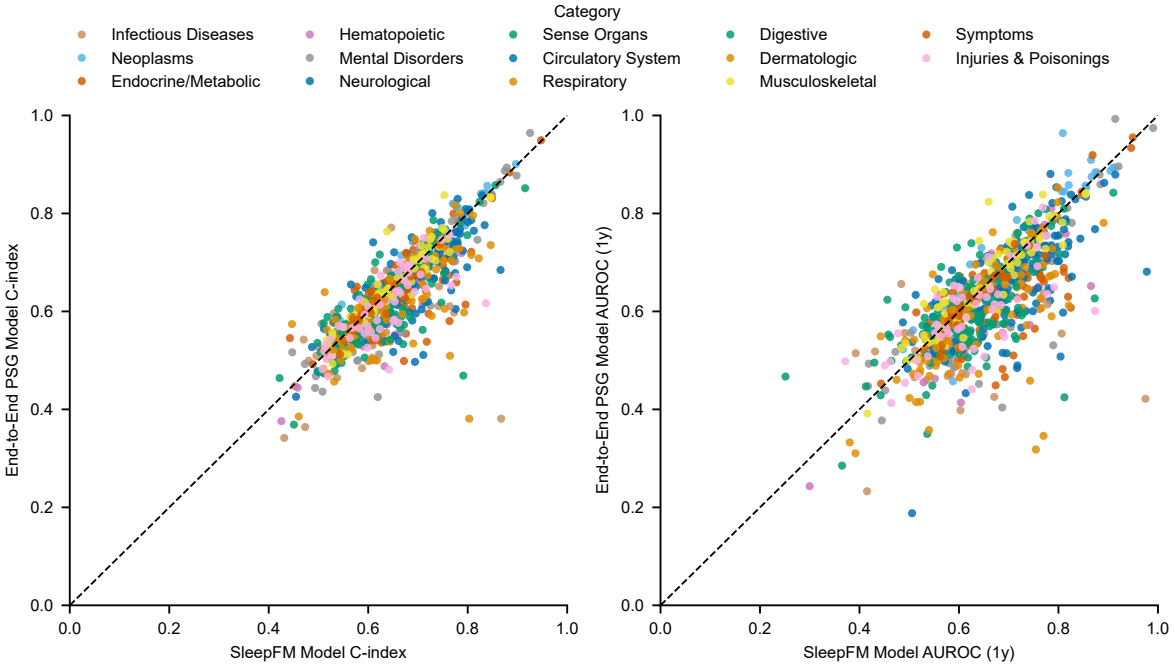

(b) Comparison with End-to-End PSG model

Supplementary Figure 6. Performance comparison on the temporal test set (Stanford data from 2020 onwards) using C-Index and 6-year AUROC metrics. Each point represents a disease phenotype. (a) Comparison against demographics baseline shows points below the diagonal, indicating SleepFM's superior performance. (b) Comparison against End-to-End PSG model demonstrates the benefits of foundation model pre-training even under temporal distribution shift. These results highlight SleepFM's robust generalization to more recent patients. Overall, most points fall below the diagonal, demonstrating that SleepFM outperforms the baseline models for the majority of conditions.

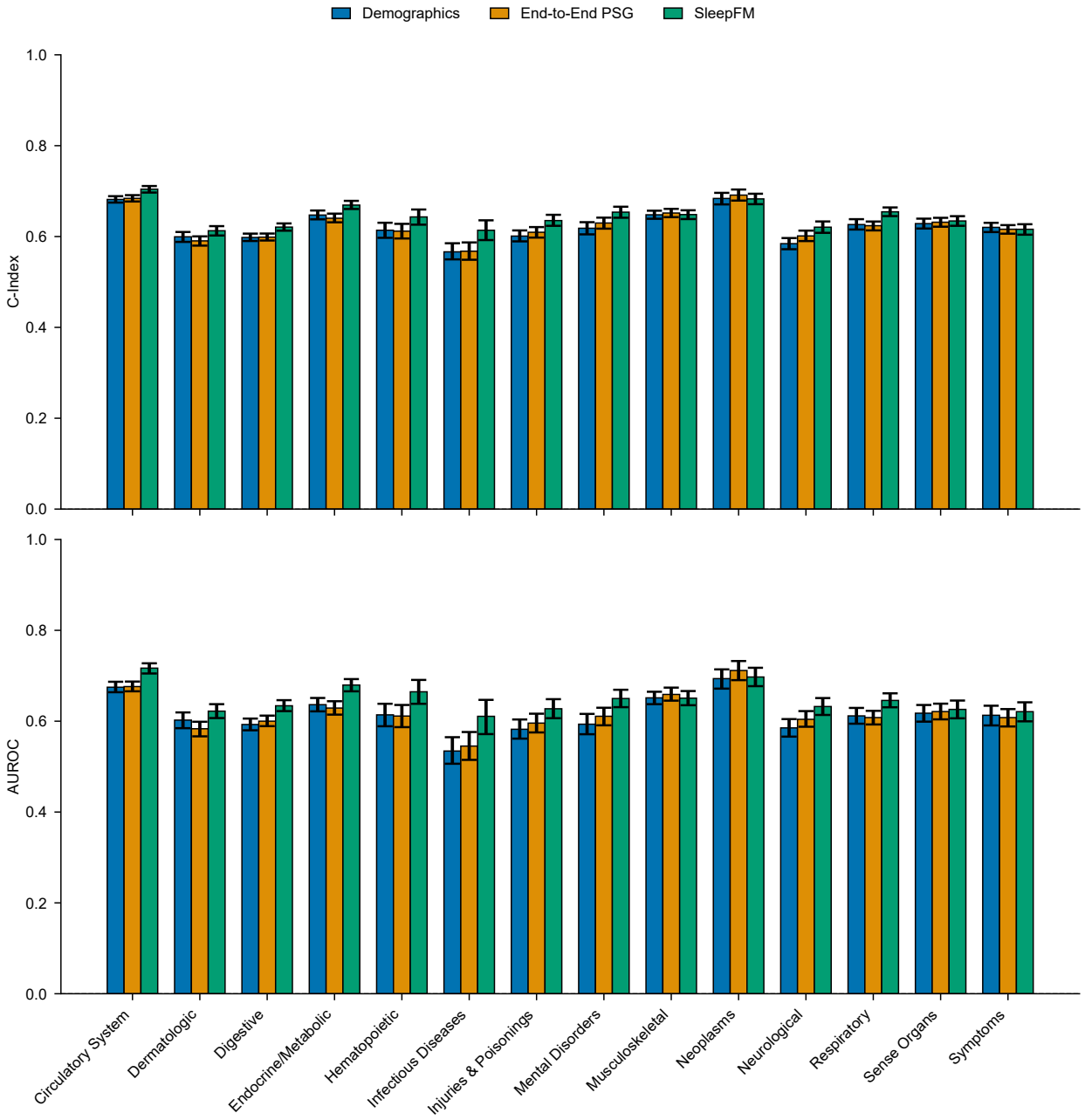

Supplementary Figure 7. Performance comparison of SleepFM with baseline models on the temporal test set (2020 onwards), showing average C-Index and 6-year AUROC metrics across disease categories. The demographics baseline uses only clinical features (age, gender, BMI, and race/ethnicity), while the End-to-End PSG baseline is trained directly on raw PSG signals without pre-training. Despite the temporal distribution shift, SleepFM maintains its performance advantages over both baselines across most disease categories, demonstrating robust generalization to more recent patients.

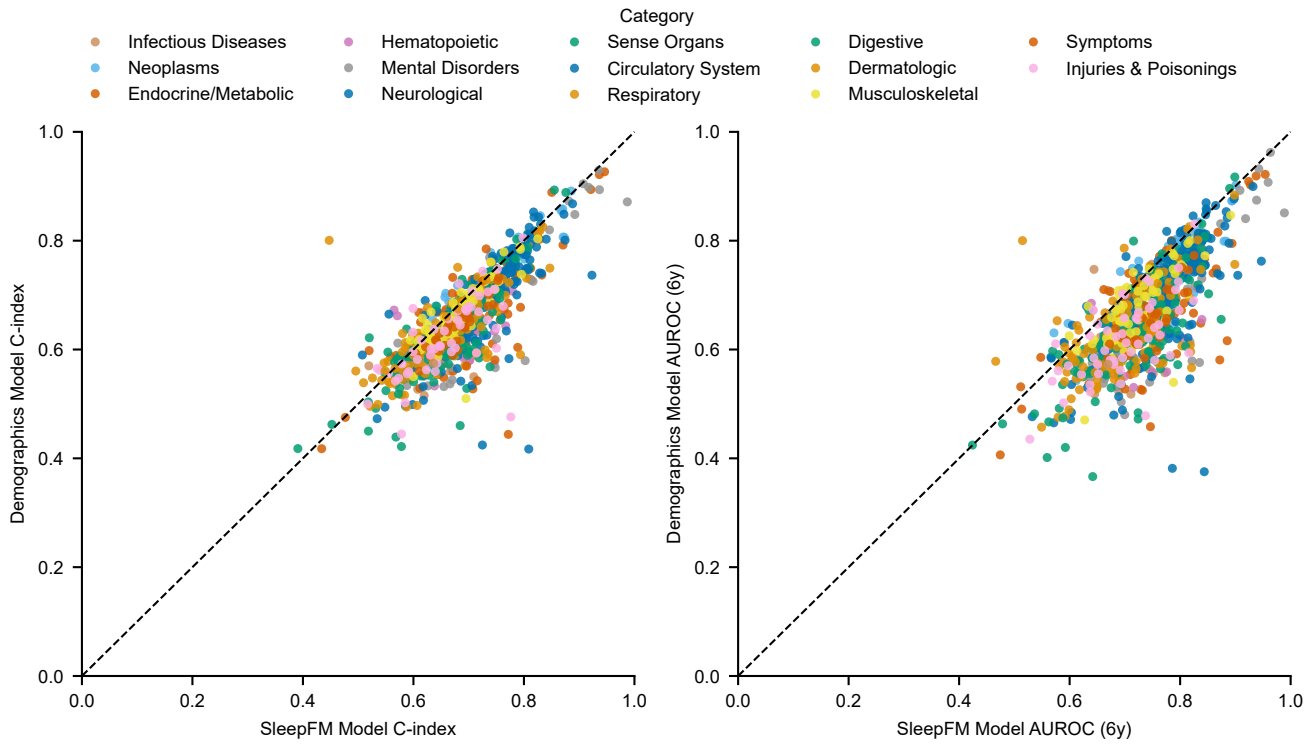

(a) Comparison with demographics-only baseline

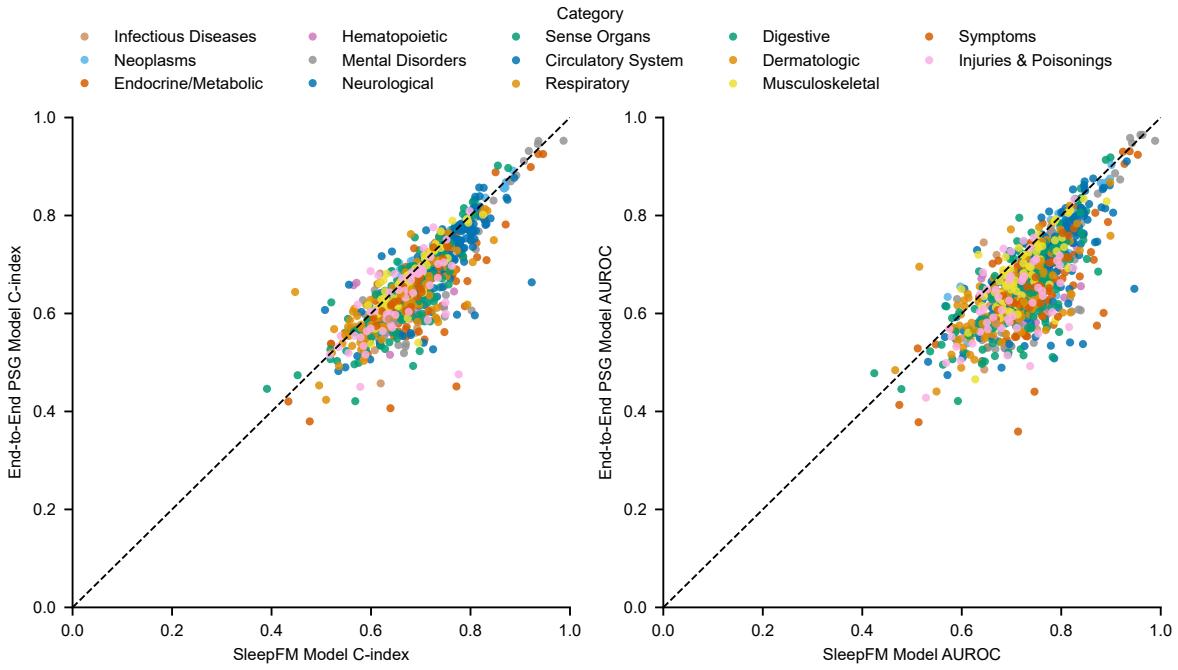

(b) Comparison with End-to-End PSG model

Supplementary Figure 8. Performance comparison of SleepFM with baseline models on the test set using C-Index and 6-year AUROC metrics. Each point represents a disease phenotype. (a) Comparison against the demographics-only baseline shows points consistently below the diagonal, indicating superior performance by SleepFM. (b) Comparison against the End-to-End PSG model highlights the advantages of foundation model pre-training over direct supervised learning from raw PSG signals. Overall, most points fall below the diagonal, demonstrating that SleepFM outperforms the baseline models for the majority of conditions.

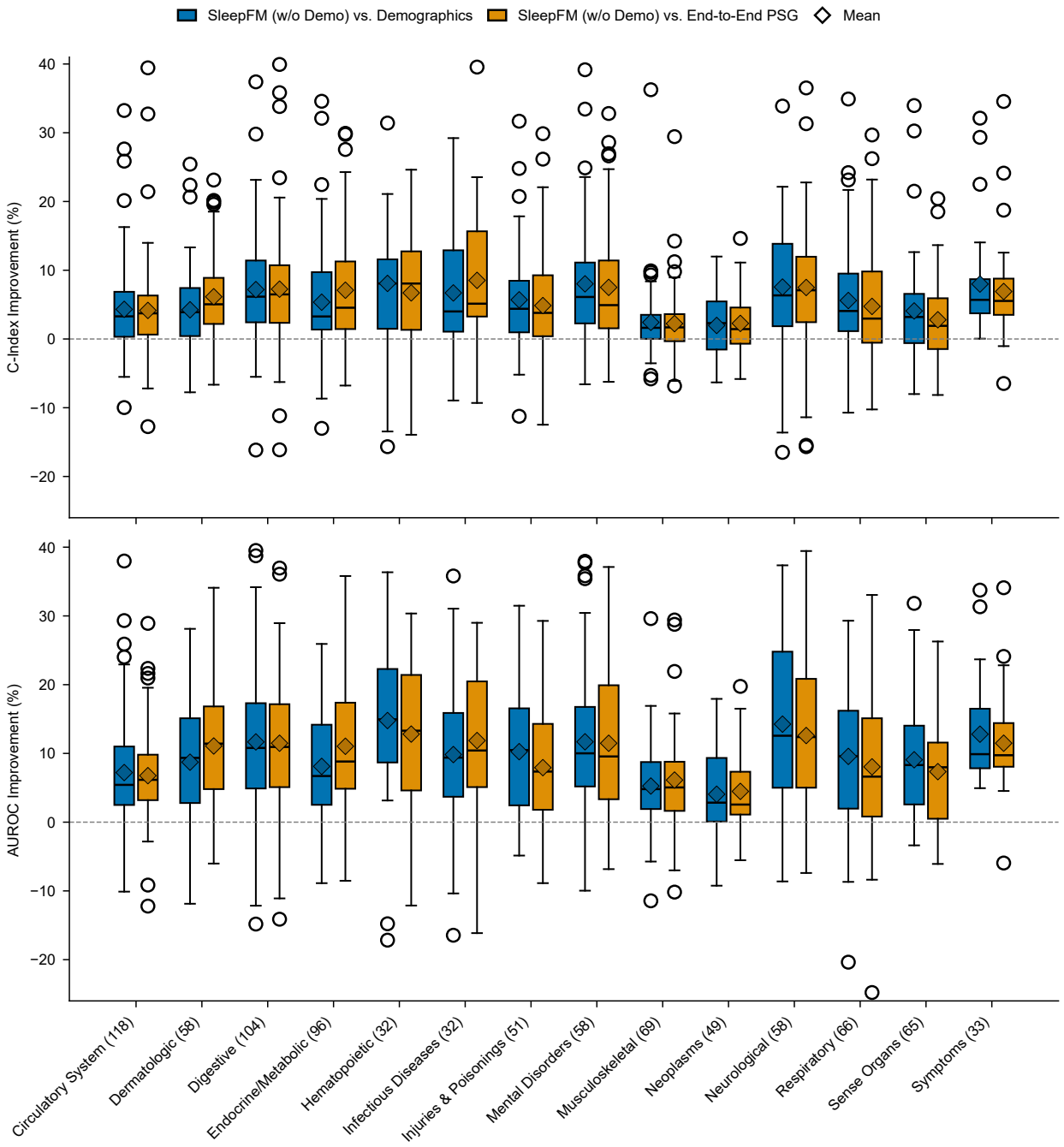

Supplementary Figure 9. Performance improvements of SleepFM over baseline models across disease categories. This version of SleepFM excludes demographic inputs, while the End-to-End PSG model includes age and sex. Results show percentage improvements in C-Index and 6-year AUROC on the test set. Compared with the demographics-only model (age, sex, BMI, and race/ethnicity), SleepFM achieves broad gains, especially for neurological and hematopoietic conditions. The comparison with the End-to-End PSG model underscores the value of foundation model pre-training for robust sleep representations. Each box shows the distribution of disease-level percentage improvements by category, with C-Index (top) and AUROC (bottom). Boxes indicate interquartile ranges (IQR), whiskers extend to 1.5×IQR, outliers are points, and diamonds mark mean improvements. The dashed line at zero denotes no improvement.

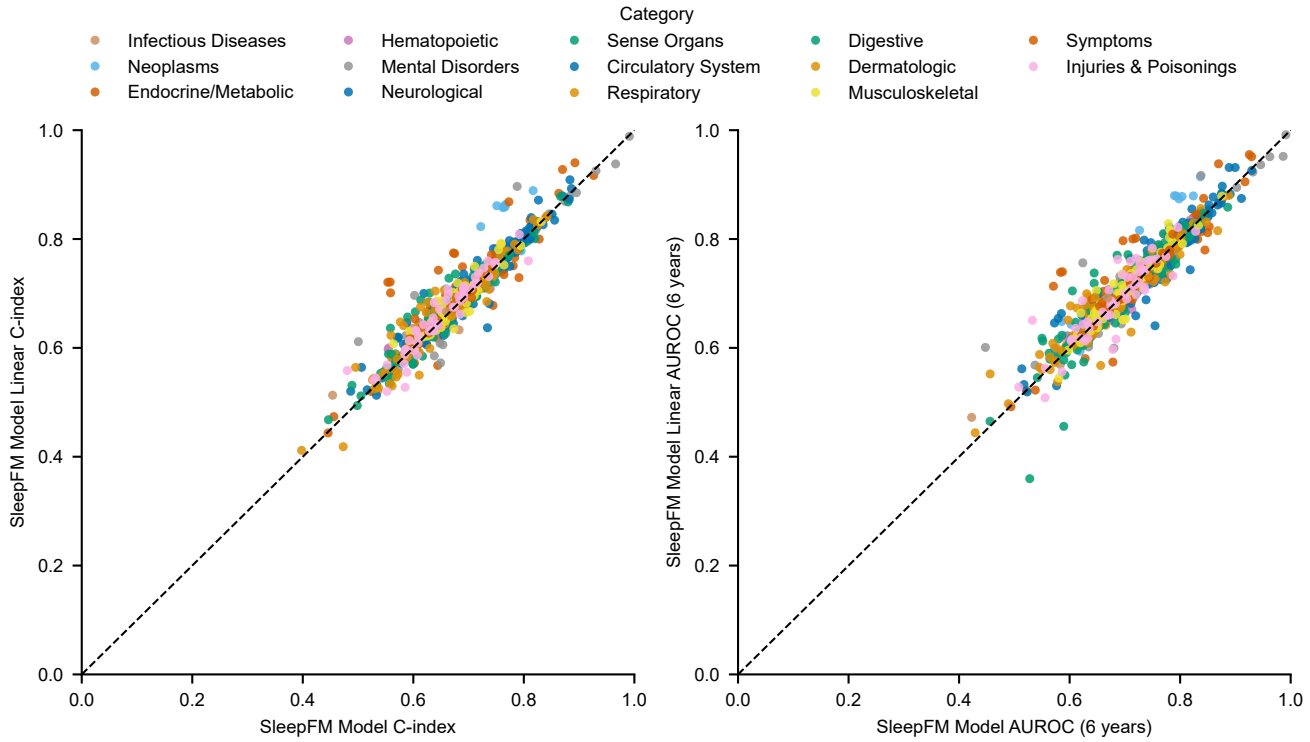

(a) Comparison between LSTM and linear finetuning heads for SleepFM.

Supplementary Figure 10. Performance comparison between different finetuning heads for SleepFM using C-Index and 6-year AUROC metrics. Each point represents a disease phenotype. The LSTM-based head shows only a modest advantage over the linear classifier, with an average improvement of 1.98% in C-Index and 1.72% in AUROC. This suggests that the strength of SleepFM lies primarily in the expressiveness of its pretrained embeddings, rather than complexity in the downstream architecture.

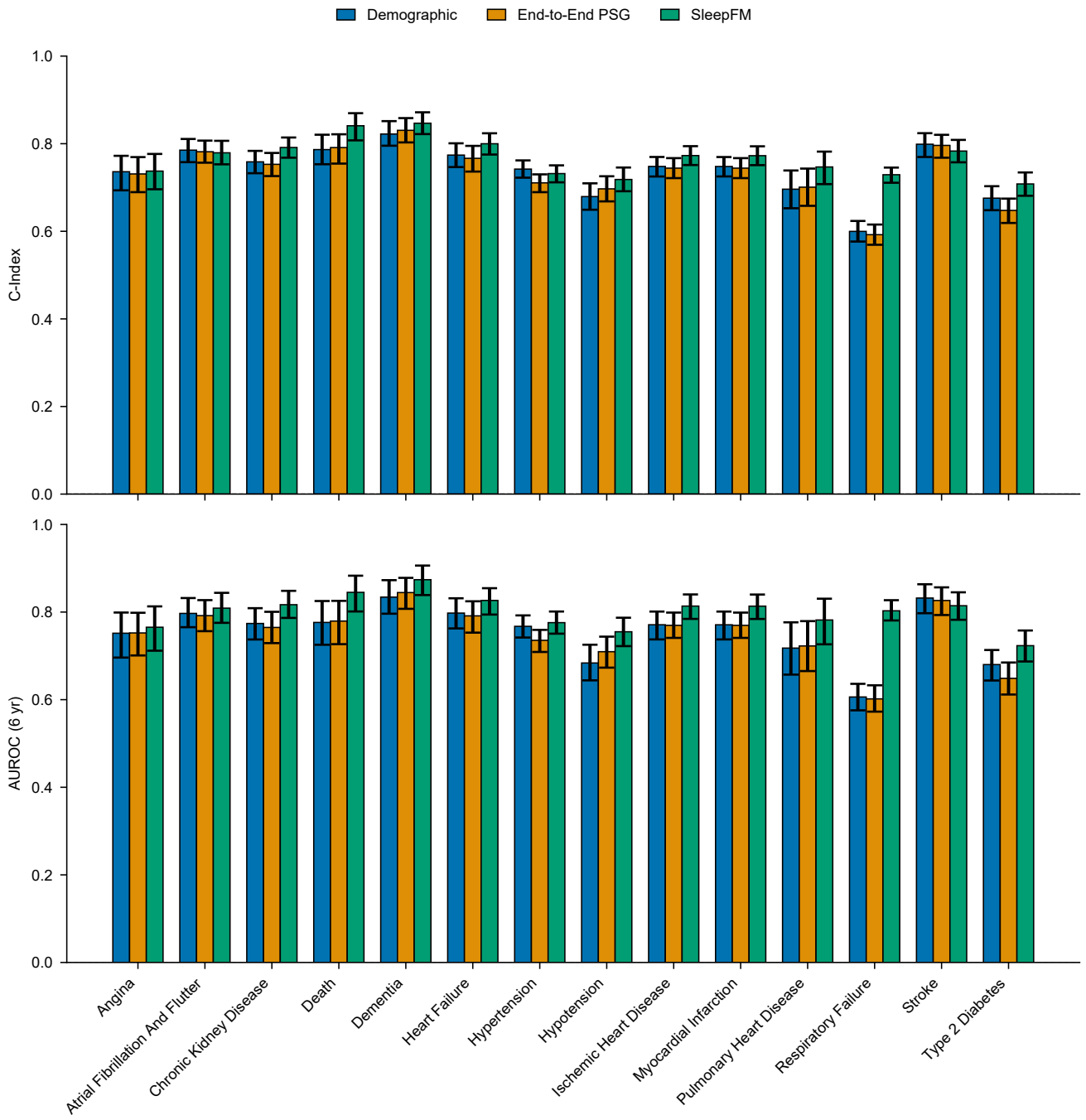

Supplementary Figure 11. Performance comparison across clinically relevant diseases selected in consultation with sleep experts. The plot compares SleepFM against two baselines: a demographics-only model using clinical features (age, gender, BMI, and race/ethnicity) and an End-to-End PSG model trained directly on raw PSG signals. Performance is evaluated on the test set using multiple metrics: C-Index and 6-year AUROC. The selected conditions include critical health outcomes such as death, heart failure, stroke, and dementia. SleepFM demonstrates superior predictive performance across these important clinical endpoints compared to both baseline approaches.

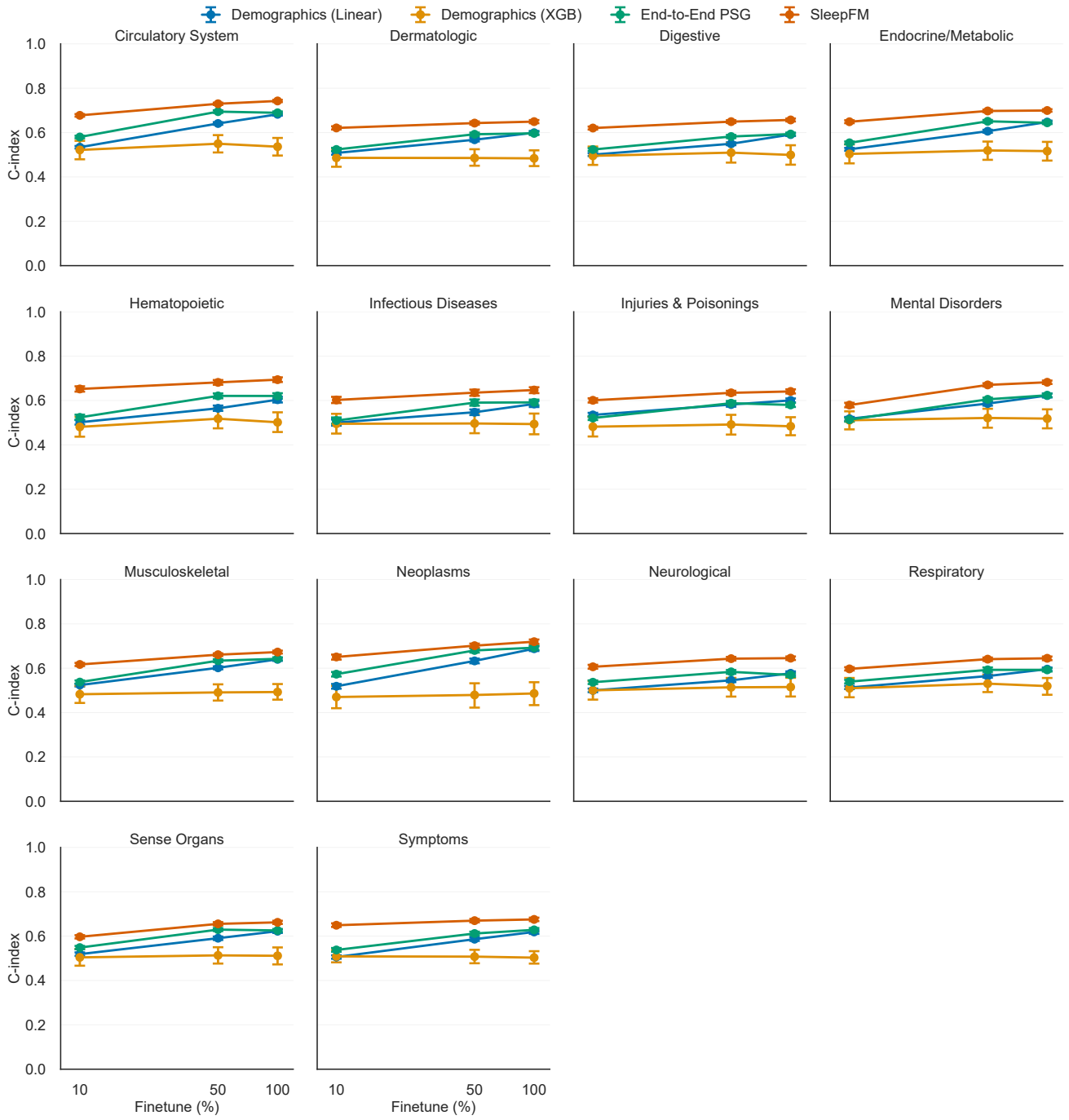

Supplementary Figure 12. Scaling behavior of fine-tuning SleepFM on the SSC dataset. We progressively increased the proportion of labeled SSC data used during fine-tuning, from 10% to 100%. The plots show C-Index performance across multiple outcome categories. Notably, SleepFM achieves strong predictive performance even with just 10% of the training data, with performance improving consistently as more labeled data is used. Here, 100% corresponds to 6,000 SSC examples—substantially fewer than the full fine-tuning dataset of 24,137 examples. Note that while the same SSC data was used during fine-tuning and seen by the SleepFM model during pretraining, the pretraining objective was entirely different and lacked disease supervision, minimizing potential bias.

Supplementary Table 1. F1 scores for SleepFM and PhysioEx models on DCSM and HMC in an external validation setting (no site-specific fine-tuning).

	DCSM	HMC
SeqSleepNet	0.62	0.64
Chambon2018	0.43	0.65
TinySleepNet	0.34	0.63
SleepFM	0.68	0.55

Supplementary Table 2. Sleep staging results (macro F1 score) when pretrained on different cohorts, finetuned and tested of SHHS.

Pretraining data set			
SSC	**MESA**	**MROS**	**Bioserenity**
0.65	0.66	0.66	0.65

Supplementary Table 3. Cross-dataset generalization results (macro F1 score) for sleep staging models trained on one cohort and tested on others. Diagonal values represent within-dataset performance.

Pretrain + Finetune	MESA (test)	MrOS (test)	Stanford (test)	Avg. transfer
MESA	0.64	0.55	0.32	0.44
MrOS	0.40	0.65	0.39	0.40
Stanford	0.30	0.38	0.54	0.34
Avg. test reception	0.35	0.47	0.36	–

Supplementary Table 4. Sleep staging results (macro F1 score) using multi-dataset pretraining and fine-tuning. All models were pretrained on MESA, MrOS, Stanford, and Bioserenity, and fine-tuned on MESA, MrOS, Stanford, and SHHS.

Test dataset	MESA	MrOS	Stanford
Macro F1	0.74	0.74	0.67

Phecode	Phenotype	Category	C-Index	AUROC (6 Years)	Prevalence (%)
290.11	Alzheimer's disease	mental disorders	0.91 (0.87, 0.94)	0.96 (0.94, 0.98)	1.18
332.0	Parkinson's disease	neurological	0.89 (0.85, 0.92)	0.93 (0.89, 0.96)	1.33
185.0	Cancer of prostate	neoplasms	0.89 (0.86, 0.91)	0.90 (0.87, 0.93)	1.97
290.1	Dementias	mental disorders	0.88 (0.85, 0.90)	0.91 (0.87, 0.94)	2.99
218.1	Uterine leiomyoma	neoplasms	0.87 (0.85, 0.89)	0.88 (0.85, 0.91)	1.68
428.4	Heart failure with preserved EF [Diastolic heart failure]	circulatory system	0.87 (0.85, 0.90)	0.90 (0.86, 0.93)	2.98
218.0	Benign neoplasm of uterus	neoplasms	0.87 (0.85, 0.89)	0.88 (0.84, 0.91)	1.71
250.25	Diabetes type 2 with peripheral circulatory disorders	endocrine/metabolic	0.87 (0.83, 0.91)	0.89 (0.85, 0.93)	1.07
174.0	Breast cancer	neoplasms	0.87 (0.83, 0.90)	0.90 (0.86, 0.93)	1.47
174.11	Malignant neoplasm of female breast	neoplasms	0.87 (0.83, 0.90)	0.89 (0.85, 0.93)	1.52
504.0	Other alveolar and parietoalveolar pneumonopathy	respiratory	0.85 (0.80, 0.89)	0.90 (0.84, 0.95)	1.1
290.0	Delirium dementia and amnestic and other cognitive disorders	mental disorders	0.85 (0.82, 0.87)	0.87 (0.84, 0.91)	4.78
401.21	Hypertensive heart disease	circulatory system	0.84 (0.82, 0.86)	0.88 (0.85, 0.91)	4.01
496.21	Obstructive chronic bronchitis	respiratory	0.83 (0.79, 0.87)	0.90 (0.86, 0.93)	1.38
276.42	Alkalosis	endocrine/metabolic	0.83 (0.77, 0.88)	0.87 (0.77, 0.93)	1.07
447.7	Aortic ectasia	circulatory system	0.83 (0.80, 0.86)	0.90 (0.87, 0.93)	2.36
172.22	Squamous cell carcinoma	neoplasms	0.83 (0.78, 0.87)	0.83 (0.78, 0.88)	1.52
474.2	Chronic tonsillitis and adenoiditis	respiratory	0.83 (0.81, 0.85)	0.82 (0.79, 0.84)	7.59
250.22	Type 2 diabetes with renal manifestations	endocrine/metabolic	0.83 (0.80, 0.85)	0.87 (0.84, 0.90)	3.16
172.11	Melanomas of skin	neoplasms	0.83 (0.77, 0.87)	0.83 (0.76, 0.90)	1.2
395.2	Nonrheumatic aortic valve disorders	circulatory system	0.83 (0.79, 0.86)	0.86 (0.82, 0.90)	2.95
741.3	Difficulty in walking	musculoskeletal	0.83 (0.79, 0.86)	0.89 (0.84, 0.93)	2.51
474.0	Acute and chronic tonsillitis	respiratory	0.82 (0.80, 0.84)	0.81 (0.79, 0.84)	7.86
440.9	Atherosclerosis of aorta	circulatory system	0.82 (0.79, 0.86)	0.86 (0.82, 0.89)	1.83
427.22	Atrial flutter	circulatory system	0.82 (0.78, 0.85)	0.88 (0.84, 0.92)	3.04
443.9	Peripheral vascular disease, unspecified	circulatory system	0.82 (0.79, 0.85)	0.85 (0.81, 0.89)	3.3
433.1	Occlusion and stenosis of precerebral arteries	circulatory system	0.82 (0.79, 0.84)	0.85 (0.81, 0.88)	3.51
426.23	Second degree AV block	circulatory system	0.82 (0.77, 0.86)	0.89 (0.85, 0.92)	1.14
290.2	Delirium due to conditions classified elsewhere	mental disorders	0.82 (0.76, 0.87)	0.81 (0.74, 0.88)	1.98
250.24	Type 2 diabetes with neurological manifestations	endocrine/metabolic	0.81 (0.77, 0.85)	0.86 (0.81, 0.90)	2.42
250.7	Diabetic retinopathy	endocrine/metabolic	0.81 (0.77, 0.85)	0.84 (0.79, 0.89)	1.79
274.2	Crystal arthropathies	endocrine/metabolic	0.81 (0.76, 0.85)	0.83 (0.75, 0.90)	1.16
433.21	Cerebral artery occlusion, with cerebral infarction	circulatory system	0.81 (0.78, 0.84)	0.85 (0.80, 0.89)	2.7
411.2	Myocardial infarction	circulatory system	0.81 (0.78, 0.84)	0.85 (0.82, 0.88)	5.53
362.27	Drusen (degenerative) of retina	sense organs	0.81 (0.77, 0.85)	0.83 (0.78, 0.88)	1.37
426.92	Cardiac defibrillator in situ	circulatory system	0.81 (0.75, 0.87)	0.85 (0.79, 0.89)	1.08
292.2	Mild cognitive impairment	mental disorders	0.81 (0.78, 0.84)	0.84 (0.80, 0.88)	3.29
440.2	Atherosclerosis of the extremities	circulatory system	0.81 (0.74, 0.86)	0.84 (0.75, 0.90)	1.21
526.3	Anomalies of jaw size/symmetry	digestive	0.81 (0.77, 0.84)	0.84 (0.80, 0.88)	2.66
433.2	Occlusion of cerebral arteries	circulatory system	0.81 (0.77, 0.84)	0.85 (0.80, 0.89)	2.81
362.2	Degeneration of macula and posterior pole of retina	sense organs	0.81 (0.78, 0.83)	0.84 (0.81, 0.87)	4.34
411.8	Other chronic ischemic heart disease, unspecified	circulatory system	0.81 (0.76, 0.85)	0.81 (0.76, 0.86)	1.64
707.2	Chronic ulcer of leg or foot	dermatologic	0.80 (0.76, 0.85)	0.84 (0.79, 0.88)	1.12
428.3	Heart failure with reduced EF [Systolic or combined heart failure]	circulatory system	0.80 (0.77, 0.84)	0.83 (0.78, 0.87)	3.7
430.0	Intracranial hemorrhage	circulatory system	0.80 (0.74, 0.86)	0.82 (0.73, 0.90)	1.49
315.0	Develomental delays and disorders	mental disorders	0.80 (0.77, 0.84)	0.84 (0.79, 0.87)	2.65
415.1	Acute pulmonary heart disease	circulatory system	0.80 (0.75, 0.85)	0.84 (0.77, 0.90)	1.73
172.1	Melanomas of skin, dx or hx	neoplasms	0.80 (0.74, 0.86)	0.79 (0.69, 0.88)	1.34
415.11	Pulmonary embolism and infarction, acute	circulatory system	0.80 (0.75, 0.85)	0.85 (0.78, 0.91)	1.71
440.0	Atherosclerosis	circulatory system	0.80 (0.77, 0.83)	0.84 (0.80, 0.87)	3.66
401.2	Hypertensive heart and/or renal disease	circulatory system	0.80 (0.77, 0.82)	0.83 (0.80, 0.86)	7.58
428.0	Congestive heart failure; nonhypertensive	circulatory system	0.80 (0.77, 0.82)	0.83 (0.79, 0.85)	6.32
740.2	Osteoarthrosis, generalized	musculoskeletal	0.80 (0.76, 0.83)	0.85 (0.80, 0.89)	2.09
426.2	Atrioventricular [AV] block	circulatory system	0.79 (0.76, 0.83)	0.84 (0.80, 0.88)	4.26
374.6	Dermatochalasis	sense organs	0.79 (0.75, 0.83)	0.85 (0.80, 0.90)	2.21
249.0	Secondary diabetes mellitus	endocrine/metabolic	0.79 (0.74, 0.84)	0.82 (0.76, 0.88)	2.63
509.2	Respiratory insufficiency	respiratory	0.79 (0.72, 0.85)	0.82 (0.72, 0.91)	1.23
743.1	Osteoporosis	musculoskeletal	0.79 (0.77, 0.82)	0.81 (0.78, 0.85)	6
411.4	Coronary atherosclerosis	circulatory system	0.79 (0.77, 0.81)	0.83 (0.81, 0.86)	10.3
743.11	Osteoporosis NOS	musculoskeletal	0.79 (0.77, 0.82)	0.82 (0.78, 0.85)	6.24
426.32	Left bundle branch block	circulatory system	0.79 (0.76, 0.83)	0.82 (0.77, 0.87)	3.91
172.3	Carcinoma in situ of skin	neoplasms	0.79 (0.73, 0.84)	0.83 (0.76, 0.89)	1.01
285.21	Anemia in chronic kidney disease	hematopoietic	0.79 (0.74, 0.83)	0.78 (0.70, 0.85)	1.89
427.11	Paroxysmal supraventricular tachycardia	circulatory system	0.79 (0.76, 0.81)	0.87 (0.84, 0.90)	7.57
362.26	Macular puckering of retina	sense organs	0.79 (0.76, 0.82)	0.83 (0.79, 0.87)	2.4
275.6	Hypercalcemia	endocrine/metabolic	0.79 (0.73, 0.84)	0.83 (0.74, 0.91)	1.59
550.4	Umbilical hernia	digestive	0.79 (0.74, 0.83)	0.84 (0.78, 0.90)	1.25
365.1	Open-angle glaucoma	sense organs	0.78 (0.73, 0.83)	0.83 (0.77, 0.88)	1.16
427.1	Paroxysmal tachycardia, unspecified	circulatory system	0.78 (0.76, 0.81)	0.87 (0.84, 0.89)	8.33
350.2	Abnormality of gait	neurological	0.78 (0.76, 0.81)	0.83 (0.80, 0.86)	7.69
427.21	Atrial fibrillation	circulatory system	0.78 (0.75, 0.81)	0.81 (0.77, 0.84)	6.29
426.21	First degree AV block	circulatory system	0.78 (0.74, 0.82)	0.83 (0.78, 0.87)	3.45
427.8	Sinoatrial node dysfunction (Bradycardia)	circulatory system	0.78 (0.73, 0.83)	0.77 (0.70, 0.84)	2.23
411.1	Unstable angina (intermediate coronary syndrome)	circulatory system	0.78 (0.74, 0.82)	0.80 (0.75, 0.85)	1.66
285.1	Acute posthemorrhagic anemia	hematopoietic	0.78 (0.75, 0.81)	0.83 (0.79, 0.87)	4.57
427.2	Atrial fibrillation and flutter	circulatory system	0.78 (0.75, 0.81)	0.81 (0.78, 0.84)	6.38
427.12	Paroxysmal ventricular tachycardia	circulatory system	0.78 (0.74, 0.82)	0.84 (0.79, 0.88)	3.54
428.1	Congestive heart failure (CHF) NOS	circulatory system	0.78 (0.74, 0.81)	0.80 (0.76, 0.84)	5.06
442.1	Aortic aneurysm	circulatory system	0.78 (0.72, 0.83)	0.82 (0.74, 0.89)	1.55
366.2	Senile cataract	sense organs	0.78 (0.75, 0.80)	0.82 (0.79, 0.85)	9.07
427.61	Supraventricular premature beats	circulatory system	0.77 (0.75, 0.80)	0.83 (0.80, 0.86)	6.95
394.1	Mitral valve stenosis and aortic valve stenosis	circulatory system	0.77 (0.72, 0.83)	0.78 (0.71, 0.85)	1.35
411.0	Ischemic Heart Disease	circulatory system	0.77 (0.75, 0.79)	0.81 (0.78, 0.84)	12.22

Supplementary Table 5. Summary of SleepFM performance metrics, including C-Index and AUROC (6 years) on the Stanford dataset. Results are sorted by C-Index, ensuring that both AUROC and C-Index exceed 0.75, with 95% confidence intervals that do not overlap with 0.5 (random chance). All conditions have statistically significant p-values (<0.01) after Bonferroni correction. Notable top conditions include Alzheimer's disease, Parkinson's disease, and dementias.

Disease	Phecode	Phenotype
Dementia	290.0	Delirium dementia and amnestic and other cognitive disorders
Dementia	290.1	Dementias
Dementia	290.16	Vascular dementia
Dementia	290.12	Dementia with cerebral degenerations
Dementia	290.11	Alzheimer's disease
Dementia	290.13	Senile dementia
Myocardial Infarction	411.0	Ischemic Heart Disease
Myocardial Infarction	411.2	Myocardial infarction
Ischemic Heart Disease	411.0	Ischemic Heart Disease
Ischemic Heart Disease	411.8	Other chronic ischemic heart disease, unspecified
Ischemic Heart Disease	411.9	Other acute and subacute forms of ischemic heart disease
Angina	411.1	Unstable angina (intermediate coronary syndrome)
Angina	411.3	Angina pectoris
Hypertension	401.0	Hypertension
Hypertension	401.1	Essential hypertension
Hypertension	401.2	Hypertensive heart and/or renal disease
Hypertension	401.21	Hypertensive heart disease
Hypertension	401.3	Other hypertensive complications
Hypertension	401.22	Hypertensive chronic kidney disease
Hypotension	458.0	Hypotension
Hypotension	458.1	Orthostatic hypotension
Hypotension	458.2	Iatrogenic hypotension
Hypotension	458.9	Hypotension NOS
Pulmonary Heart Disease	415.0	Pulmonary heart disease
Pulmonary Heart Disease	415.2	Chronic pulmonary heart disease
Pulmonary Heart Disease	415.1	Acute pulmonary heart disease
Pulmonary Heart Disease	415.21	Primary pulmonary hypertension
Pulmonary Heart Disease	415.11	Pulmonary embolism and infarction, acute
Atrial Fibrillation and Flutter	427.0	Cardiac dysrhythmias
Atrial Fibrillation and Flutter	427.2	Atrial fibrillation and flutter
Atrial Fibrillation and Flutter	427.21	Atrial fibrillation
Atrial Fibrillation and Flutter	427.22	Atrial flutter
Respiratory Failure	509.0	Respiratory failure, insufficiency, arrest
Respiratory Failure	509.1	Respiratory failure
Respiratory Failure	509.2	Respiratory insufficiency
Respiratory Failure	509.3	Pulmonary insufficiency or respiratory failure following trauma and surgery
Respiratory Failure	509.5	Respiratory arrest
Respiratory Failure	509.8	Dependence on respirator [Ventilator] or supplemental oxygen

Supplementary Table 6. Hand-selected diseases and their corresponding phecode groupings. These diseases were chosen for their relevance to sleep, in consultation with a sleep expert. All phecode groupings were reviewed and curated by a medical professional.

Phecode	Phenotype	Category	Wake	Stage1/2	Stage3	REM	Best
290.12	Dementia With Cerebral Degenerations	Mental Disorders	0.88 (0.82, 0.93)	0.87 (0.78, 0.93)	0.80 (0.68, 0.90)	0.82 (0.69, 0.91)	Wake
440.1	Atherosclerosis Of Renal Artery	Circulatory System	0.78 (0.65, 0.88)	0.76 (0.53, 0.94)	0.73 (0.50, 0.89)	0.74 (0.55, 0.90)	Wake
427.22	Atrial Flutter	Circulatory System	0.77 (0.73, 0.81)	0.77 (0.72, 0.81)	0.75 (0.70, 0.79)	0.75 (0.72, 0.79)	Wake
290.1	Dementias	Mental Disorders	0.77 (0.73, 0.80)	0.75 (0.71, 0.79)	0.75 (0.71, 0.79)	0.75 (0.71, 0.80)	Wake
306.1	Mental Disorders Durring/After Pregnancy	Mental Disorders	0.77 (0.68, 0.86)	0.72 (0.53, 0.86)	0.70 (0.51, 0.87)	0.67 (0.48, 0.83)	Wake
474.0	Acute And Chronic Tonsillitis	Respiratory	0.76 (0.74, 0.79)	0.76 (0.73, 0.79)	0.75 (0.72, 0.78)	0.76 (0.74, 0.79)	Wake
440.21	Atherosclerosis Of Native Arteries Of The Extremities With Ulceration Or Gangrene	Circulatory System	0.82 (0.63, 0.95)	0.95 (0.89, 1.00)	0.83 (0.74, 0.93)	0.83 (0.71, 0.95)	Stage 1/2
290.13	Senile Dementia	Mental Disorders	0.90 (0.85, 0.97)	0.94 (0.89, 0.99)	0.66 (0.39, 1.00)	0.89 (0.85, 0.94)	Stage 1/2
264.9	Lack Of Normal Physiological Development, Unspecified	Endocrine/Metabolic	0.87 (0.78, 0.95)	0.91 (0.84, 0.96)	0.91 (0.84, 0.96)	0.86 (0.77, 0.94)	Stage 1/2
313.3	Autism	Mental Disorders	0.88 (0.82, 0.93)	0.88 (0.83, 0.93)	0.88 (0.81, 0.93)	0.87 (0.79, 0.92)	Stage 1/2
411.8	Other Chronic Ischemic Heart Disease, Unspecified	Circulatory System	0.77 (0.73, 0.82)	0.83 (0.79, 0.86)	0.73 (0.69, 0.77)	0.78 (0.72, 0.82)	Stage 1/2
426.24	Atrioventricular Block, Complete	Circulatory System	0.82 (0.76, 0.87)	0.82 (0.75, 0.89)	0.80 (0.74, 0.87)	0.82 (0.76, 0.87)	Stage 1/2
250.25	Diabetes Type 2 With Peripheral Circulatory Disorders	Endocrine/Metabolic	0.81 (0.76, 0.87)	0.82 (0.76, 0.88)	0.75 (0.69, 0.80)	0.81 (0.76, 0.86)	Stage 1/2
496.21	Obstructive Chronic Bronchitis	Respiratory	0.74 (0.68, 0.79)	0.82 (0.78, 0.86)	0.71 (0.65, 0.76)	0.78 (0.73, 0.83)	Stage 1/2
264.0	Lack Of Normal Physiological Development	Endocrine/Metabolic	0.78 (0.68, 0.87)	0.81 (0.72, 0.88)	0.78 (0.67, 0.87)	0.79 (0.70, 0.87)	Stage 1/2
426.92	Cardiac Defibrillator In Situ	Circulatory System	0.76 (0.68, 0.82)	0.79 (0.72, 0.87)	0.79 (0.74, 0.85)	0.74 (0.67, 0.81)	Stage 1/2
276.42	Alkalosis	Endocrine/Metabolic	0.74 (0.65, 0.82)	0.79 (0.71, 0.85)	0.72 (0.63, 0.80)	0.77 (0.70, 0.83)	Stage 1/2
250.22	Type 2 Diabetes With Renal Manifestations	Endocrine/Metabolic	0.72 (0.68, 0.76)	0.79 (0.75, 0.82)	0.75 (0.70, 0.79)	0.77 (0.73, 0.81)	Stage 1/2
331.0	Other Cerebral Degenerations	Neurological	0.74 (0.65, 0.81)	0.79 (0.72, 0.85)	0.75 (0.67, 0.81)	0.74 (0.67, 0.80)	Stage 1/2
427.4	Cardiac Arrest And Ventricular Fibrillation	Circulatory System	0.69 (0.60, 0.77)	0.78 (0.70, 0.85)	0.68 (0.58, 0.78)	0.66 (0.58, 0.75)	Stage 1/2
256.4	Polycystic Ovaries	Endocrine/Metabolic	0.76 (0.66, 0.84)	0.78 (0.70, 0.85)	0.73 (0.66, 0.79)	0.63 (0.54, 0.73)	Stage 1/2
250.1	Type 1 Diabetes	Endocrine/Metabolic	0.69 (0.61, 0.76)	0.78 (0.72, 0.83)	0.64 (0.56, 0.71)	0.71 (0.65, 0.77)	Stage 1/2
440.9	Atherosclerosis Of Aorta	Circulatory System	0.73 (0.68, 0.79)	0.77 (0.72, 0.81)	0.69 (0.63, 0.75)	0.75 (0.70, 0.80)	Stage 1/2
707.2	Chronic Ulcer Of Leg Or Foot	Dermatologic	0.72 (0.64, 0.79)	0.77 (0.71, 0.82)	0.69 (0.63, 0.75)	0.71 (0.63, 0.77)	Stage 1/2
707.1	Decubitus Ulcer	Dermatologic	0.74 (0.67, 0.81)	0.77 (0.72, 0.82)	0.69 (0.61, 0.76)	0.75 (0.68, 0.81)	Stage 1/2
256.0	Ovarian Dysfunction	Endocrine/Metabolic	0.74 (0.65, 0.81)	0.77 (0.69, 0.84)	0.71 (0.64, 0.77)	0.63 (0.54, 0.71)	Stage 1/2
287.32	Secondary Thrombocytopenia	Hematopoietic	0.75 (0.67, 0.82)	0.77 (0.68, 0.84)	0.68 (0.57, 0.77)	0.72 (0.62, 0.80)	Stage 1/2
426.9	Cardiac Pacemaker/Device In Situ	Circulatory System	0.72 (0.68, 0.76)	0.76 (0.72, 0.81)	0.75 (0.71, 0.80)	0.71 (0.67, 0.75)	Stage 1/2
426.21	First Degree Av Block	Circulatory System	0.75 (0.71, 0.79)	0.76 (0.72, 0.80)	0.69 (0.64, 0.74)	0.74 (0.69, 0.79)	Stage 1/2
428.3	Heart Failure With Reduced Ef [Systolic Or Combined Heart Failure]	Circulatory System	0.74 (0.71, 0.78)	0.76 (0.73, 0.80)	0.71 (0.67, 0.75)	0.73 (0.70, 0.77)	Stage 1/2
430.0	Intracranial Hemorrhage	Circulatory System	0.73 (0.65, 0.80)	0.76 (0.70, 0.81)	0.70 (0.63, 0.77)	0.74 (0.67, 0.81)	Stage 1/2
433.8	Late Effects Of Cerebrovascular Disease	Circulatory System	0.74 (0.66, 0.80)	0.76 (0.69, 0.81)	0.70 (0.62, 0.76)	0.69 (0.61, 0.76)	Stage 1/2
443.9	Peripheral Vascular Disease, Unspecified	Circulatory System	0.75 (0.71, 0.78)	0.76 (0.72, 0.80)	0.69 (0.65, 0.73)	0.76 (0.72, 0.79)	Stage 1/2
415.11	Pulmonary Embolism And Infarction, Acute	Circulatory System	0.72 (0.66, 0.77)	0.76 (0.70, 0.81)	0.74 (0.68, 0.79)	0.70 (0.63, 0.77)	Stage 1/2
250.24	Type 2 Diabetes With Neurological Manifestations	Endocrine/Metabolic	0.72 (0.66, 0.77)	0.76 (0.71, 0.81)	0.68 (0.63, 0.72)	0.75 (0.71, 0.79)	Stage 1/2
172.11	Melanomas Of Skin	Neoplasms	0.68 (0.60, 0.75)	0.76 (0.70, 0.82)	0.75 (0.67, 0.82)	0.70 (0.63, 0.77)	Stage 1/2
332.0	Parkinson'S Disease	Neurological	0.76 (0.69, 0.81)	0.76 (0.70, 0.81)	0.73 (0.67, 0.78)	0.75 (0.68, 0.82)	Stage 1/2
377.1	Optic Atrophy	Sense Organs	0.70 (0.64, 0.77)	0.76 (0.70, 0.82)	0.66 (0.59, 0.73)	0.69 (0.63, 0.77)	Stage 1/2
415.1	Acute Pulmonary Heart Disease	Circulatory System	0.72 (0.66, 0.77)	0.75 (0.69, 0.81)	0.74 (0.68, 0.80)	0.70 (0.63, 0.76)	Stage 1/2
440.0	Atherosclerosis	Circulatory System	0.72 (0.68, 0.75)	0.75 (0.71, 0.79)	0.69 (0.65, 0.73)	0.71 (0.67, 0.75)	Stage 1/2
428.0	Congestive Heart Failure; Nonhypertensive	Circulatory System	0.72 (0.69, 0.75)	0.75 (0.72, 0.78)	0.72 (0.69, 0.75)	0.73 (0.70, 0.76)	Stage 1/2
457.2	Encounter For Long-Term (Current) Use Of Antiplatelets/Antithrombotics	Circulatory System	0.71 (0.66, 0.76)	0.75 (0.72, 0.79)	0.71 (0.67, 0.76)	0.72 (0.67, 0.77)	Stage 1/2
426.32	Left Bundle Branch Block	Circulatory System	0.74 (0.71, 0.78)	0.75 (0.71, 0.79)	0.72 (0.68, 0.76)	0.74 (0.70, 0.78)	Stage 1/2
509.1	Respiratory Failure	Respiratory	0.70 (0.66, 0.74)	0.75 (0.71, 0.79)	0.68 (0.64, 0.73)	0.72 (0.67, 0.76)	Stage 1/2
509.2	Respiratory Insufficiency	Respiratory	0.71 (0.64, 0.77)	0.75 (0.70, 0.81)	0.71 (0.63, 0.78)	0.69 (0.61, 0.76)	Stage 1/2
426.91	Cardiac Pacemaker In Situ	Circulatory System	0.74 (0.69, 0.78)	0.78 (0.73, 0.82)	0.79 (0.74, 0.83)	0.73 (0.68, 0.77)	Stage 3
425.2	Secondary/Extrinsic Cardiomyopathies	Circulatory System	0.59 (0.49, 0.69)	0.60 (0.51, 0.68)	0.77 (0.66, 0.86)	0.58 (0.48, 0.69)	Stage 3
428.4	Heart Failure With Preserved Ef [Diastolic Heart Failure]	Circulatory System	0.80 (0.76, 0.83)	0.81 (0.78, 0.85)	0.76 (0.73, 0.80)	0.82 (0.78, 0.85)	REM
290.16	Vascular Dementia	Mental Disorders	0.80 (0.72, 0.87)	0.76 (0.67, 0.84)	0.77 (0.67, 0.86)	0.80 (0.71, 0.87)	REM
362.29	Macular Degeneration (Senile) Of Retina Nos	Sense Organs	0.77 (0.72, 0.83)	0.78 (0.72, 0.83)	0.70 (0.62, 0.77)	0.79 (0.74, 0.84)	REM
315.2	Speech And Language Disorder	Mental Disorders	0.77 (0.67, 0.85)	0.74 (0.65, 0.82)	0.77 (0.68, 0.84)	0.78 (0.68, 0.85)	REM
401.21	Hypertensive Heart Disease	Circulatory System	0.72 (0.68, 0.76)	0.74 (0.71, 0.78)	0.74 (0.70, 0.77)	0.77 (0.73, 0.80)	REM
411.9	Other Acute And Subacute Forms Of Ischemic Heart Disease	Circulatory System	0.71 (0.62, 0.79)	0.69 (0.59, 0.79)	0.67 (0.58, 0.77)	0.77 (0.69, 0.85)	REM
426.8	Other Cardiac Conduction Disorders	Circulatory System	0.76 (0.72, 0.79)	0.75 (0.71, 0.79)	0.69 (0.65, 0.73)	0.77 (0.74, 0.81)	REM
290.0	Delirium Dementia And Amnestic And Other Cognitive Disorders	Mental Disorders	0.75 (0.72, 0.79)	0.74 (0.70, 0.77)	0.73 (0.70, 0.76)	0.77 (0.73, 0.80)	REM
290.2	Delirium Due To Conditions Classified Elsewhere	Mental Disorders	0.75 (0.70, 0.80)	0.73 (0.67, 0.79)	0.69 (0.63, 0.75)	0.77 (0.72, 0.82)	REM
474.2	Chronic Tonsillitis And Adenoiditis	Respiratory	0.77 (0.74, 0.79)	0.77 (0.74, 0.79)	0.75 (0.72, 0.78)	0.77 (0.74, 0.79)	REM
250.7	Diabetic Retinopathy	Endocrine/Metabolic	0.74 (0.67, 0.79)	0.73 (0.68, 0.78)	0.67 (0.61, 0.73)	0.76 (0.71, 0.81)	REM
264.2	Failure To Thrive (Childhood)	Endocrine/Metabolic	0.74 (0.62, 0.86)	0.73 (0.56, 0.86)	0.66 (0.51, 0.83)	0.75 (0.66, 0.86)	REM
260.2	Severe Protein-Calorie Malnutrition	Endocrine/Metabolic	0.73 (0.67, 0.78)	0.70 (0.64, 0.75)	0.62 (0.55, 0.68)	0.75 (0.70, 0.80)	REM
333.1	Essential Tremor	Neurological	0.69 (0.63, 0.76)	0.70 (0.62, 0.77)	0.65 (0.58, 0.71)	0.75 (0.68, 0.82)	REM
504.0	Other Alveolar And Parietoalveolar Pneumonopathy	Respiratory	0.72 (0.65, 0.79)	0.73 (0.65, 0.80)	0.75 (0.67, 0.83)	0.75 (0.67, 0.83)	REM

Supplementary Table 7. Performance comparison of models trained on different sleep stages across conditions. For each sleep stage, C-Index values are reported with 95% confidence intervals in parentheses. Only conditions where at least one sleep stage achieves a C-Index above 0.75 are included. Results are grouped by disease category and sorted alphabetically within each category. Stage 1/2 demonstrates the highest predictive performance across 39 conditions, followed by REM sleep with 15 conditions.

Phecode	Phenotype	Category	BAS	Respiratory	EKG	EMG	Best
313.3	Autism	Mental Disorders	0.89 (0.85, 0.93)	0.84 (0.77, 0.90)	0.86 (0.80, 0.91)	0.85 (0.80, 0.91)	BAS
290.12	Dementia With Cerebral Degenerations	Mental Disorders	0.88 (0.78, 0.95)	0.82 (0.75, 0.89)	0.83 (0.73, 0.91)	0.76 (0.67, 0.84)	BAS
290.16	Vascular Dementia	Mental Disorders	0.87 (0.82, 0.92)	0.78 (0.68, 0.87)	0.83 (0.75, 0.89)	0.78 (0.70, 0.85)	BAS
331.0	Other Cerebral Degenerations	Neurological	0.85 (0.80, 0.90)	0.74 (0.64, 0.82)	0.71 (0.62, 0.77)	0.74 (0.65, 0.82)	BAS
447.7	Aortic Ectasia	Circulatory System	0.82 (0.79, 0.85)	0.81 (0.78, 0.85)	0.80 (0.76, 0.84)	0.82 (0.78, 0.85)	BAS
250.7	Diabetic Retinopathy	Endocrine/Metabolic	0.82 (0.77, 0.86)	0.78 (0.74, 0.83)	0.80 (0.76, 0.84)	0.75 (0.69, 0.80)	BAS
264.0	Lack Of Normal Physiological Development	Endocrine/Metabolic	0.82 (0.74, 0.89)	0.77 (0.68, 0.85)	0.75 (0.65, 0.85)	0.80 (0.72, 0.87)	BAS
332.0	Parkinson'S Disease	Neurological	0.82 (0.76, 0.87)	0.82 (0.77, 0.86)	0.79 (0.73, 0.84)	0.78 (0.72, 0.83)	BAS
250.22	Type 2 Diabetes With Renal Manifestations	Endocrine/Metabolic	0.81 (0.78, 0.84)	0.78 (0.75, 0.81)	0.81 (0.78, 0.84)	0.77 (0.73, 0.80)	BAS
290.1	Dementias	Mental Disorders	0.81 (0.77, 0.84)	0.80 (0.76, 0.83)	0.78 (0.74, 0.81)	0.78 (0.74, 0.81)	BAS
362.29	Macular Degeneration (Senile) Of Retina Nos	Sense Organs	0.81 (0.76, 0.86)	0.74 (0.68, 0.80)	0.69 (0.61, 0.77)	0.75 (0.69, 0.81)	BAS
707.1	Decubitus Ulcer	Dermatologic	0.80 (0.74, 0.86)	0.71 (0.63, 0.79)	0.74 (0.67, 0.81)	0.78 (0.72, 0.83)	BAS
290.0	Delirium Dementia And Amnestic And Other Cognitive Disorders	Mental Disorders	0.80 (0.76, 0.83)	0.79 (0.75, 0.81)	0.78 (0.75, 0.81)	0.76 (0.72, 0.78)	BAS
504.0	Other Alveolar And Parietoalveolar Pneumonopathy	Respiratory	0.80 (0.73, 0.87)	0.80 (0.72, 0.87)	0.77 (0.70, 0.84)	0.79 (0.73, 0.86)	BAS
290.11	Alzheimer'S Disease	Mental Disorders	0.79 (0.74, 0.84)	0.76 (0.69, 0.82)	0.72 (0.66, 0.79)	0.74 (0.68, 0.79)	BAS
433.21	Cerebral Artery Occlusion, With Cerebral Infarction	Circulatory System	0.78 (0.74, 0.82)	0.75 (0.70, 0.79)	0.75 (0.71, 0.79)	0.77 (0.73, 0.81)	BAS
433.2	Occlusion Of Cerebral Arteries	Circulatory System	0.78 (0.73, 0.82)	0.74 (0.70, 0.79)	0.75 (0.70, 0.79)	0.77 (0.73, 0.81)	BAS
443.9	Peripheral Vascular Disease, Unspecified	Circulatory System	0.78 (0.74, 0.82)	0.75 (0.71, 0.79)	0.77 (0.73, 0.80)	0.75 (0.71, 0.79)	BAS
250.23	Type 2 Diabetes With Ophthalmic Manifestations	Endocrine/Metabolic	0.78 (0.71, 0.83)	0.74 (0.68, 0.79)	0.76 (0.71, 0.82)	0.71 (0.65, 0.77)	BAS
315.0	Develomental Delays And Disorders	Mental Disorders	0.78 (0.73, 0.82)	0.77 (0.73, 0.81)	0.77 (0.73, 0.81)	0.72 (0.67, 0.77)	BAS
333.2	Myoclonus	Neurological	0.78 (0.70, 0.85)	0.62 (0.54, 0.70)	0.68 (0.58, 0.77)	0.69 (0.60, 0.78)	BAS
433.1	Occlusion And Stenosis Of Precerebral Arteries	Circulatory System	0.77 (0.73, 0.80)	0.74 (0.70, 0.78)	0.73 (0.69, 0.77)	0.75 (0.71, 0.79)	BAS
264.2	Failure To Thrive (Childhood)	Endocrine/Metabolic	0.77 (0.67, 0.86)	0.67 (0.51, 0.83)	0.62 (0.46, 0.80)	0.76 (0.63, 0.86)	BAS
292.2	Mild Cognitive Impairment	Mental Disorders	0.77 (0.73, 0.81)	0.73 (0.68, 0.77)	0.73 (0.68, 0.77)	0.73 (0.69, 0.76)	BAS
202.0	Cancer Of Other Lymphoid, Histiocytic Tissue	Neoplasms	0.77 (0.70, 0.84)	0.75 (0.65, 0.83)	0.75 (0.66, 0.83)	0.73 (0.65, 0.81)	BAS
430.0	Intracranial Hemorrhage	Circulatory System	0.76 (0.70, 0.82)	0.69 (0.63, 0.76)	0.71 (0.64, 0.78)	0.70 (0.64, 0.76)	BAS
433.8	Late Effects Of Cerebrovascular Disease	Circulatory System	0.76 (0.70, 0.81)	0.69 (0.63, 0.76)	0.72 (0.65, 0.79)	0.70 (0.64, 0.75)	BAS
260.6	Anorexia	Endocrine/Metabolic	0.76 (0.72, 0.80)	0.72 (0.67, 0.77)	0.70 (0.64, 0.75)	0.73 (0.68, 0.77)	BAS
202.2	Non-Hodgkins Lymphoma	Neoplasms	0.76 (0.67, 0.84)	0.74 (0.62, 0.84)	0.72 (0.62, 0.82)	0.71 (0.62, 0.79)	BAS
350.2	Abnormality Of Gait	Neurological	0.76 (0.73, 0.78)	0.73 (0.70, 0.76)	0.73 (0.70, 0.76)	0.73 (0.70, 0.76)	BAS
362.26	Macular Puckering Of Retina	Sense Organs	0.76 (0.71, 0.79)	0.73 (0.68, 0.78)	0.71 (0.67, 0.76)	0.73 (0.69, 0.78)	BAS
362.2	Degeneration Of Macula And Posterior Pole Of Retina	Sense Organs	0.75 (0.72, 0.78)	0.73 (0.69, 0.76)	0.70 (0.67, 0.73)	0.72 (0.69, 0.75)	BAS
290.13	Senile Dementia	Mental Disorders	0.88 (0.78, 1.00)	0.92 (0.86, 0.99)	0.89 (0.87, 0.91)	0.67 (0.54, 0.83)	RESP
428.4	Heart Failure With Preserved Ef [Diastolic Heart Failure]	Circulatory System	0.83 (0.79, 0.86)	0.85 (0.82, 0.87)	0.84 (0.80, 0.87)	0.81 (0.78, 0.84)	RESP
401.21	Hypertensive Heart Disease	Circulatory System	0.81 (0.78, 0.84)	0.83 (0.80, 0.86)	0.82 (0.79, 0.85)	0.79 (0.76, 0.82)	RESP
440.1	Atherosclerosis Of Renal Artery	Circulatory System	0.73 (0.52, 0.94)	0.82 (0.69, 0.94)	0.81 (0.65, 0.93)	0.77 (0.62, 0.96)	RESP
496.21	Obstructive Chronic Bronchitis	Respiratory	0.76 (0.71, 0.81)	0.82 (0.77, 0.86)	0.80 (0.76, 0.85)	0.77 (0.71, 0.83)	RESP
426.23	Second Degree Av Block	Circulatory System	0.78 (0.73, 0.83)	0.81 (0.76, 0.84)	0.76 (0.70, 0.81)	0.79 (0.73, 0.83)	RESP
250.24	Type 2 Diabetes With Neurological Manifestations	Endocrine/Metabolic	0.78 (0.74, 0.83)	0.81 (0.76, 0.85)	0.80 (0.76, 0.83)	0.76 (0.71, 0.80)	RESP
741.3	Difficulty In Walking	Musculoskeletal	0.77 (0.72, 0.81)	0.81 (0.77, 0.84)	0.78 (0.73, 0.82)	0.76 (0.72, 0.81)	RESP
277.4	Disorders Of Bilirubin Excretion	Endocrine/Metabolic	0.79 (0.71, 0.85)	0.80 (0.72, 0.86)	0.70 (0.62, 0.77)	0.74 (0.65, 0.81)	RESP
276.11	Hyperosmolality And/Or Hypernatremia	Endocrine/Metabolic	0.74 (0.63, 0.83)	0.80 (0.72, 0.88)	0.78 (0.71, 0.85)	0.76 (0.66, 0.83)	RESP
315.2	Speech And Language Disorder	Mental Disorders	0.78 (0.69, 0.86)	0.80 (0.73, 0.86)	0.77 (0.69, 0.84)	0.74 (0.65, 0.82)	RESP
411.2	Myocardial Infarction	Circulatory System	0.78 (0.75, 0.81)	0.79 (0.76, 0.81)	0.78 (0.76, 0.81)	0.76 (0.73, 0.79)	RESP
250.1	Type 1 Diabetes	Endocrine/Metabolic	0.74 (0.67, 0.80)	0.78 (0.73, 0.83)	0.75 (0.69, 0.80)	0.71 (0.63, 0.77)	RESP
172.11	Melanomas Of Skin	Neoplasms	0.72 (0.65, 0.78)	0.78 (0.72, 0.83)	0.76 (0.69, 0.83)	0.71 (0.65, 0.77)	RESP
172.22	Squamous Cell Carcinoma	Neoplasms	0.71 (0.65, 0.77)	0.78 (0.73, 0.83)	0.75 (0.70, 0.80)	0.74 (0.68, 0.80)	RESP
427.11	Paroxysmal Supraventricular Tachycardia	Circulatory System	0.76 (0.73, 0.78)	0.77 (0.75, 0.80)	0.77 (0.74, 0.79)	0.76 (0.73, 0.79)	RESP
427.1	Paroxysmal Tachycardia, Unspecified	Circulatory System	0.76 (0.73, 0.78)	0.77 (0.75, 0.79)	0.77 (0.75, 0.79)	0.76 (0.73, 0.78)	RESP
505.0	Other Pulmonary Inflamation Or Edema	Respiratory	0.73 (0.65, 0.81)	0.77 (0.71, 0.83)	0.72 (0.65, 0.79)	0.70 (0.63, 0.77)	RESP
509.1	Respiratory Failure	Respiratory	0.72 (0.68, 0.76)	0.77 (0.72, 0.81)	0.76 (0.72, 0.80)	0.75 (0.71, 0.79)	RESP
509.2	Respiratory Insufficiency	Respiratory	0.69 (0.62, 0.77)	0.77 (0.69, 0.83)	0.76 (0.70, 0.82)	0.72 (0.64, 0.80)	RESP
415.1	Acute Pulmonary Heart Disease	Circulatory System	0.72 (0.67, 0.78)	0.76 (0.71, 0.82)	0.76 (0.71, 0.81)	0.73 (0.67, 0.78)	RESP
428.0	Congestive Heart Failure; Nonhypertensive	Circulatory System	0.74 (0.71, 0.77)	0.76 (0.73, 0.79)	0.76 (0.72, 0.79)	0.72 (0.69, 0.75)	RESP
415.11	Pulmonary Embolism And Infarction, Acute	Circulatory System	0.73 (0.67, 0.79)	0.76 (0.71, 0.81)	0.76 (0.71, 0.81)	0.73 (0.67, 0.78)	RESP
440.21	Atherosclerosis Of Native Arteries Of The Extremities With Ulceration Or Gangrene	Circulatory System	0.90 (0.82, 0.95)	0.86 (0.75, 0.94)	0.93 (0.87, 0.98)	0.86 (0.79, 0.92)	EKG
264.9	Lack Of Normal Physiological Development, Unspecified	Endocrine/Metabolic	0.86 (0.77, 0.93)	0.88 (0.82, 0.93)	0.90 (0.84, 0.95)	0.88 (0.81, 0.94)	EKG
426.24	Atrioventricular Block, Complete	Circulatory System	0.87 (0.80, 0.92)	0.85 (0.77, 0.91)	0.87 (0.82, 0.91)	0.81 (0.75, 0.88)	EKG
426.92	Cardiac Defibrillator In Situ	Circulatory System	0.79 (0.73, 0.84)	0.79 (0.73, 0.85)	0.87 (0.82, 0.91)	0.75 (0.69, 0.82)	EKG
250.25	Diabetes Type 2 With Peripheral Circulatory Disorders	Endocrine/Metabolic	0.83 (0.78, 0.88)	0.83 (0.80, 0.87)	0.86 (0.82, 0.89)	0.81 (0.75, 0.86)	EKG
411.8	Other Chronic Ischemic Heart Disease, Unspecified	Circulatory System	0.76 (0.70, 0.81)	0.77 (0.72, 0.82)	0.84 (0.80, 0.88)	0.75 (0.69, 0.80)	EKG
426.91	Cardiac Pacemaker In Situ	Circulatory System	0.77 (0.73, 0.81)	0.74 (0.69, 0.79)	0.82 (0.78, 0.86)	0.74 (0.69, 0.79)	EKG
276.42	Alkalosis	Endocrine/Metabolic	0.81 (0.74, 0.87)	0.81 (0.74, 0.87)	0.81 (0.74, 0.87)	0.77 (0.70, 0.84)	EKG
287.32	Secondary Thrombocytopenia	Hematopoietic	0.62 (0.52, 0.73)	0.77 (0.69, 0.84)	0.81 (0.73, 0.87)	0.69 (0.59, 0.77)	EKG
427.22	Atrial Flutter	Circulatory System	0.77 (0.73, 0.80)	0.80 (0.76, 0.83)	0.80 (0.77, 0.84)	0.74 (0.70, 0.78)	EKG
428.3	Heart Failure With Reduced Ef [Systolic Or Combined Heart Failure]	Circulatory System	0.75 (0.71, 0.79)	0.78 (0.75, 0.82)	0.80 (0.75, 0.84)	0.74 (0.70, 0.77)	EKG
426.8	Other Cardiac Conduction Disorders	Circulatory System	0.74 (0.70, 0.78)	0.80 (0.76, 0.83)	0.80 (0.77, 0.83)	0.72 (0.68, 0.76)	EKG
474.0	Acute And Chronic Tonsillitis	Respiratory	0.78 (0.75, 0.80)	0.77 (0.74, 0.79)	0.80 (0.78, 0.82)	0.74 (0.71, 0.77)	EKG
474.2	Chronic Tonsillitis And Adenoiditis	Respiratory	0.78 (0.76, 0.81)	0.78 (0.75, 0.80)	0.80 (0.78, 0.83)	0.75 (0.72, 0.77)	EKG
427.4	Cardiac Arrest And Ventricular Fibrillation	Circulatory System	0.66 (0.57, 0.74)	0.72 (0.63, 0.80)	0.79 (0.72, 0.85)	0.71 (0.64, 0.78)	EKG
426.9	Cardiac Pacemaker/Device In Situ	Circulatory System	0.74 (0.70, 0.78)	0.72 (0.68, 0.77)	0.79 (0.75, 0.83)	0.71 (0.66, 0.75)	EKG
249.0	Secondary Diabetes Mellitus	Endocrine/Metabolic	0.78 (0.73, 0.83)	0.78 (0.74, 0.82)	0.79 (0.75, 0.83)	0.75 (0.70, 0.79)	EKG
440.9	Atherosclerosis Of Aorta	Circulatory System	0.74 (0.70, 0.78)	0.76 (0.71, 0.81)	0.78 (0.73, 0.82)	0.70 (0.65, 0.74)	EKG
426.2	Atrioventricular [Av] Block	Circulatory System	0.72 (0.69, 0.76)	0.76 (0.72, 0.79)	0.78 (0.74, 0.81)	0.72 (0.67, 0.75)	EKG
428.2	Heart Failure Nos	Circulatory System	0.73 (0.64, 0.81)	0.74 (0.65, 0.82)	0.78 (0.70, 0.86)	0.69 (0.59, 0.77)	EKG
395.2	Nonrheumatic Aortic Valve Disorders	Circulatory System	0.77 (0.73, 0.81)	0.74 (0.70, 0.78)	0.78 (0.74, 0.81)	0.71 (0.66, 0.76)	EKG
427.8	Sinoatrial Node Dysfunction (Bradycardia)	Circulatory System	0.73 (0.67, 0.78)	0.78 (0.74, 0.82)	0.78 (0.74, 0.83)	0.70 (0.65, 0.75)	EKG
285.21	Anemia In Chronic Kidney Disease	Hematopoietic	0.76 (0.70, 0.81)	0.77 (0.72, 0.82)	0.78 (0.74, 0.82)	0.73 (0.67, 0.78)	EKG
426.21	First Degree Av Block	Circulatory System	0.70 (0.66, 0.74)	0.74 (0.70, 0.78)	0.77 (0.73, 0.81)	0.70 (0.66, 0.74)	EKG
401.2	Hypertensive Heart And/Or Renal Disease	Circulatory System	0.75 (0.72, 0.78)	0.77 (0.74, 0.79)	0.77 (0.74, 0.79)	0.73 (0.70, 0.75)	EKG
426.32	Left Bundle Branch Block	Circulatory System	0.72 (0.68, 0.75)	0.74 (0.70, 0.77)	0.77 (0.73, 0.81)	0.72 (0.68, 0.75)	EKG
395.3	Nonrheumatic Tricuspid Valve Disorders	Circulatory System	0.63 (0.56, 0.70)	0.75 (0.69, 0.80)	0.77 (0.72, 0.82)	0.65 (0.59, 0.71)	EKG
411.9	Other Acute And Subacute Forms Of Ischemic Heart Disease	Circulatory System	0.73 (0.64, 0.81)	0.76 (0.69, 0.83)	0.77 (0.70, 0.82)	0.70 (0.61, 0.78)	EKG
275.6	Hypercalcemia	Endocrine/Metabolic	0.75 (0.69, 0.80)	0.75 (0.69, 0.81)	0.77 (0.70, 0.82)	0.74 (0.66, 0.80)	EKG
427.12	Paroxysmal Ventricular Tachycardia	Circulatory System	0.75 (0.71, 0.79)	0.76 (0.71, 0.79)	0.76 (0.72, 0.80)	0.76 (0.71, 0.80)	EKG
571.51	Cirrhosis Of Liver Without Mention Of Alcohol	Digestive	0.67 (0.58, 0.76)	0.73 (0.65, 0.80)	0.76 (0.67, 0.82)	0.71 (0.62, 0.79)	EKG
440.2	Atherosclerosis Of The Extremities	Circulatory System	0.74 (0.68, 0.80)	0.72 (0.65, 0.79)	0.75 (0.68, 0.81)	0.68 (0.62, 0.74)	EKG
426.3	Bundle Branch Block	Circulatory System	0.71 (0.68, 0.74)	0.73 (0.69, 0.76)	0.75 (0.72, 0.78)	0.70 (0.67, 0.73)	EKG
420.3	Endocarditis	Circulatory System	0.66 (0.54, 0.77)	0.73 (0.63, 0.82)	0.75 (0.68, 0.82)	0.61 (0.50, 0.71)	EKG
427.6	Premature Beats	Circulatory System	0.73 (0.71, 0.75)	0.74 (0.71, 0.76)	0.75 (0.73, 0.77)	0.72 (0.70, 0.74)	EKG

Supplementary Table 8. Performance comparison of different modalities across conditions. For each modality, C-Index values are reported with 95% confidence intervals in parentheses. Only conditions where at least one modality achieves a C-Index above 0.75 are included. Results are grouped by disease category and sorted alphabetically within each category. BAS and EKG demonstrate the highest predictive performance, followed closely by RESP. EMG is the least predictive, with no top conditions where it performs best.

Category	BAS	EKG	EMG	RESP	SleepFM
circulatory system	0.71	0.73	0.69	0.72	0.75
dermatologic	0.63	0.63	0.63	0.63	0.66
digestive	0.63	0.65	0.64	0.65	0.67
endocrine/metabolic	0.67	0.68	0.66	0.68	0.71
hematopoietic	0.67	0.69	0.66	0.69	0.70
infectious diseases	0.63	0.63	0.63	0.64	0.66
injuries & poisonings	0.61	0.64	0.62	0.64	0.66
mental disorders	0.66	0.66	0.65	0.66	0.70
musculoskeletal	0.64	0.64	0.64	0.64	0.68
neoplasms	0.67	0.68	0.66	0.67	0.73
neurological	0.65	0.65	0.64	0.64	0.67
respiratory	0.62	0.64	0.62	0.64	0.66
sense organs	0.65	0.64	0.63	0.64	0.68
symptoms	0.66	0.66	0.66	0.66	0.68

Supplementary Table 9. Performance comparison between SleepFM trained on all modalities versus models trained on individual modalities alone. The table shows average C-Index across disease categories for each configuration. While certain modalities perform relatively well on their own, combining all modalities yields the highest performance, demonstrating the complementary nature of multimodal signals in PSG. These results support the benefit of leveraging multimodal data during training and highlight how different physiological signals contribute to disease prediction.

Category	BAS	EKG	EMG	RESP	SleepFM
circulatory system	0.75	0.77	0.74	0.76	0.79
dermatologic	0.69	0.69	0.69	0.69	0.70
digestive	0.69	0.70	0.70	0.70	0.72
endocrine/metabolic	0.72	0.72	0.71	0.72	0.75
hematopoietic	0.72	0.73	0.72	0.74	0.74
infectious diseases	0.68	0.67	0.68	0.68	0.70
injuries & poisonings	0.66	0.69	0.67	0.68	0.70
mental disorders	0.71	0.70	0.70	0.69	0.74
musculoskeletal	0.70	0.69	0.69	0.68	0.72
neoplasms	0.72	0.72	0.71	0.72	0.76
neurological	0.71	0.70	0.70	0.70	0.72
respiratory	0.67	0.68	0.67	0.68	0.70
sense organs	0.71	0.69	0.69	0.70	0.73
symptoms	0.73	0.73	0.73	0.73	0.75

Supplementary Table 10. Performance comparison between SleepFM trained on all modalities versus models trained on individual modalities alone. The table shows average AUROC across disease categories for each configuration. While certain modalities perform relatively well on their own, combining all modalities yields the highest performance, demonstrating the complementary nature of multimodal signals in PSG. These results support the benefit of leveraging multimodal data during training and highlight how different physiological signals contribute to disease prediction.

Phecode	Phenotype	Category	SleepFM	Demographics	End-to-End PSG
290.13	Senile dementia	mental disorders	0.99 (0.98, 1.00)	0.87 (0.75, 0.96)	0.95 (0.91, 0.98)
440.21	Atherosclerosis of native arteries of the extremities with ulceration or gangrene	circulatory system	0.92 (0.88, 0.95)	0.74 (0.64, 0.89)	0.66 (0.50, 0.89)
358.0	Myoneural disorders	neurological	0.81 (0.73, 0.88)	0.42 (0.28, 0.55)	0.60 (0.48, 0.71)
264.2	Failure to thrive (childhood)	endocrine/metabolic	0.77 (0.68, 0.88)	0.44 (0.26, 0.67)	0.45 (0.26, 0.67)
315.0	Develomental delays and disorders	mental disorders	0.80 (0.77, 0.84)	0.58 (0.51, 0.64)	0.61 (0.54, 0.67)
509.2	Respiratory insufficiency	respiratory	0.79 (0.72, 0.85)	0.59 (0.51, 0.67)	0.62 (0.53, 0.69)
277.4	Disorders of bilirubin excretion	endocrine/metabolic	0.79 (0.70, 0.85)	0.60 (0.46, 0.75)	0.61 (0.47, 0.75)
344.0	Other paralytic syndromes	neurological	0.77 (0.72, 0.83)	0.58 (0.48, 0.69)	0.60 (0.48, 0.69)
626.8	Infertility, female	genitourinary	0.89 (0.84, 0.93)	0.80 (0.73, 0.87)	0.88 (0.83, 0.92)
614.51	Cervicitis and endocervicitis	genitourinary	0.88 (0.85, 0.91)	0.79 (0.74, 0.83)	0.86 (0.83, 0.89)
619.2	Disorders of uterus, NEC	genitourinary	0.87 (0.84, 0.90)	0.79 (0.76, 0.82)	0.84 (0.81, 0.88)
609.0	Male infertility and abnormal spermatozoa	genitourinary	0.82 (0.78, 0.86)	0.71 (0.66, 0.76)	0.82 (0.78, 0.86)
504.0	Other alveolar and parietoalveolar pneumonopathy	respiratory	0.85 (0.80, 0.89)	0.75 (0.68, 0.81)	0.75 (0.68, 0.81)
619.3	Noninflammatory disorders of cervix	genitourinary	0.86 (0.82, 0.89)	0.77 (0.72, 0.81)	0.82 (0.79, 0.85)
250.25	Diabetes type 2 with peripheral circulatory disorders	endocrine/metabolic	0.87 (0.83, 0.91)	0.79 (0.74, 0.85)	0.78 (0.72, 0.84)
426.24	Atrioventricular block, complete	circulatory system	0.87 (0.83, 0.92)	0.80 (0.73, 0.87)	0.83 (0.76, 0.89)
348.8	Encephalopathy, not elsewhere classified	neurological	0.77 (0.70, 0.83)	0.63 (0.56, 0.71)	0.71 (0.64, 0.77)
276.42	Alkalosis	endocrine/metabolic	0.83 (0.77, 0.88)	0.74 (0.66, 0.80)	0.71 (0.63, 0.78)
249.0	Secondary diabetes mellitus	endocrine/metabolic	0.79 (0.74, 0.84)	0.68 (0.63, 0.72)	0.67 (0.62, 0.71)
447.7	Aortic ectasia	circulatory system	0.83 (0.80, 0.86)	0.74 (0.69, 0.79)	0.78 (0.74, 0.82)
280.2	Iron deficiency anemia secondary to blood loss (chronic)	hematopoietic	0.77 (0.73, 0.81)	0.64 (0.59, 0.69)	0.64 (0.60, 0.69)
218.1	Uterine leiomyoma	neoplasms	0.87 (0.85, 0.89)	0.81 (0.79, 0.83)	0.87 (0.84, 0.89)
300.9	Posttraumatic stress disorder	mental disorders	0.75 (0.70, 0.79)	0.62 (0.56, 0.68)	0.64 (0.59, 0.69)
331.0	Other cerebral degenerations	neurological	0.83 (0.76, 0.88)	0.74 (0.65, 0.82)	0.79 (0.70, 0.87)
290.2	Delirium due to conditions classified elsewhere	mental disorders	0.82 (0.76, 0.87)	0.73 (0.67, 0.78)	0.77 (0.71, 0.82)
218.0	Benign neoplasm of uterus	neoplasms	0.87 (0.85, 0.89)	0.81 (0.79, 0.83)	0.87 (0.85, 0.89)
276.4	Acid-base balance disorder	endocrine/metabolic	0.77 (0.72, 0.82)	0.66 (0.61, 0.72)	0.67 (0.61, 0.72)
250.24	Type 2 diabetes with neurological manifestations	endocrine/metabolic	0.81 (0.77, 0.85)	0.73 (0.68, 0.77)	0.71 (0.68, 0.75)
315.2	Speech and language disorder	mental disorders	0.81 (0.74, 0.87)	0.73 (0.63, 0.82)	0.73 (0.64, 0.82)
530.2	Esophageal bleeding (varices/hemorrhage)	digestive	0.76 (0.72, 0.79)	0.65 (0.60, 0.71)	0.69 (0.64, 0.74)
260.6	Anorexia	endocrine/metabolic	0.76 (0.71, 0.80)	0.65 (0.59, 0.72)	0.68 (0.62, 0.74)
458.2	Iatrogenic hypotension	circulatory system	0.76 (0.68, 0.83)	0.66 (0.58, 0.74)	0.67 (0.60, 0.74)
585.31	Renal dialysis	genitourinary	0.78 (0.73, 0.82)	0.68 (0.63, 0.74)	0.66 (0.60, 0.71)
426.8	Other cardiac conduction disorders	circulatory system	0.79 (0.75, 0.82)	0.70 (0.65, 0.74)	0.71 (0.66, 0.75)
276.11	Hyperosmolality and/or hypernatremia	endocrine/metabolic	0.76 (0.66, 0.86)	0.67 (0.58, 0.75)	0.68 (0.59, 0.76)
264.0	Lack of normal physiological development	endocrine/metabolic	0.77 (0.67, 0.86)	0.69 (0.56, 0.81)	0.69 (0.55, 0.81)
707.2	Chronic ulcer of leg or foot	dermatologic	0.80 (0.76, 0.85)	0.73 (0.68, 0.79)	0.70 (0.65, 0.75)
622.1	Polyp of corpus uteri	genitourinary	0.85 (0.81, 0.89)	0.79 (0.75, 0.83)	0.85 (0.81, 0.88)
594.3	Calculus of ureter	genitourinary	0.75 (0.69, 0.81)	0.67 (0.60, 0.73)	0.67 (0.62, 0.73)
250.7	Diabetic retinopathy	endocrine/metabolic	0.81 (0.77, 0.85)	0.75 (0.69, 0.80)	0.74 (0.69, 0.79)
513.8	Disorders of diaphragm	respiratory	0.75 (0.65, 0.84)	0.67 (0.56, 0.76)	0.68 (0.57, 0.77)
592.11	Acute cystitis	genitourinary	0.81 (0.78, 0.83)	0.74 (0.72, 0.77)	0.74 (0.71, 0.77)
285.1	Acute posthemorrhagic anemia	hematopoietic	0.78 (0.75, 0.81)	0.71 (0.67, 0.74)	0.72 (0.68, 0.75)
440.2	Atherosclerosis of the extremities	circulatory system	0.81 (0.74, 0.86)	0.75 (0.68, 0.80)	0.75 (0.69, 0.81)
362.27	Drusen (degenerative) of retina	sense organs	0.81 (0.77, 0.85)	0.75 (0.69, 0.80)	0.83 (0.79, 0.87)
501.0	Pneumonitis due to inhalation of food or vomitus	respiratory	0.75 (0.70, 0.80)	0.68 (0.62, 0.73)	0.69 (0.62, 0.76)
415.11	Pulmonary embolism and infarction, acute	circulatory system	0.80 (0.75, 0.85)	0.74 (0.68, 0.79)	0.75 (0.69, 0.81)
427.11	Paroxysmal supraventricular tachycardia	circulatory system	0.79 (0.76, 0.81)	0.72 (0.69, 0.76)	0.73 (0.70, 0.76)
415.1	Acute pulmonary heart disease	circulatory system	0.80 (0.75, 0.85)	0.74 (0.68, 0.80)	0.75 (0.69, 0.81)
411.8	Other chronic ischemic heart disease, unspecified	circulatory system	0.81 (0.76, 0.85)	0.75 (0.69, 0.79)	0.77 (0.72, 0.81)
440.22	Atherosclerosis of native arteries of the extremities with intermittent claudication	circulatory system	0.80 (0.73, 0.86)	0.75 (0.68, 0.83)	0.74 (0.65, 0.81)
411.9	Other acute and subacute forms of ischemic heart disease	circulatory system	0.78 (0.72, 0.85)	0.72 (0.64, 0.79)	0.72 (0.66, 0.79)
509.1	Respiratory failure	respiratory	0.77 (0.73, 0.80)	0.70 (0.65, 0.74)	0.69 (0.64, 0.73)
740.2	Osteoarthrosis, generalized	musculoskeletal	0.80 (0.76, 0.83)	0.74 (0.69, 0.79)	0.79 (0.74, 0.82)

Supplementary Table 11. Top conditions where sleep recordings provide substantial predictive value beyond demographic information alone. For each condition, we compare the predictive performance (C-Index) of SleepFM against demographic-only and end-to-end PSG models. The table highlights conditions where SleepFM achieved both strong absolute performance (C-Index > 0.75) and demonstrated meaningful improvement over demographic features (difference in C-Index > 0.5). Conditions are ranked by their relative improvement over demographics, emphasizing areas where sleep patterns contribute most significantly to prediction accuracy. Notable top conditions where SleepFM performs much better than baseline, include dementia, respiratory insufficiency, and developmental delays and disorders.

Phecode	Phenotype	Category	SleepFM	Demographics	End-to-End PSG
290.13	Senile dementia	mental disorders	0.99 (0.98, 1.00)	0.87 (0.75, 0.96)	0.95 (0.91, 0.98)
440.21	Atherosclerosis of native arteries of the extremities with ulceration or gangrene	circulatory system	0.92 (0.88, 0.95)	0.74 (0.64, 0.89)	0.66 (0.50, 0.89)
358.0	Myoneural disorders	neurological	0.81 (0.73, 0.88)	0.42 (0.28, 0.55)	0.60 (0.48, 0.71)
264.2	Failure to thrive (childhood)	endocrine/metabolic	0.77 (0.68, 0.88)	0.44 (0.26, 0.67)	0.45 (0.26, 0.67)
315.0	Develomental delays and disorders	mental disorders	0.80 (0.77, 0.84)	0.58 (0.51, 0.64)	0.61 (0.54, 0.67)
509.2	Respiratory insufficiency	respiratory	0.79 (0.72, 0.85)	0.59 (0.51, 0.67)	0.62 (0.53, 0.69)
277.4	Disorders of bilirubin excretion	endocrine/metabolic	0.79 (0.70, 0.85)	0.60 (0.46, 0.75)	0.61 (0.47, 0.75)
344.0	Other paralytic syndromes	neurological	0.77 (0.72, 0.83)	0.58 (0.48, 0.69)	0.60 (0.48, 0.69)
504.0	Other alveolar and parietoalveolar pneumonopathy	respiratory	0.85 (0.80, 0.89)	0.75 (0.68, 0.81)	0.75 (0.68, 0.81)
250.25	Diabetes type 2 with peripheral circulatory disorders	endocrine/metabolic	0.87 (0.83, 0.91)	0.79 (0.74, 0.85)	0.78 (0.72, 0.84)
426.24	Atrioventricular block, complete	circulatory system	0.87 (0.83, 0.92)	0.80 (0.73, 0.87)	0.83 (0.76, 0.89)
348.8	Encephalopathy, not elsewhere classified	neurological	0.77 (0.70, 0.83)	0.63 (0.56, 0.71)	0.71 (0.64, 0.77)
276.42	Alkalosis	endocrine/metabolic	0.83 (0.77, 0.88)	0.74 (0.66, 0.80)	0.71 (0.63, 0.78)
249.0	Secondary diabetes mellitus	endocrine/metabolic	0.79 (0.74, 0.84)	0.68 (0.63, 0.72)	0.67 (0.62, 0.71)
447.7	Aortic ectasia	circulatory system	0.83 (0.80, 0.86)	0.74 (0.69, 0.79)	0.78 (0.74, 0.82)
280.2	Iron deficiency anemia secondary to blood loss (chronic)	hematopoietic	0.77 (0.73, 0.81)	0.64 (0.59, 0.69)	0.64 (0.60, 0.69)
218.1	Uterine leiomyoma	neoplasms	0.87 (0.85, 0.89)	0.81 (0.79, 0.83)	0.87 (0.84, 0.89)
300.9	Posttraumatic stress disorder	mental disorders	0.75 (0.70, 0.79)	0.62 (0.56, 0.68)	0.64 (0.59, 0.69)
331.0	Other cerebral degenerations	neurological	0.83 (0.76, 0.88)	0.74 (0.65, 0.82)	0.79 (0.70, 0.87)
290.2	Delirium due to conditions classified elsewhere	mental disorders	0.82 (0.76, 0.87)	0.73 (0.67, 0.78)	0.77 (0.71, 0.82)
218.0	Benign neoplasm of uterus	neoplasms	0.87 (0.85, 0.89)	0.81 (0.79, 0.83)	0.87 (0.85, 0.89)
276.4	Acid-base balance disorder	endocrine/metabolic	0.77 (0.72, 0.82)	0.66 (0.61, 0.72)	0.67 (0.61, 0.72)
250.24	Type 2 diabetes with neurological manifestations	endocrine/metabolic	0.81 (0.77, 0.85)	0.73 (0.68, 0.77)	0.71 (0.68, 0.75)
315.2	Speech and language disorder	mental disorders	0.81 (0.74, 0.87)	0.73 (0.63, 0.82)	0.73 (0.64, 0.82)
530.2	Esophageal bleeding (varices/hemorrhage)	digestive	0.76 (0.72, 0.79)	0.65 (0.60, 0.71)	0.69 (0.64, 0.74)
260.6	Anorexia	endocrine/metabolic	0.76 (0.71, 0.80)	0.65 (0.59, 0.72)	0.68 (0.62, 0.74)
458.2	Iatrogenic hypotension	circulatory system	0.76 (0.68, 0.83)	0.66 (0.58, 0.74)	0.67 (0.60, 0.74)
426.8	Other cardiac conduction disorders	circulatory system	0.79 (0.75, 0.82)	0.70 (0.65, 0.74)	0.71 (0.66, 0.75)
276.11	Hyperosmolality and/or hypernatremia	endocrine/metabolic	0.76 (0.66, 0.86)	0.67 (0.58, 0.75)	0.68 (0.59, 0.76)
264.0	Lack of normal physiological development	endocrine/metabolic	0.77 (0.67, 0.86)	0.69 (0.56, 0.81)	0.69 (0.55, 0.81)
707.2	Chronic ulcer of leg or foot	dermatologic	0.80 (0.76, 0.85)	0.73 (0.68, 0.79)	0.70 (0.65, 0.75)
250.7	Diabetic retinopathy	endocrine/metabolic	0.81 (0.77, 0.85)	0.75 (0.69, 0.80)	0.74 (0.69, 0.79)
513.8	Disorders of diaphragm	respiratory	0.75 (0.65, 0.84)	0.67 (0.56, 0.76)	0.68 (0.57, 0.77)
285.1	Acute posthemorrhagic anemia	hematopoietic	0.78 (0.75, 0.81)	0.71 (0.67, 0.74)	0.72 (0.68, 0.75)
440.2	Atherosclerosis of the extremities	circulatory system	0.81 (0.74, 0.86)	0.75 (0.68, 0.80)	0.75 (0.69, 0.81)
362.27	Drusen (degenerative) of retina	sense organs	0.81 (0.77, 0.85)	0.75 (0.69, 0.80)	0.83 (0.79, 0.87)
501.0	Pneumonitis due to inhalation of food or vomitus	respiratory	0.75 (0.70, 0.80)	0.68 (0.62, 0.73)	0.69 (0.62, 0.76)
415.11	Pulmonary embolism and infarction, acute	circulatory system	0.80 (0.75, 0.85)	0.74 (0.68, 0.79)	0.75 (0.69, 0.81)
427.11	Paroxysmal supraventricular tachycardia	circulatory system	0.79 (0.76, 0.81)	0.72 (0.69, 0.76)	0.73 (0.70, 0.76)
415.1	Acute pulmonary heart disease	circulatory system	0.80 (0.75, 0.85)	0.74 (0.68, 0.80)	0.75 (0.69, 0.81)
411.8	Other chronic ischemic heart disease, unspecified	circulatory system	0.81 (0.76, 0.85)	0.75 (0.69, 0.79)	0.77 (0.72, 0.81)
440.22	Atherosclerosis of native arteries of the extremities with intermittent claudication	circulatory system	0.80 (0.73, 0.86)	0.75 (0.68, 0.83)	0.74 (0.65, 0.81)
411.9	Other acute and subacute forms of ischemic heart disease	circulatory system	0.78 (0.72, 0.85)	0.72 (0.64, 0.79)	0.72 (0.66, 0.79)
509.1	Respiratory failure	respiratory	0.77 (0.73, 0.80)	0.70 (0.65, 0.74)	0.69 (0.64, 0.73)
740.2	Osteoarthrosis, generalized	musculoskeletal	0.80 (0.76, 0.83)	0.74 (0.69, 0.79)	0.79 (0.74, 0.82)
427.1	Paroxysmal tachycardia, unspecified	circulatory system	0.78 (0.76, 0.81)	0.73 (0.70, 0.75)	0.73 (0.71, 0.76)
427.4	Cardiac arrest and ventricular fibrillation	circulatory system	0.77 (0.68, 0.84)	0.71 (0.63, 0.78)	0.73 (0.65, 0.81)
569.2	Gastrointestinal complications	digestive	0.76 (0.70, 0.81)	0.69 (0.62, 0.77)	0.66 (0.59, 0.72)
427.12	Paroxysmal ventricular tachycardia	circulatory system	0.78 (0.74, 0.82)	0.72 (0.68, 0.77)	0.72 (0.67, 0.77)
260.2	severe protein-calorie malnutrition	endocrine/metabolic	0.79 (0.74, 0.83)	0.73 (0.68, 0.78)	0.71 (0.67, 0.76)
285.2	Anemia of chronic disease	hematopoietic	0.76 (0.72, 0.79)	0.70 (0.66, 0.75)	0.71 (0.67, 0.75)
459.9	Circulatory disease NEC	circulatory system	0.77 (0.74, 0.79)	0.71 (0.68, 0.74)	0.71 (0.68, 0.75)
276.13	Hyperpotassemia	endocrine/metabolic	0.75 (0.71, 0.80)	0.70 (0.65, 0.75)	0.70 (0.65, 0.74)
574.2	Calculus of bile duct	digestive	0.76 (0.70, 0.80)	0.70 (0.63, 0.78)	0.70 (0.63, 0.78)
250.1	Type 1 diabetes	endocrine/metabolic	0.75 (0.69, 0.81)	0.70 (0.64, 0.75)	0.68 (0.62, 0.75)

Supplementary Table 12. Top conditions where sleep recordings demonstrate strong predictive performance for 6-year risk assessment. For each condition, we compare the 6-year AUROC of SleepFM against demographic-only and end-to-end PSG models. The table includes conditions where SleepFM achieved both strong absolute performance (AUROC > 0.75) and substantial improvement over the demographic baseline. Conditions are ranked by their relative improvement over demographics, highlighting diseases where sleep patterns provide the most significant additional predictive value. Notable top conditions where SleepFM performs much better than baseline, include dementia, respiratory insufficiency, and developmental delays and disorders.

Phecode	Phenotype	Category	C-Index		AUROC (6 Years)	
			SleepFM	Demographics	SleepFM	Demographics
290.13	Senile dementia	mental disorders	0.99 (0.98, 1.00)	0.87 (0.75, 0.96)	0.99 (0.98, 1.00)	0.85 (0.75, 0.97)
440.21	Atherosclerosis of native arteries of the extremities with ulceration or gangrene	circulatory system	0.92 (0.88, 0.95)	0.74 (0.64, 0.89)	0.95 (0.91, 0.98)	0.76 (0.72, 0.80)
358.0	Myoneural disorders	neurological	0.81 (0.73, 0.88)	0.42 (0.28, 0.55)	0.84 (0.75, 0.91)	0.38 (0.25, 0.53)
264.2	Failure to thrive (childhood)	endocrine/metabolic	0.77 (0.68, 0.88)	0.44 (0.26, 0.67)	0.75 (0.65, 0.87)	0.46 (0.29, 0.66)
315.0	Develomental delays and disorders	mental disorders	0.80 (0.77, 0.84)	0.58 (0.51, 0.64)	0.84 (0.79, 0.87)	0.58 (0.49, 0.66)
509.2	Respiratory insufficiency	respiratory	0.79 (0.72, 0.85)	0.59 (0.51, 0.67)	0.82 (0.72, 0.91)	0.57 (0.46, 0.67)
277.4	Disorders of bilirubin excretion	endocrine/metabolic	0.79 (0.70, 0.85)	0.60 (0.46, 0.75)	0.89 (0.84, 0.93)	0.62 (0.41, 0.80)
344.0	Other paralytic syndromes	neurological	0.77 (0.72, 0.83)	0.58 (0.48, 0.69)	0.82 (0.75, 0.88)	0.55 (0.41, 0.68)
504.0	Other alveolar and parietoalveolar pneumonopathy	respiratory	0.85 (0.80, 0.89)	0.75 (0.68, 0.81)	0.90 (0.84, 0.95)	0.76 (0.66, 0.84)
250.25	Diabetes type 2 with peripheral circulatory disorders	endocrine/metabolic	0.87 (0.83, 0.91)	0.79 (0.74, 0.85)	0.89 (0.85, 0.93)	0.79 (0.72, 0.87)
426.24	Atrioventricular block, complete	circulatory system	0.87 (0.83, 0.92)	0.80 (0.73, 0.87)	0.89 (0.84, 0.94)	0.80 (0.70, 0.88)
348.8	Encephalopathy, not elsewhere classified	neurological	0.77 (0.70, 0.83)	0.63 (0.56, 0.71)	0.78 (0.70, 0.86)	0.63 (0.54, 0.73)
276.42	Alkalosis	endocrine/metabolic	0.83 (0.77, 0.88)	0.74 (0.66, 0.80)	0.87 (0.77, 0.93)	0.75 (0.64, 0.84)
249.0	Secondary diabetes mellitus	endocrine/metabolic	0.79 (0.74, 0.84)	0.68 (0.63, 0.72)	0.82 (0.76, 0.88)	0.67 (0.59, 0.74)
447.7	Aortic ectasia	circulatory system	0.83 (0.80, 0.86)	0.74 (0.69, 0.79)	0.90 (0.87, 0.93)	0.74 (0.67, 0.80)
280.2	Iron deficiency anemia secondary to blood loss (chronic)	hematopoietic	0.77 (0.73, 0.81)	0.64 (0.59, 0.69)	0.84 (0.79, 0.89)	0.66 (0.59, 0.72)
218.1	Uterine leiomyoma	neoplasms	0.87 (0.85, 0.89)	0.81 (0.79, 0.83)	0.88 (0.85, 0.91)	0.80 (0.77, 0.83)
300.9	Posttraumatic stress disorder	mental disorders	0.75 (0.70, 0.79)	0.62 (0.56, 0.68)	0.82 (0.76, 0.87)	0.61 (0.54, 0.68)
331.0	Other cerebral degenerations	neurological	0.83 (0.76, 0.88)	0.74 (0.65, 0.82)	0.85 (0.77, 0.91)	0.75 (0.65, 0.84)
290.2	Delirium due to conditions classified elsewhere	mental disorders	0.82 (0.76, 0.87)	0.73 (0.67, 0.78)	0.81 (0.74, 0.88)	0.71 (0.64, 0.78)
218.0	Benign neoplasm of uterus	neoplasms	0.87 (0.85, 0.89)	0.81 (0.79, 0.83)	0.88 (0.84, 0.91)	0.80 (0.77, 0.83)
276.4	Acid-base balance disorder	endocrine/metabolic	0.77 (0.72, 0.82)	0.66 (0.61, 0.72)	0.79 (0.73, 0.85)	0.67 (0.59, 0.74)
250.24	Type 2 diabetes with neurological manifestations	endocrine/metabolic	0.81 (0.77, 0.85)	0.73 (0.68, 0.77)	0.86 (0.81, 0.90)	0.74 (0.68, 0.80)
315.2	Speech and language disorder	mental disorders	0.81 (0.74, 0.87)	0.73 (0.63, 0.82)	0.83 (0.74, 0.90)	0.72 (0.60, 0.83)
530.2	Esophageal bleeding (varices/hemorrhage)	digestive	0.76 (0.72, 0.79)	0.65 (0.60, 0.71)	0.87 (0.84, 0.90)	0.66 (0.57, 0.73)
260.6	Anorexia	endocrine/metabolic	0.76 (0.71, 0.80)	0.65 (0.59, 0.72)	0.84 (0.79, 0.88)	0.65 (0.55, 0.74)
458.2	Iatrogenic hypotension	circulatory system	0.76 (0.68, 0.83)	0.66 (0.58, 0.74)	0.77 (0.65, 0.87)	0.66 (0.53, 0.77)
426.8	Other cardiac conduction disorders	circulatory system	0.79 (0.75, 0.82)	0.70 (0.65, 0.74)	0.82 (0.77, 0.87)	0.69 (0.62, 0.75)
276.11	Hyperosmolality and/or hypernatremia	endocrine/metabolic	0.76 (0.66, 0.86)	0.67 (0.58, 0.75)	0.77 (0.59, 0.94)	0.78 (0.68, 0.88)
264.0	Lack of normal physiological development	endocrine/metabolic	0.77 (0.67, 0.86)	0.69 (0.56, 0.81)	0.72 (0.60, 0.84)	0.64 (0.49, 0.78)
707.2	Chronic ulcer of leg or foot	dermatologic	0.80 (0.76, 0.85)	0.73 (0.68, 0.79)	0.84 (0.79, 0.88)	0.75 (0.67, 0.81)
250.7	Diabetic retinopathy	endocrine/metabolic	0.81 (0.77, 0.85)	0.75 (0.69, 0.80)	0.84 (0.79, 0.89)	0.77 (0.70, 0.82)
513.8	Disorders of diaphragm	respiratory	0.75 (0.65, 0.84)	0.67 (0.56, 0.76)	0.73 (0.58, 0.86)	0.63 (0.48, 0.77)
285.1	Acute posthemorrhagic anemia	hematopoietic	0.78 (0.75, 0.81)	0.71 (0.67, 0.74)	0.83 (0.79, 0.87)	0.71 (0.66, 0.77)
440.2	Atherosclerosis of the extremities	circulatory system	0.81 (0.74, 0.86)	0.75 (0.68, 0.80)	0.84 (0.75, 0.90)	0.77 (0.68, 0.84)
362.27	Drusen (degenerative) of retina	sense organs	0.81 (0.77, 0.85)	0.75 (0.69, 0.80)	0.83 (0.78, 0.88)	0.72 (0.65, 0.78)
501.0	Pneumonitis due to inhalation of food or vomitus	respiratory	0.75 (0.70, 0.80)	0.68 (0.62, 0.73)	0.75 (0.69, 0.81)	0.65 (0.56, 0.72)
415.11	Pulmonary embolism and infarction, acute	circulatory system	0.80 (0.75, 0.85)	0.74 (0.68, 0.79)	0.85 (0.78, 0.91)	0.76 (0.68, 0.83)
427.11	Paroxysmal supraventricular tachycardia	circulatory system	0.79 (0.76, 0.81)	0.72 (0.69, 0.76)	0.87 (0.84, 0.90)	0.74 (0.69, 0.78)
415.1	Acute pulmonary heart disease	circulatory system	0.80 (0.75, 0.85)	0.74 (0.68, 0.80)	0.84 (0.77, 0.90)	0.76 (0.68, 0.82)
411.8	Other chronic ischemic heart disease, unspecified	circulatory system	0.81 (0.76, 0.85)	0.75 (0.69, 0.79)	0.81 (0.76, 0.86)	0.73 (0.66, 0.79)
440.22	Atherosclerosis of native arteries of the extremities with intermittent claudication	circulatory system	0.80 (0.73, 0.86)	0.75 (0.68, 0.83)	0.82 (0.74, 0.89)	0.75 (0.67, 0.84)
411.9	Other acute and subacute forms of ischemic heart disease	circulatory system	0.78 (0.72, 0.85)	0.72 (0.64, 0.79)	0.79 (0.71, 0.88)	0.74 (0.65, 0.82)
509.1	Respiratory failure	respiratory	0.77 (0.73, 0.80)	0.70 (0.65, 0.74)	0.76 (0.71, 0.82)	0.69 (0.63, 0.75)
740.2	Osteoarthrosis, generalized	musculoskeletal	0.80 (0.76, 0.83)	0.74 (0.69, 0.79)	0.85 (0.80, 0.89)	0.77 (0.71, 0.83)
427.1	Paroxysmal tachycardia, unspecified	circulatory system	0.78 (0.76, 0.81)	0.73 (0.70, 0.75)	0.87 (0.84, 0.89)	0.74 (0.70, 0.77)
427.4	Cardiac arrest and ventricular fibrillation	circulatory system	0.77 (0.68, 0.84)	0.71 (0.63, 0.78)	0.76 (0.66, 0.86)	0.73 (0.65, 0.81)
569.2	Gastrointestinal complications	digestive	0.76 (0.70, 0.81)	0.69 (0.62, 0.77)	0.79 (0.71, 0.87)	0.68 (0.59, 0.77)
427.12	Paroxysmal ventricular tachycardia	circulatory system	0.78 (0.74, 0.82)	0.72 (0.68, 0.77)	0.84 (0.79, 0.88)	0.71 (0.65, 0.77)
260.2	severe protein-calorie malnutrition	endocrine/metabolic	0.79 (0.74, 0.83)	0.73 (0.68, 0.78)	0.83 (0.75, 0.90)	0.77 (0.70, 0.84)
285.2	Anemia of chronic disease	hematopoietic	0.76 (0.72, 0.79)	0.70 (0.66, 0.75)	0.77 (0.72, 0.82)	0.69 (0.62, 0.75)
459.9	Circulatory disease NEC	circulatory system	0.77 (0.74, 0.79)	0.71 (0.68, 0.74)	0.84 (0.80, 0.87)	0.74 (0.69, 0.78)
276.13	Hyperpotassemia	endocrine/metabolic	0.75 (0.71, 0.80)	0.70 (0.65, 0.75)	0.79 (0.73, 0.85)	0.69 (0.64, 0.75)
574.2	Calculus of bile duct	digestive	0.76 (0.70, 0.80)	0.70 (0.63, 0.78)	0.79 (0.72, 0.85)	0.72 (0.65, 0.79)
250.1	Type 1 diabetes	endocrine/metabolic	0.75 (0.69, 0.81)	0.70 (0.64, 0.75)	0.77 (0.70, 0.82)	0.72 (0.65, 0.78)

Supplementary Table 13. Comparison of performance metrics, including C-Index and AUROC (6 Years) for SleepFM and demographics model. Conditions are ranked by their relative improvement over demographics model, retaining only conditions where the C-Index for SleepFM exceeds 0.75. All metrics include 95% confidence intervals calculated using bootstrapping.

Phecode	Phenotype	Category	C-Index		AUROC (6 Years)	
			SleepFM	End-to-End PSG	SleepFM	End-to-End PSG
440.21	Atherosclerosis of native arteries of the extremities with ulceration or gangrene	circulatory system	0.92 (0.88, 0.95)	0.66 (0.50, 0.89)	0.95 (0.92, 0.98)	0.65 (0.61, 0.69)
264.2	Failure to thrive (childhood)	endocrine/metabolic	0.77 (0.68, 0.88)	0.45 (0.26, 0.67)	0.75 (0.65, 0.87)	0.44 (0.26, 0.66)
358.0	Myoneural disorders	neurological	0.81 (0.73, 0.88)	0.60 (0.48, 0.71)	0.84 (0.75, 0.91)	0.54 (0.40, 0.69)
315.0	Develomental delays and disorders	mental disorders	0.80 (0.77, 0.84)	0.61 (0.54, 0.67)	0.84 (0.79, 0.87)	0.61 (0.52, 0.69)
509.2	Respiratory insufficiency	respiratory	0.79 (0.72, 0.85)	0.62 (0.53, 0.69)	0.82 (0.72, 0.91)	0.64 (0.54, 0.73)
277.4	Disorders of bilirubin excretion	endocrine/metabolic	0.79 (0.70, 0.85)	0.61 (0.47, 0.75)	0.89 (0.84, 0.93)	0.60 (0.41, 0.78)
344.0	Other paralytic syndromes	neurological	0.77 (0.72, 0.83)	0.60 (0.48, 0.69)	0.82 (0.75, 0.88)	0.54 (0.40, 0.68)
276.42	Alkalosis	endocrine/metabolic	0.83 (0.77, 0.88)	0.71 (0.63, 0.78)	0.87 (0.77, 0.93)	0.71 (0.59, 0.81)
250.25	Diabetes type 2 with peripheral circulatory disorders	endocrine/metabolic	0.87 (0.83, 0.91)	0.78 (0.72, 0.84)	0.89 (0.85, 0.93)	0.79 (0.70, 0.87)
504.0	Other alveolar and parietoalveolar pneumonopathy	respiratory	0.85 (0.80, 0.89)	0.75 (0.68, 0.81)	0.90 (0.84, 0.95)	0.76 (0.66, 0.84)
249.0	Secondary diabetes mellitus	endocrine/metabolic	0.79 (0.74, 0.84)	0.67 (0.62, 0.71)	0.82 (0.76, 0.88)	0.66 (0.59, 0.72)
250.24	Type 2 diabetes with neurological manifestations	endocrine/metabolic	0.81 (0.77, 0.85)	0.71 (0.68, 0.75)	0.86 (0.81, 0.90)	0.73 (0.67, 0.78)
280.2	Iron deficiency anemia secondary to blood loss (chronic)	hematopoietic	0.77 (0.73, 0.81)	0.64 (0.60, 0.69)	0.84 (0.79, 0.89)	0.66 (0.60, 0.71)
707.2	Chronic ulcer of leg or foot	dermatologic	0.80 (0.76, 0.85)	0.70 (0.65, 0.75)	0.84 (0.79, 0.88)	0.73 (0.67, 0.79)
276.4	Acid-base balance disorder	endocrine/metabolic	0.77 (0.72, 0.82)	0.67 (0.61, 0.72)	0.79 (0.73, 0.85)	0.67 (0.60, 0.74)
300.9	Posttraumatic stress disorder	mental disorders	0.75 (0.70, 0.79)	0.64 (0.59, 0.69)	0.82 (0.76, 0.87)	0.63 (0.56, 0.69)
315.2	Speech and language disorder	mental disorders	0.81 (0.74, 0.87)	0.73 (0.64, 0.82)	0.83 (0.74, 0.90)	0.71 (0.60, 0.83)
569.2	Gastrointestinal complications	digestive	0.76 (0.70, 0.81)	0.66 (0.59, 0.72)	0.79 (0.71, 0.87)	0.65 (0.57, 0.73)
426.8	Other cardiac conduction disorders	circulatory system	0.79 (0.75, 0.82)	0.71 (0.66, 0.75)	0.82 (0.77, 0.87)	0.69 (0.62, 0.76)
458.2	Iatrogenic hypotension	circulatory system	0.76 (0.68, 0.83)	0.67 (0.60, 0.74)	0.77 (0.65, 0.87)	0.67 (0.56, 0.77)
250.7	Diabetic retinopathy	endocrine/metabolic	0.81 (0.77, 0.85)	0.74 (0.69, 0.79)	0.84 (0.79, 0.89)	0.76 (0.69, 0.82)
276.11	Hyperosmolality and/or hypernatremia	endocrine/metabolic	0.76 (0.66, 0.86)	0.68 (0.59, 0.76)	0.77 (0.59, 0.94)	0.74 (0.62, 0.85)
264.0	Lack of normal physiological development	endocrine/metabolic	0.77 (0.67, 0.86)	0.69 (0.55, 0.81)	0.72 (0.60, 0.84)	0.63 (0.48, 0.77)
440.22	Atherosclerosis of native arteries of the extremities with intermittent claudication	circulatory system	0.80 (0.73, 0.86)	0.74 (0.65, 0.81)	0.82 (0.74, 0.89)	0.74 (0.65, 0.83)
274.11	Gouty arthropathy	endocrine/metabolic	0.76 (0.71, 0.81)	0.68 (0.63, 0.73)	0.77 (0.70, 0.84)	0.67 (0.60, 0.74)
509.1	Respiratory failure	respiratory	0.77 (0.73, 0.80)	0.69 (0.64, 0.73)	0.76 (0.71, 0.82)	0.68 (0.62, 0.74)
260.2	severe protein-calorie malnutrition	endocrine/metabolic	0.79 (0.74, 0.83)	0.71 (0.67, 0.76)	0.83 (0.75, 0.90)	0.72 (0.64, 0.80)
550.4	Umbilical hernia	digestive	0.79 (0.74, 0.83)	0.72 (0.64, 0.79)	0.84 (0.78, 0.90)	0.75 (0.66, 0.83)
513.8	Disorders of diaphragm	respiratory	0.75 (0.65, 0.84)	0.68 (0.57, 0.77)	0.73 (0.58, 0.86)	0.63 (0.48, 0.79)
260.6	Anorexia	endocrine/metabolic	0.76 (0.71, 0.80)	0.68 (0.62, 0.74)	0.84 (0.79, 0.88)	0.68 (0.58, 0.77)
530.2	Esophageal bleeding (varices/hemorrhage)	digestive	0.76 (0.72, 0.79)	0.69 (0.64, 0.74)	0.87 (0.84, 0.90)	0.69 (0.61, 0.75)
440.2	Atherosclerosis of the extremities	circulatory system	0.81 (0.74, 0.86)	0.75 (0.69, 0.81)	0.84 (0.75, 0.90)	0.78 (0.71, 0.85)
411.9	Other acute and subacute forms of ischemic heart disease	circulatory system	0.78 (0.72, 0.85)	0.72 (0.66, 0.79)	0.79 (0.71, 0.88)	0.75 (0.68, 0.82)
227.0	Benign neoplasm of other endocrine glands and related structures	neoplasms	0.75 (0.66, 0.84)	0.69 (0.59, 0.77)	0.82 (0.69, 0.93)	0.72 (0.59, 0.83)
250.1	Type 1 diabetes	endocrine/metabolic	0.75 (0.69, 0.81)	0.68 (0.62, 0.75)	0.77 (0.70, 0.82)	0.70 (0.64, 0.78)
285.1	Acute posthemorrhagic anemia	hematopoietic	0.78 (0.75, 0.81)	0.72 (0.68, 0.75)	0.83 (0.79, 0.87)	0.73 (0.68, 0.78)
415.1	Acute pulmonary heart disease	circulatory system	0.80 (0.75, 0.85)	0.75 (0.69, 0.81)	0.84 (0.77, 0.90)	0.76 (0.69, 0.83)
348.8	Encephalopathy, not elsewhere classified	neurological	0.77 (0.70, 0.83)	0.71 (0.64, 0.77)	0.78 (0.70, 0.86)	0.70 (0.62, 0.78)
427.11	Paroxysmal supraventricular tachycardia	circulatory system	0.79 (0.76, 0.81)	0.73 (0.70, 0.76)	0.87 (0.84, 0.90)	0.75 (0.70, 0.79)
427.12	Paroxysmal ventricular tachycardia	circulatory system	0.78 (0.74, 0.82)	0.72 (0.67, 0.77)	0.84 (0.79, 0.88)	0.72 (0.65, 0.78)
428.2	Heart failure NOS	circulatory system	0.77 (0.70, 0.84)	0.71 (0.64, 0.78)	0.81 (0.74, 0.88)	0.72 (0.64, 0.80)
427.1	Paroxysmal tachycardia, unspecified	circulatory system	0.78 (0.76, 0.81)	0.73 (0.71, 0.76)	0.87 (0.84, 0.89)	0.75 (0.71, 0.79)
501.0	Pneumonitis due to inhalation of food or vomitus	respiratory	0.75 (0.70, 0.80)	0.69 (0.62, 0.76)	0.75 (0.69, 0.81)	0.66 (0.57, 0.74)
276.13	Hyperpotassemia	endocrine/metabolic	0.75 (0.71, 0.80)	0.70 (0.65, 0.74)	0.79 (0.73, 0.85)	0.69 (0.63, 0.74)
459.9	Circulatory disease NEC	circulatory system	0.77 (0.74, 0.79)	0.71 (0.68, 0.75)	0.84 (0.80, 0.87)	0.74 (0.69, 0.78)
574.2	Calculus of bile duct	digestive	0.76 (0.70, 0.80)	0.70 (0.63, 0.78)	0.79 (0.72, 0.85)	0.72 (0.64, 0.80)

Supplementary Table 14. Comparison of performance metrics, including C-Index and AUROC (6 Years) for SleepFM and End-to-End PSG model. Conditions are ranked by their relative improvement over End-to-End PSG model, retaining only conditions where the C-Index for SleepFM exceeds 0.75. All metrics include 95% confidence intervals calculated using bootstrapping.

Modality	Channel	Prevalence (%)
RESP	Airflow	100.00
RESP	HR	99.92
RESP	Abdominal	73.92
RESP	SaO2	73.92
RESP	Thoracic	73.92
RESP	ABD	26.08
RESP	Chest	26.08
RESP	SpO2	26.08
BAS	C3	99.85
BAS	C4	99.85
BAS	LOC	73.92
BAS	ROC	73.92
BAS	A1	73.74
BAS	A2	73.74
BAS	M1	26.11
BAS	M2	26.11
BAS	E1	26.08
BAS	E2	26.08
EKG	ECG L	73.77
EKG	ECG R	73.77
EKG	ECGL	26.08
EKG	ECGR	26.08
EKG	ECG L-ECG R	0.15
EMG	Leg L	73.92
EMG	Leg R	73.92
EMG	L Chin	73.77
EMG	R Chin	73.77
EMG	LChin	26.08
EMG	LegL	26.08
EMG	LegR	26.08
EMG	RChin	26.08
EMG	L Chin-R Chin	0.15

Supplementary Table 15. Channels and prevalence percentages by modality for MROS.

Modality	Channel	Prevalence (%)
RESP	Abdo	100.00
RESP	HR	100.00
RESP	Snore	100.00
RESP	SpO2	100.00
RESP	Thor	100.00
RESP	Therm	99.37
BAS	EEG1	100.00
BAS	EEG2	100.00
BAS	EEG3	100.00
BAS	EOG-L	100.00
BAS	EOG-R	100.00
EKG	EKG	100.00
EMG	EMG	100.00
EMG	Leg	100.00
EMG	Pleth	100.00

Supplementary Table 16. Channels and prevalence percentages by modality for MESA.

Modality	Channel	Prevalence (%)
RESP	ABDO RES	100.00
RESP	SaO2	100.00
RESP	THOR RES	100.00
RESP	AIRFLOW	75.94
RESP	H.R.	68.69
RESP	NEW AIR	46.64
RESP	New Air	9.43
RESP	NEWAIR	4.14
RESP	AIRFLOW-0	1.08
RESP	AIRFLOW-1	1.08
EKG	ECG	100.00
BAS	EEG	100.00
BAS	EOG(L)	100.00
BAS	EOG(R)	100.00
BAS	EEG(sec)	97.95
BAS	EEG 2	1.15
BAS	EEG2	0.65
BAS	EEG sec	0.15
BAS	EEG(SEC)	0.09
EMG	EMG	100.00
EMG	LEG(L)	0.02
EMG	LEG(R)	0.02

Supplementary Table 17. Channels and prevalence percentages by modality for SHHS.

Modality	Channel	Prevalence (%)
BAS	LOC	70.10
BAS	ROC	70.10
BAS	A1A2	68.81
BAS	C3M2	60.02
BAS	C4M1	60.02
BAS	O1M2	60.02
BAS	O2M1	60.02
BAS	F3M2	58.78
BAS	F4M1	58.78
BAS	C3A2	36.61
RESP	Abd	83.75
RESP	SpO2	72.65
RESP	Snore	70.40
RESP	Pulse	27.17
RESP	SAO2	26.81
RESP	SNOR	16.34
RESP	PPG	13.07
RESP	ABD	12.29
RESP	Abdomen	2.03
RESP	Thorax	2.03
EMG	LLeg	75.01
EMG	RLeg	75.01
EMG	Chin	67.73
EMG	CHIN	26.86
EMG	LLEG	18.28
EMG	RLEG	18.28
EMG	InterEMG	2.91
EMG	Pleth	2.42
EMG	CHINEMG	1.96
EMG	LLEGEMG	1.96
EKG	ECG	92.22
EKG	EKG	2.35
EKG	ECGI-0	1.83
EKG	ECGI-1	1.83
EKG	ECGII-0	1.83
EKG	ECGII-1	1.83
EKG	ECG1	1.27
EKG	ECGI	1.23
EKG	ECG2	0.41
EKG	ECG II	0.23

Supplementary Table 18. Channels and prevalence percentages by modality for BioSerenity.

Modality	Channel	Prevalence (%)
RESP	Snore	88.04
RESP	Chest	83.96
RESP	SpO2	66.98
RESP	Abd	65.96
RESP	Pulse Rate	45.14
RESP	Nasal	43.81
RESP	Nasal Pressure	43.49
RESP	Oral Therm	42.88
RESP	Pulse	39.97
RESP	Oral-CO2	37.94
BAS	E1-Cz	43.53
BAS	C3-Cz	43.31
BAS	C4-Cz	43.31
BAS	M1-Cz	43.31
BAS	M2-Cz	43.31
BAS	O1-Cz	43.31
BAS	C3	43.11
BAS	C4	43.11
BAS	O1	43.11
BAS	O2	43.11
EMG	Chin	31.40
EMG	Chin2	28.35
EMG	Chin EMG	27.09
EMG	Chin_Ctr-Cz	26.01
EMG	Chin_L-Cz	26.01
EMG	Chin_R-Cz	26.01
EMG	Feet-R	19.18
EMG	Pleth	17.60
EMG	Arms-1	17.52
EMG	Arms-2	17.52
EKG	EKG_L-Cz	43.31
EKG	EKG_R-Cz	43.31
EKG	ECG	17.78
EKG	EKG-L	12.01
EKG	EKG-R	12.01
EKG	ECG II	11.87
EKG	EKG	9.07
EKG	ECG 2	1.48
EKG	EKG2	0.02
EKG	ECG1-EC	0.00

Supplementary Table 19. Channels and prevalence percentages by modality for SSC.